# Investigation of Subgrade and Performance Characteristics of Cement-Treated Base Materials for Road Pavement System Enhancement: A Case Study in Addis Ababa

Yared Zikuala Mulugeta

A Thesis Submitted to the Department of Civil Engineering,
School of Civil Engineering and Architecture

Presented in Partial Fulfillment of the Requirement for the Degree of
Master`s in Civil Engineering
(Specialization in Geotechnical Engineering)

Office of Post Graduate Studies
Adama Science and Technology University

November, 2024
Adama, Ethiopia

# Investigation of Subgrade and Performance Characteristics of Cement-Treated Base Materials for Road Pavement System Enhancement: A Case Study in Addis Ababa

Yared Zikuala Mulugeta

Main Advisor: Argaw Asha Ashango (Ph.D.)

A Thesis Submitted to the Department of Civil Engineering, School of Civil Engineering and Architecture

Presented in Partial Fulfillment of the Requirement for the Degree of Master`s in Civil Engineering

(Specialization in Geotechnical Engineering)

Office of Post Graduate Studies
Adama Science and Technology University

November, 2024
Adama, Ethiopia

## DECLARATION

I declare that this thesis entitled **"Investigation of Subgrade and Performance Characteristics of Cement-Treated Base Materials for Road Pavement System Enhancement: A Case Study in Addis Ababa"** is my work and has not been submitted to any university for a similar purpose. Proper citations duly recognize the references used in this thesis.

| | | |
|---|---|---|
| Yared Zikuala Mulugeta | ________________ | ________________ |
| Name of student | Signature | Date |

# RECOMMENDATION

I/we, the advisor(s) of this thesis, at this moment certify that I/we have read the revised version of the thesis entitled **"Investigation of Subgrade and Performance Characteristics of Cement-Treated Base Materials for Road Pavement System Enhancement: A Case Study in Addis Ababa"** prepared under my/our guidance by **Yared Zikuala Mulugeta** submitted in partial fulfillment of the requirements for the degree of Masters of Science in Civil Engineering. Therefore, I/we recommend submitting the revised version of the thesis to the department following the applicable procedures.

| | | |
|---|---|---|
| Argaw Asha Ashango (Ph.D.) | ________________________ | ____________________ |
| Advisor | Signature | Date |
| _______________ | _______________ | _______________ |
| Co-advisor/Co-supervisor | Signature | Date |

# APPROVAL PAGE

I at this moment certify that the recommendation and suggestion given by the thesis review committee are appropriately incorporated into the final thesis entitled **"Investigation of Subgrade and Performance Characteristics of Cement-Treated Base Materials for Road Pavement System Enhancement: A Case Study in Addis Ababa"** by Yared Zikuala Mulugeta.

| | | |
|---|---|---|
| Argaw Asha Ashango (Ph.D.) | ____________ | ______________ |
| Advisor | Signature | Date |
| _____________ | ____________ | _____________ |
| Co-advisor/Co-supervisor | Signature | Date |

We, the undersigned, members of the Board of Examiners of the thesis by Yared Zikuala Mulugeta have read and evaluated the thesis entitled **"Investigation of Subgrade and Performance Characteristics of Cement-Treated Base Materials for Road Pavement System Enhancement: A Case Study in Addis Ababa"** and examined the candidate during the open defense. This is, therefore, to certify that the thesis is accepted for partial fulfillment of the requirement of the degree of Master of Science in Civil Engineering.

| | | |
|---|---|---|
| ___________________________ | _____________________ | ___________________ |
| Chairperson | Signature | Date |
| ___________________________ | _____________________ | ___________________ |
| Internal Examiner | Signature | Date |
| ___________________________ | _____________________ | ___________________ |
| External Examiner | Signature | Date |

Finally, approval and acceptance of the thesis are contingent upon submission of its final copy to the Office of Postgraduate Studies (OPGS) through the Department Graduate Council (DGC) and School Graduate Committee (SGC).

| | | |
|---|---|---|
| ___________________________ | _____________________ | ___________________ |
| Department Head | Signature | Date |
| ___________________________ | _____________________ | ___________________ |
| School Dean | Signature | Date |
| ___________________________ | _____________________ | ___________________ |
| Office of Postgraduate Studies, Dean | Signature | Date |

# ACKNOWLEDGEMENT

I would like to express my deepest gratitude to all those who contributed to the completion of this thesis. Your support, guidance, and encouragement have been invaluable throughout this journey.

First and foremost, I am profoundly grateful to my thesis advisor, Dr. Argaw Asha, for his unwavering support, expert guidance, and encouragement. His mentorship and insightful feedback have been instrumental in shaping the direction and quality of this research.

I extend my sincere thanks to the Civil Engineering Department faculty members for their dedication to education and research, which provided the foundation upon which this work is built. Special thanks go to Mr. Shume, Mr. Mesele, Mr. Leta, and Mr. Demeke for their invaluable assistance with the experiments at the ASTU laboratory. I am also deeply grateful to Mr. Robel, head of the China First Highway Engineering Co. LTD Laboratory, for allowing me to conduct part of my experiments in their facilities. Furthermore, my deepest appreciation goes to Engineer Mesfin Teshome, General Manager of White Knight Construction Management Consulting Engineers PLC, for his unwavering support and guidance.

I would also like to express my sincere thanks to my friends Mr. Zerihun Mamo, Mr. Musse Gizachew, Mr. Anteneh Endashaw, Mr. Biniyam Abebayehu, and Miss Mihiret Rebo, whose valuable feedback and insights greatly enhanced the quality of this work.

My heartfelt appreciation goes to my family for their unending love, encouragement, and belief in my abilities. Your unwavering support has sustained me throughout this endeavor.

Lastly, I extend my gratitude to the countless researchers and scholars whose work laid the groundwork for this study. Your contributions to the field of Geotechnical Engineering have been a constant source of inspiration.

# TABLE OF CONTENTS

# LIST OF FIGURES

# LIST OF TABLES

# LIST OF ABBREVIATIONS AND ACRONYMS

| | |
|---|---|
| $\varepsilon t$ | Horizontal tensile strains in the bottom of the asphalt concrete layer |
| $\varepsilon$ | Horizontal tensile strains in the bottom of the cement-treated layer |
| $\sigma v$ | Vertical compressive stress on top of the cement-treated layer |
| $\varepsilon v$ | Vertical compressive strains at the surface of the subgrade |
| $\mu$ | Poisson's Ratio |
| AASHTO | American Association of State Highway and Transportation Officials |
| ACV | Aggregate crushing value |
| BS | British standard specification |
| CM | Centimeter |
| CH | high plastic clay |
| ML | low plastic silty |
| CBR | California Bearing Ratio |
| D | Depth |
| E | Easting |
| E | Modulus of elasticity |
| Ec | Cement-treated layer modulus |
| ESAL | Equivalent Single Axle Load |
| ERA | Ethiopia road authority |
| Elv | Elevation |
| FHWA | Federal Highway Administration |
| FI | Flakiness index |
| GPS | Global position system |
| H | Height |
| ITS | Indirect Tensile Strength |
| Km | Kilometer |
| Km/hr | Kilo meter per hour |
| Kg | Kilo gram |
| L | Length |
| LAA | Los Angeles Abrasion |

| | |
|---|---|
| LHS | Left hand side |
| LL | Liquid limit |
| LS | Liner shrinkage |
| M | Meter |
| M3 | Cubic meter |
| mm | Millimeter |
| N | Northing |
| N | Equivalent Number of Standard Axles (80 kN) |
| Nil | None |
| NP | Non-plastic |
| MDD | Maximum dry density |
| NaSo4 | Sodium sulfate |
| OMC | Optimum moisture content. |
| PI | Plasticity index. |
| PL | Plasticity limit. |
| SADOT | South African Department of Transport |
| SAMDM | South African Mechanistic Design Method |
| SANRAL | South African National Roads Agency Limited |
| SR | Tensile Strain Relationship |
| TMH | Technical Methods for Highways |
| TRH | Technical Recommendations for Highways |
| UCS | Unconfident Compressive Strength |
| USACE | United States Army Corps of Engineers |

# ABSTRACT

*In Ethiopia, conventional asphalt pavements with granular base and sub-base layers often face issues like premature deterioration, high maintenance costs, and poor drainage. These problems stem from factors such as substandard construction practices, weak subgrade strength, and overloading, leading to rutting and fatigue cracking. This study investigates cement-treated base (CTB) as a viable alternative to improve pavement performance and reduce costs. A thorough subgrade assessment was conducted, including soil classification, compaction, and strength testing to meet engineering standards. CTB provides several advantages over traditional base materials, such as increased structural capacity, enhanced resistance to cracking, and improved fatigue performance. Its stiffer base minimizes deflections under heavy traffic, extending the pavement's lifespan. Additionally, CTB's high bearing strength allows for a thinner base layer, which optimizes material usage and accelerates construction. Mechanical testing showed that a cement content of 5% yielded an unconfined compressive strength of 5.22 MPa, within the target range of 4.5–7 MPa, resulting in a mix that effectively resists deformation and distributes loads. Microstructural analyses using X-ray Diffraction (XRD) and Scanning Electron Microscopy (SEM) identified calcium silicate hydrates (C-S-H) as critical components contributing to CTB's strength and durability, with SEM images displaying a dense microstructure that enhances crack resistance. Performance assessments using IITPAVE software indicated that CTB outperforms conventional materials in reducing subgrade rutting and fatigue. Cost analysis revealed that CTB is approximately 15-20% less expensive than traditional granular base systems due to its increased load-bearing capacity, allowing for a thinner layer and reducing material and construction costs. Furthermore, numerical modeling with PLAXIS 3D demonstrated that using CTB as a base layer significantly reduces settlement compared to Dense Bituminous Macadam (DBM), particularly when supporting asphalt concrete (AC) and soil layers. This supports the concept of an inverted pavement system, where a CTB layer under asphalt minimizes settlement and enhances load-bearing capacity, offering a cost-effective and durable solution for Ethiopia's high-traffic roads with weak subgrades.*

***Key Words/Terms*: Subgrade soil, Cement-Treated Base, IITPAVE, PLAXIS 3D, Unconfined Compressive Strength**

# 1. INTRODUCTION

## 1.1 Background of the Study

Road infrastructure plays a pivotal role in facilitating economic development, social connectivity, and transportation efficiency in both urban and rural areas. However, the performance and longevity of road pavements are often challenged by factors such as traffic loading, environmental conditions, and subgrade soil properties. Consequently, there is a pressing need to develop innovative pavement materials and construction techniques to enhance the durability and resilience of transportation networks (Hasan et al., 2022).

The most crucial component of the entire highway construction process is the design and construction of the pavement. Pavement structural strength, traffic volume, and surface condition all affect how well the road transportation industry performs overall. In order to minimize and adjust positively to both acute and chronic stress, a pavement structure's primary purpose is to transfer applied traffic loads to the roadbed and system. The development of resilience pavements ought to incorporate a system that can preserve, enhance, and repair their fundamental tasks. Distributing the transmitted stresses from the wheel load from the layer to the soil base is the fundamental job of the pavement construction; this aids in preventing the pavement from buckling (Plati & Pomoni, 2019).

Flexible pavements follow a stress distribution pattern in which wheel load is distributed from the top layer to the bottom layer through grain-to-grain contact. A strong layer is used at the top, whereas a weak layer (i.e., subgrade) is used at the bottom. The critical locations of strains are at the bottom of the asphalt layer and on top of the subgrade (Khan et al., 2022).

The inverted pavement system is an alternative to rigid and flexible pavement. A pavement system that has a low-strength unbound layer atop a cement-bound layer is known as inverted pavement. This unbound layer is sealed with asphalt, has a high bearing capacity, and functions as a crack relief layer (Jiang, Titi, et al., 2022). In Inverted pavement, the essential stress/strain locations are at the top of the subgrade (compressive strain) and bottom of the cemented layer (tensile strain). In a flexible system, the aggregate layer is usually positioned above the subbase layer, and the thicker layers of hot mix asphalt (HMA) are layered on top of the aggregate layer; an inverted pavement comprises a rigid base layer treated with cement, a thin layer of asphalt, and a compacted aggregate layer sandwiched between the two layers of asphalt (Daniel & Velasquez, 2023).

Cement-treated base (CTB) materials have emerged as a promising solution for improving the performance of road pavements. CTB comprises a blend of cementitious materials, aggregates, and water, which, when compacted and cured, form a durable and stable base layer for road pavements. The incorporation of cementitious binders enhances the strength, stiffness, and resistance to moisture-induced distresses, making CTB an attractive alternative to traditional base materials such as untreated aggregates or asphalt-treated bases (Bressi et al., 2022).

Despite the growing interest in CTB, there remains a need for comprehensive research to understand its engineering behavior under various geotechnical and environmental conditions. This necessitates a thorough investigation of subgrade properties, material characteristics, mix design optimization, and long-term performance assessment to ensure the effective implementation of CTB in road construction projects (Chhabra et al., 2021).

Furthermore, advancements in computational tools and numerical modeling software IITPAVE offer new opportunities to analyze and predict the performance of road pavements. Integrating such tools into the research framework can provide valuable insights into the behavior of CTB materials, allowing for sophisticated analyses of stress distribution, deformation patterns, and failure mechanisms under different loading and environmental scenarios (Biswal et al., 2020).

This study investigates the elaborate interplay between the geotechnical characteristics and performance aspects of CTB materials, aiming to contribute to the knowledge base of pavement and geotechnical engineering. By unraveling the complexities associated with these materials, the research seeks to provide valuable insights that excel conventional practices, offering a pathway towards more resilient, sustainable, and cost-effective road pavements. As we embark on this exploration, the symbiotic relationship between geotechnical details and material performance takes center stage, promising to redefine the paradigm of road pavement design and construction for a future characterized by increased demands for efficiency, durability, and environmental responsibility.

## 1.2 Statement of the Problem

Road infrastructure plays a vital role in facilitating transportation and economic development. However, traditional road pavement systems often face significant challenges, including premature deterioration, high maintenance costs, shorter lifespans, and inadequate drainage (Solla et al., 2021). The flexible pavement has problems of deformation, cracking, and disintegration due to stress from heavy vehicles and water intrusion. The failure of granular bases may occur due to the loss of interlocking between aggregate, which cannot transfer the wheel load to the ground underneath properly which fails pavement (Hassani et al., 2020).

Building roads and highways requires significant financial expense. By employing innovative techniques and the most cost-effective and appropriate materials, this expense can be reduced to the absolute minimum. The poor state of the highways is actually the main reason for the introduction of CTB. Pavement sustains severe damage quickly in locations with high traffic and weather. Highways experience uneven settlement, the development of potholes, and side-shoulder failure as a result of prolonged precipitation. The majority of the damage is brought about by the permeability, voids, and weak foundation layer (Plati, 2019).

In this context, the adoption of cement-treated base (CTB) materials emerges as a promising solution for enhancing road pavement performance. CTB offers improved strength, stiffness, and durability compared to conventional base materials, attributed to the incorporation of cementitious binders that enhance engineering properties.

This study aims to address these challenges by conducting a thorough geotechnical investigation and performance characteristics, thereby contributing to the optimization of designs, enhanced stability, and the promotion of sustainable construction practices in the development of road infrastructure.

### 1.3 Research Questions

1. What are the key geotechnical properties of the subgrade soil that influence its suitability for pavement construction?
2. How does the addition of cement to base materials affect their mechanical properties and overall performance in pavement applications?
3. How effectively does the PLAXIS 3D and the IITPAVE software simulate rutting and fatigue performance in pavement structures utilizing cement-treated base materials?

4. What is the cost-effectiveness of using cement-treated base materials compared to conventional pavement materials in terms of initial construction and long-term maintenance?

## 1.4 Objectives of the Study

### 1.4.1 General Objective

The main objective of this study is to investigate the subgrade soil and performance characteristics of cement-treated base materials for enhancing road pavement systems

### 1.4.2 Specific Objectives

- To investigate the geotechnical properties of the subgrade soil
- To explore and understand the concept of cement-treated base (CTB) materials
- To simulate the performance evaluation of pavement structures using PLAXIS 3D and IITPAVE
- To perform a cost comparison between cement-treated base (CTB) materials and conventional pavement methods

## 1.5 Significance of the Study

The current study holds paramount significance in advancing geotechnical engineering and infrastructure development by conducting a thorough laboratory investigation of subgrade soil, encompassing index properties, compaction, and California Bearing Ratio (CBR). This is an important study in several ways, particularly when road construction in Ethiopia is considered.

The present research about geotechnical properties at the subgrade level contributes vital information about the foundation conditions necessary for the design of durable and long-lasting road infrastructure. To understand the subgrade characteristics, optimize pavement designs, and reduce premature failures to eventually minimize the costs of maintenance.

Attention to cement-treated base (CTB) materials opens up a realistic alternative solution for conventional pavement construction. CTB is capable of enhancing the structural adequacy of roads, taking into account improved resistance to deformation, rutting, and fatigue cracking. Understanding that this study explores CTB as a viable solution to these issues addresses one of the main persistent challenges of road deterioration in Ethiopia and offers a pathway to more resilient infrastructure.

The Performance criteria of CTB pavement type, considering rutting and fatigue criteria, was assessed by the research using IITPAVE software to determine the stress, strain, and deflection of each pavement layer; thus, the proposed designs for CTB were thus meet the required engineering standards. With this approach, the expected life and pavement behavior under heavy traffic loads can be fully assessed, leading to safer and more reliable highways.

The use of PLAXIS 3D software allows for sophisticated modeling of complex geotechnical systems, including the interaction between CTB materials and underlying subgrade soil. This enhances the understanding of the mechanical properties, stress distribution, and deformation behavior of the CTB layer under real-world conditions. By utilizing this software, your study provides a more precise and reliable simulation of how CTB materials perform under traffic loads and environmental factors, offering insights into long-term pavement behavior

This study is therefore of paramount importance in comparing the cost of CTB materials and conventional pavement methods for this field of study. The findings were enable the decision-makers to understand the financial implications of adopting CTB and eventually result in cost-effective construction practices that can stretch limited resources further while delivering better road performance. It were, therefore, make a huge contribution to change in geotechnical engineering practices in Ethiopia by embracing CTB materials. The study contributes to more resilient, cost-effective, and durable road infrastructure necessary for economic growth and development.

In general, the current study collectively contributes to the advancement of best practices, fostering the development of sustainable, resilient, and economically viable road infrastructure.

## 1.5 Scope of the Study

The current study proposes a comprehensive investigation encompassing the geotechnical properties of subgrade soil, the study of cement treated base material and optimization of material application rates, performance criteria for subgrade rutting, fatigue cracking of the bituminous layer and fatigue resistance for cement treated base materials and to determine the cumulative damage analysis of the axle load survey to check the performance of the CTB pavement, and cost-comparison analysis of the CTB pavement and the traditional conventional pavement.

The scope involves detailed laboratory analyses to characterize the subgrade soil, focusing on index properties, compaction characteristics, and California Bearing Ratio (CBR), with the aim of understanding its behavior for stable road pavement design. Simultaneously, the study were to determine the optimal application rates of cement and aggregate through dedicated laboratory investigations, emphasizing sustainability by minimizing material usage.

The simulation of IITPAVE software to determine the pavement's stress, strain and deflection to determine the performance criteria of subgrade rutting and fatigue deformation integration of the pavement to understand the enhancing precision of pavement design.

A critical aspect of the study involves a comprehensive cost-comparison analysis to assess the economic feasibility of employing cement-treated base materials compared to conventional alternatives, providing decision-makers with essential insights.

The study also aims to advance geotechnical engineering practices, optimize construction methodologies, and contribute to developing resilient, sustainable, and economically viable road infrastructure.

## 1.6 Limitations of the study

This study on Cement-Treated Base (CTB) materials in Ethiopian road construction faced several key limitations. Due to time constraints and the unavailability of critical field performance testing equipment, such as the Falling Weight Deflectometer (FWD), the Benkelman Beam Deflection Method could not be conducted. Furthermore, the analysis of Cumulative Fatigue Damage (CFD) for the CTB layer was restricted by the lack of reliable traffic data and the time-consuming nature of the process.

## 1.7 Research Organization

This research is structured into key chapters that systematically address the objectives, ensuring a coherent flow of information. The organization allows for a logical progression from identifying the research problem to presenting the findings and recommendations.

Chapter One provides the introduction, including an overview of the study's background, a clear statement of the research problem, and the study's objectives. Additionally, the limitations, scope, and significance of the study are briefly outlined to establish the framework for the research.

Chapter Two of this research presents a comprehensive literature review that covers essential topics related to the study. It explores the geotechnical properties of subgrade soils, the principles and applications of Cement-Treated Base (CTB) materials, and common pavement issues such as rutting and fatigue. Additionally, this chapter reviews the application of IITPAVE software for performance evaluations and provides a summary of relevant studies comparing the cost-effectiveness of CTB versus conventional pavement methods. This thorough review lays the foundation for the research methodology and subsequent analysis.

Chapter Three provides an overview of the materials and methods used in the study. It begins with a description of the study area and the materials utilized, followed by a detailed explanation of the laboratory tests conducted to investigate subgrade soil properties and analyze the performance of Cement-Treated Base (CTB) materials. The chapter also outlines the approach for evaluating pavement performance using IITPAVE software and the methodology for conducting a cost comparison between CTB and conventional pavement methods. A step-by-step explanation of the data collection, testing procedures, and analysis methods is included to ensure the research is transparent and reproducible.

Chapter Four presents the analysis of laboratory test results and provides a detailed discussion of the subgrade investigation conducted in the study area. This includes all relevant quality tests, such as soil classification, compaction, and strength tests. The chapter also covers the testing and evaluation of Cement-Treated Base (CTB) materials, focusing on their mechanical properties and performance, particularly in relation to subgrade rutting, fatigue resistance, and cumulative fatigue damage, as assessed using PLAXIS 3D and IITPAVE software. Additionally, a cost-comparison analysis is included, evaluating the economic viability of CTB materials compared to traditional construction methods.

The final chapter provides a summary of the key findings of the research, drawing conclusions based on the analysis conducted. It also presents recommendations for practical applications in road construction and suggests areas for further research to expand the understanding of Cement-Treated Base (CTB) materials and their long-term performance in pavement systems.

# 2. Literature Review

## 2.1 Conventional road pavement systems

Traditional road pavement systems have served as the backbone of transportation infrastructure, adhering to a conventional layering approach designed to provide stability, durability, and efficient load distribution. The conventional sequence comprises distinct layers, each contributing to the overall structural integrity of the road. Flexible pavement has been developed for many years, and it is the most common pavement type that can be used for high-volume interstate highways, airport runways, and aprons subjected to heavy aircraft wheel loads (Tian et al., 2021).

Flexible pavements follow a pattern of stress distribution, transferring wheel force from the upper to the bottom layer by grain-to-grain contact. A weak layer, or subgrade, is used at the bottom, and a strong layer at the top. The base of the asphalt layer and the top of the subgrade are where the strains are most obvious. Schematic Layer for traditional road (conventional pavement) systems and figure 2.1 below shows the schematic layer for traditional road (conventional pavement) systems (Singh & Sahoo, 2020).

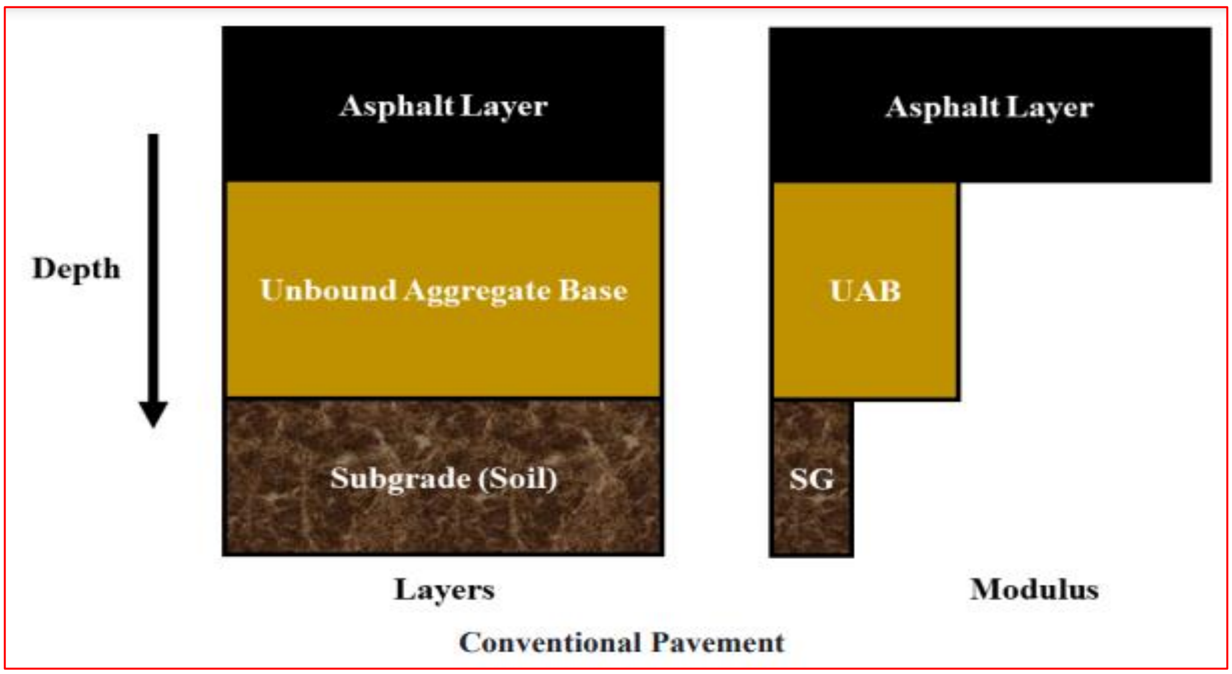


**Figure 2.1 Schematic Layer for traditional road (conventional pavement) systems**

## 2.2 Inverted Road Base Pavement Systems on the Concepts of CTB

The concept of inverted pavement was first introduced in South Africa, and many practical applications have been regarded as competent pavement structures and a cost-effective alternative to conventional pavements since the 1970s (Khan et al., 2022).The improvements of inverted pavement in service performance compared to the conventional pavement make it a practical design for heavy traffic loads in South Africa (Khan et al., 2022).

Inverted pavement systems represent an innovative paradigm in road construction, challenging the conventional layering sequence to optimize structural performance and address contemporary challenges. This approach strategically rearranges the placement of load-bearing materials, offering potential benefits in terms of stability, durability, and sustainability. Figure 2.2 shows the schematic layer configuration of inverted base pavement systems.

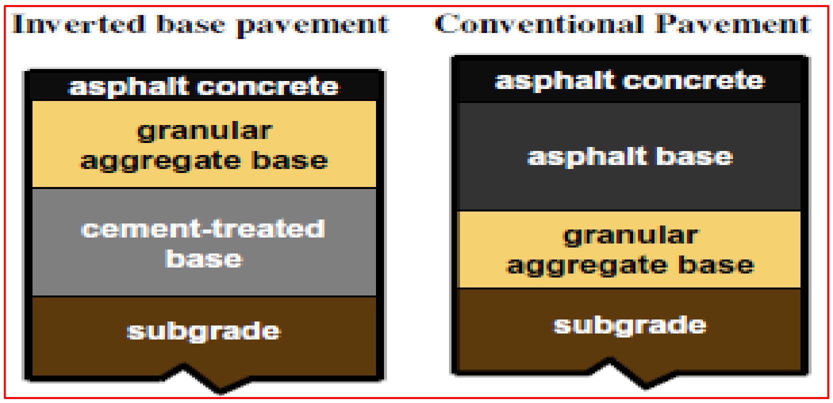


**Figure 2.2 Schematic layer arrangement comparison of an inverted base pavement and a conventional asphalt pavement.**

The stress distribution pattern in flexible pavements transfers wheel force from the uppermost layer to the lowermost layer through grain-to-grain contact. There is a subgrade, or weak layer, at the bottom and a strong layer at the top. The top of the subgrade and the bottom of the asphalt layer are where the strains are most visible. Instead of flexible pavement, there is inverted pavement technology. A pavement system that has a low-strength unbound layer underneath a cement-bound layer is known as "inverted pavement." Because of its high bearing capacity, this unbound layer is covered in an asphalt layer that serves as a fracture relief layer (Jiang et al., 2021).

The critical stress/strain points in an inverted pavement are at the bottom of the cemented layer (tensile strain) and top of the subgrade (compressive strain). An inverted pavement, on the other hand, is made up of a rigid base layer treated with cement, a thin layer of asphalt, and a compacted aggregate layer sandwiched between the two. In a flexible system, the aggregate layer is typically placed on top of the subbase layer, followed by thicker layers of hot mix asphalt (HMA) (Papadopoulos & Santamarina, 2017b).

The distribution of stress in inverted pavement differs from that of ordinary pavement. In a conventional pavement system, the modulus value drops with layer height below the layer's structural capabilities. Inverted pavement has a different modulus value distribution than conventional pavement. The modulus distributions of inverted pavement systems and semi-rigid pavements are comparable. In an inverted pavement, the cement foundation layer has the highest modulus and is the strongest (Jiang, Titi, et al., 2022).

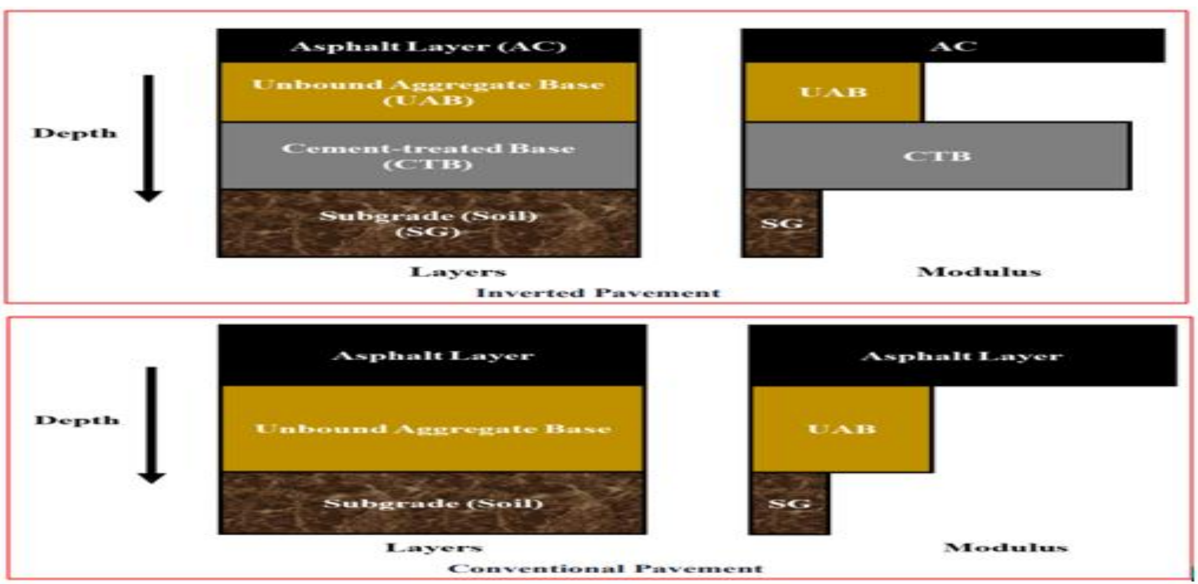


**Figure 2.3 Schematic comparison of an Inverted Base Pavement and a Conventional Asphalt Pavement**

A well-compacted upper thin asphalt concrete (AC) layer and a lower cement-treated base (CTB) layer are sandwiched between two stiffer layers of upper thin asphalt concrete (AC) and lower inverted pavement, which is a sort of flexible pavement. Its structure defies that of a typical pavement. Figure 2.3's schematic diagram compares and contrasts the inverted pavement with traditional pavement constructions to highlight their differences. It is evident from Figure

2.3 that the layer order is the primary design distinction between them. The stiffer layers are often built at the top of the conventional pavement construction. As pavement depth increases, the layer's rigidity diminishes.

According to a recent study by Papadopoulos and Santamarina, using a thin layer of asphalt in an inverted pavement functions more as a membrane (seal coat for lower layers) than a beam (Papadopoulos & Santamarina, 2017b). Because of the stronger base layer, the inverted pavement system protects the subgrade layer more successfully than traditional pavement systems (Cortes et al., 2012). These pavement kinds are also referred to as G1 base pavements, upside-down pavements, sandwich pavements, and stone interlayer pavements (Lewis et al. 2012).

### 2.3 Properties of Individual Layers of Inverted Pavement as Compared to Conventional Pavement

The various components of an inverted pavement consisting of a bituminous layer, aggregate, and cement stabilized layer are discussed in the following sections.

#### 2.3.1 Bituminous Layer

The inverted pavement has a thin coating of bituminous substance. The thin bituminous layer acts as a functioning layer most of the time. This thin bituminous layer provides a great riding quality to an inverted pavement by acting as a membrane instead of a beam (Papadopoulos & Santamarina, 2017a). Studies show that tensile strain increases near the load's edges, or locations where high shear is occurring, but decreases with decreasing thickness at the bottom of the bituminous layer (De Almeida, 2021). Depending on the weather, the bituminous layer thickness cannot be greater than 25–50 mm to take advantage of this behavior.

Inverted pavements have longer fatigue lifetimes due to the thin bituminous layer at the base layer interface creating relatively low tensile strains, in addition to the cost savings associated with a thin layer. Additionally, when a thin bituminous layer is employed, shear stress from braking and accelerating raises the tension in the bituminous layer (Papadopoulos & Santamarina, 2017b). Thus, with thin bituminous layers, top-down hairline cracking is a typical mechanism of failure and is simpler to handle than bottom-up cracking.

### 2.3.2 Aggregate Layer

Because of their thinner HMA surface layers, inverted pavement technologies provide more cost-effective solutions for high-performance pavement structures. Inverted pavements have the following main benefits: Three primary goals for pavement structures were established by Barksdale and Toddres (1983): maximizing the use of the un-stabilized aggregate layer, improving the compaction of the aggregate layer placed over the cement stabilized layers, and eliminating or drastically reducing reflection cracking.

#### 2.3.2.1 Stress Dependency of aggregate layer in an inverted pavement

Conventional pavements employ stiff upper layers to transmit traffic stresses onto less rigid bottom levels. In contrast, an inverted pavement is made up of two high modulus layers: an asphalt layer and a base layer stabilized by cement, which is encased in thin layers of aggregate asphalt. The aggregate layer nearest to the load has horizontal compression(Jiang, Huang, et al., 2022).

Stress softening is the drop in modulus brought on by a rise in octahedral shear stress, whereas stress hardening is the increase in unbound layer modulus brought on by an increase in bulk stress. The aggregate layer stiffens with increasing load (Biswal et al., 2020) and this shows the stress-hardening behavior of the aggregate layer in an inverted pavement.

According to research conducted by (Biswal et al., 2020), A Falling Weight Deflect meter (FWD) was used to measure the stress dependence of the unbound aggregate layer at different load levels. The findings demonstrated that base layer stress-hardening dominates, even though subgrade exhibits both stress-hardening and softening behavior. The aggregate layer exhibits high elastic modulus values up to 689 MPa due to its stress-hardening feature. This high of modulus can diffuse the generated tension

IRC: 37-2018 guideline also specifies the typical modulus value of well-graded crack relief granular layer of 450MPa for the analysis of pavement where Poisson’s ratio may be taken as 0.35 (IRC:37-2018, n.d.).

The listed three types of materials are also called G1, G2, and G4 type of material in South African design research (Khan et al., 2022). The South African practices generally adopt a minimum unbound aggregate base layer of apparent density of 86 percent (solid particle density) equal to 100 to 105% of modified proctor (AASHTO T-180) density level during the construction of aggregate layer.

In South Africa, the slushing process is typically used to compact aggregate foundation, however conventional methods are also utilized in other regions. Using multiple applications of water, the layer is compacted in the slushing procedure until air bubbles develop on the surface. At the end, the surface seems coarser due to the expulsion of particulates. The procedure can be recognized by the absence of air bubbles behind the roller's wheel. Whether or not to apply to slush, there is no discernible difference in the compaction density attained. Higher densities are typically attained by having a hard foundation, such as a cemented layer beneath an aggregate layer (Forest, 2017).

### 2.3.3 Cement Treated Base Layer

The inverted pavement's strongest layer is this one. It can support the highest weight, and unlike traditional pavement, it uses a different load-transfer method. In an inverted pavement, the cemented layer functions as a semi-rigid base layer, and weight transfer is accomplished differently over a larger area than in a standard pavement, where load transfer occurs through grain-to-grain contact. The primary load-bearing layer of the pavement is the cement-stabilized layer. In contrast to conventional pavements, inverted pavements have a higher base layer stress distribution because the cement-stabilized layer's UCS value is greater.

Cemented base layers may consist of aggregates or soils or both stabilized with chemical stabilizers such as cement, lime, lime-fly ash, or other stabilizers which are required to give a minimum strength of 4.5 to 7 MPa in 7/28 days (IRC 37, 2012). While conventional cement should attain the above strength in seven days, lime or lime-fly ash stabilized granular materials and soils should meet the above strength requirement in 28 days since strength gain in such materials is a slow process (IRC, 2010)

Though the initial modulus of the cementitious bases may be in the range of 10000 to 15000 MPa, the long-term modulus of the cemented layer may be taken as fifty percent of the initial modulus due to shrinkage cracks and construction traffic (Theyse et al., 1996) Australian research recommend the use of Equation 2.2 for the cemented layer. Curing cemented bases after construction is very important for achieving the required strength as described in IRC: SP-

89 and curing should start immediately by spraying bitumen emulsion or periodical mist spray of water without flooding or other methods (IRC, 2010).

$$\mathbf{E_{ctb} = 1000 * UCS} \qquad \textbf{[2.1]}$$

Where UCS = 28-day strength of the cementitious granular material

## 2.4 Strength Parameter for Cement Treated Base

According to the fatigue equation, flexural strength is necessary for the fatigue analysis. According to MEPDG, the modulus of rupture for bases that have undergone chemical stabilization can be estimated to be 20% of the unconfined compressive strength after 28 days. These studies advise doing the same. For cementitious bases, the following default modulus of rupture values is advised (MEPDG) (IRC:37-2018, n.d.).

The cemented base layer was clarified further by the description of research findings by several investigators that followed.

The compaction method does not significantly affect the strength and modulus value of the cemented base layer at densities comparable to those attained through the use of a gyratory compactor and the usual proctor test (Zvonarić et al., 2021).

When high carbon calcium-based fly ash (14%) combined with Reclaimed Pavement Material (RPM) is added to the cemented foundation layer, the resilient modulus increases from 257 MPa to 2984 and 4334 MPa at 7 and 28 days, respectively. Also, after seven and twenty-eight days of curing, respectively, the addition of fly ash decreased the plastic strains by nearly five times, from 2.77% to 0.58% and 0.56% (Patel et al., 2019).

Furthermore, Yueqin et al. (2015) investigated the usage of crushed brick in the sub-base and pavement base layers combined with cement. The primary objective of the study was to ascertain whether crushed brick aggregates (CBA) could be applied to asphalt pavement using cement stabilization. The authors examined a wide range of mechanical and empirical properties, such as compressive strength, split strength, compressive resilient modulus, fatigue performance, and shrinkage performance. They investigated the various properties for six different CBA contents: 0%, 20%, 40%, 60%, 80%, and 100%, all at a constant cement of 5%. According to Yueqin et al., the CBA content of the base and sub-base layers should not exceed 46.3% and 74.2%, respectively, in order to satisfy the requirements for Unconfined Compressive Strength (UCS) and Splitting Strength (SPS).

In Oman, studies have been conducted on the stabilization of Reclaimed Asphalt Pavement (RAP) aggregate using cement for the base layer. They altered the RAP/virgin aggregate combinations (100%, 90/10, 80/20, 70/30, and 0/100%) as well as the cement content (0, 3, 5, and 7%).The stabilized layer of RAP aggregate serves as a structural layer and can be used as a base layer, according to tests on compaction and unconfined compressive strength.(Taha et al., 2002).

### 2.4.1 Construction parameters of the cement-treated layer

#### 2.4.1.1 Cement Content

In Brazil, according to Dutra (2017), the determination of the cement content for the cement-treated layer is obtained by the ratio between the mass difference of the mixture, with cement and without cement, by the mass of the mixture without cement, multiplied by 100. The percentage by mass of cement to be incorporated into the aggregates for constituting the mixture must be fixed to meet the USC at 28 days.

In South Africa, the Initial Consumption of Stabilizer (ICS) has been used to calculate the proportion of cement or lime required to meet the requirement of clay minerals in soils and gravels. As per SANRAL (2014), the ICS test involves the preparation of samples with different stabilizer contents, typically 0%, 1%, 2%, 3%, 4%, and 10%, followed by the addition of water to produce a paste. Furthermore, SANRAL (2014) states that additional testing should be conducted to determine the optimal stabilizer type and content to obtain the necessary strength if stabilization looks to be successful, practicable, and economical that is, if the ICS is not too high that is, if it is not more than around 3.5%.

#### 2.4.1.2 Strength

The Brazilian specifications of cement-treated layers (Dutra, 2017) do not fix the strengths for the cement-treated layer In South Africa, UCS is given at two densities (97 % and 100 % modified AASHTO density). According to SANRAL (2014) the test methods are different and the strength classes of cements are now based on the strength after 28 days and not 7 days as recommended in Technical Recommendations for Highways (TRH4, 1996).

ITS and UCS testing are carried out during construction for quality control purposes. The minimum and maximum strengths for the cement-treated layer in Brazil are recommended by DER/SP (2006a) (Table 2.1).

**Table 2.1: Strength parameter suggest in Brazil and in South Africa** (De Almeida, 2021)

| Organization | Country | N° of days | UCS (MPa) | ITS (MPa) |
|---|---|---|---|---|
| DER/SP(2006a) | Brazil | 28 | Min 4 - Max 6.2 | Min 0.7 - Max 1 |
| SANRAL (2014) | South Africa | 28<br>100%MDD | C1- Min 6 - Max 12<br>C2- Min 3 - Max 6<br>C3- Min 1.5 - Max 3<br>C4- Min 0.75 - Max 1.5 | C1- Not mentioned<br>C2- Not mentioned<br>C3- Min 0.25<br>C4- Min 0.20 |
| | | 28<br>97%MDD | C1- Min 4 - Max 6<br>C2- Min 2 - Max 4<br>C3- Min 1 - Max 2<br>C4- Min 0.5 - Max 1 | Not applicable |

#### 2.4.1.3 Cement treated layer thickness

The knowledge about the minimum and maximum thicknesses of the cement-treated layer is very important to ensure compatibility and to counter segregation during paving. Table 2.2 shows the minimum and maximum thicknesses layer adopted by Brazil, South Africa and United States.

**Table 2.2: Minimum and maximum thicknesses layer adopted by Brazil, The United States and South Africa**

| Author/Organization | Country | Minimum and maximum thicknesses |
|---|---|---|
| DNIT (2017) | Brazil | 120 mm – 180 mm |
| DER/SP (2005c) | Brazil | 120 mm – 180 mm |
| TRH4 (1996) | South Africa | 125 mm – 300 mm |
| Caltrans (2010) | United States | 76.2 mm - 152.4 mm |

In South Africa, according to design catalogue provided in TRH4 (1996), the minimum and the maximum of the cement-treated layer varied between 125 mm and 300 mm. However, nowadays, in practice, the minimum and maximum thicknesses vary between 125 mm and 200 mm (De Almeida, 2021).

#### 2.4.1.4 Compaction Techniques

In Brazil, for many years the compaction energy that has been adopted as a reference for the execution of the cement-treated layer is the Intermediate Proctor, according recommend in Dutra, (2017). In the last years, the DNIT started to update its specifications, and then in DNIT (2017), the Modified Proctor must be adopted in determining the bulk density, maximum dry density, and optimum moisture content. Shall note that the specification of the cement-treated layer (Dutra, 2017) is currently in the process of approval by the responsible organs. Table 2-25 shows the compaction criterion currently applied in Brazil.

In South Africa, according to TRH13 (1986), the typical design strength given for the four classes of cemented materials (C1, C2, C3, and C4) is given at two densities (97 % and 100 % modified AASHTO density). The strength at 100 % modified AASHTO density is given since it is easy to compact samples to 100 % density, and the strength at 97 %, which can be determined from a strength/density relationship, is equivalent to the strength at the field density usually specified for a stabilized based. Table 2.3 shows the compaction criterion currently applied in South Africa.

**Table 2-3: Compaction criterion in Brazil and in South Africa**

| Organization | Country | Compaction Criterion |
|---|---|---|
| DNIT (2017) | Brazil | ⇒Degree of compaction Min = 100%;<br>⇒Modified Proctor density. |
| DER (2005c) | | ⇒Degree of compaction Min = 100%;<br>⇒Intermediate Proctor density. |
| SANRAL (2014) | South Africa | ⇒Degree of compaction Min = 97%;<br>⇒Modified AASHTO density |

In South Africa, in general, the maximum cement-treated layer to be constructed and compacted in single layers is 200 mm, but it depends on the ability of the roller to compact the layer. Moreover, there is no guarantee that the construction of two 100 mm layers would have good bond between the layers. In case of a cement-treated layer being greater than 200 mm, the construction is done in two layers. According to Visser, (2017) the cement-treated layer is constructed in two layers, as it is difficult to compact 250 mm of material without breaking down the particles.

#### 2.4.1.5 Moisture Content

According to Brita et al (2015), the water and cement ratio is a conditioning factor for the strength gain of the cement-treated layer. However, the Brazilian specifications do not mention this peculiarity of the mixture (Brita et al., 2015). Furthermore, according to the author, if it is not possible to carry out a complete dosage study of the mixture, the mixture can be prepared with a moisture content of 1.0 % below that of the reference (optimum moisture content), fixing the cement content between 3.0 % and 4.0 % by weight.

Brita et al., (2015) Concluded that the reduction of the moisture content to around 1 % below the optimum moisture content tends to increase the strength and stiffness of the cement-treated layer, while the increase in moisture content reduces these mechanical parameters. The recommendations made by the main organizations in Brazil (DNIT, 2017 and DER/SP, 2005c) and in South Africa (SANRAL, 2014) are presented in Table 2.4.

**Table 2-4: Moisture content requirements in Brazil and in South Africa**

| Organization | Country | Moisture content requirements |
|---|---|---|
| DNIT (2017) | Brazil | The moisture content of the cement-treated layer, immediately before compaction, must be within the range of -2.0% to +1.0%, in relation to the optimum moisture content obtained from compaction in the laboratory. |
| DER/SP (2005c) | Brazil | |
| SANRAL (2014) | South Africa | Stabilised materials should be compacted at a moisture content below 80% of saturation, to reduce cracking in the stabilized layers. |

### 2.4.1.6 Processing Time

In Brazil, (DER/SP, 2005c) and DNIT (2017) recommend that the time of mixing and compaction should not be longer than the beginning of the cement setting In South Africa, according to TRH13 (1985) mixing and compaction should be efficient to minimize the decrease in density and strength due the early reactions between stabilizer, water and soil. In case of utilization of Portland cement, the maximum time is 6 hours for completion of compaction and finishing after the stabilizing agent comes into contact with soil.

### 2.4.1.7 Curing

In South Africa, according to TRH13 (1986), after the treated layer is completed it should be protected against drying for 7 days and traffic should be not allowed on the layer during this period. TRH13 also recommends that one of the following curing methods should be used: Frequent light water spraying to ensure that the layer and even the surface remain continuously damp; a full, heavy water bowser may damage the layer and light or half-full bowsers or side spraying should be used. A layer of sand about 40 mm thick were improve the moisture retention. The surface of the layer must not be subjected to wetting and drying cycles since this has a detrimental effect on the treated layer; watering and covering with plastic sheeting; application of a curing membrane consisting of spray-grade emulsion, and covering the treated material while it is still damp with material that may be required for the new layer; this must be carried out in such a way that the treated layer is not damaged.

### 2.4 Design procedures for inverted pavement

Designing a pavement is a complex task. Many fatigue models check whether the pavement is suitable to accommodate the traffic predicted. However, it is not enough to just have access to several models and the latest generation software, it is necessary to have knowledge of what is being done, to know the advantages and limitations of each model.

According to the literature review, it was noticed that the concept of pavement design is very similar between countries with a few changes on the materials and local conditions. During design, all layers need to be carefully evaluated, as the failure of one layer compromises the integrity of the others. The main parameters evaluated in a traditional pavement design method are:

- ✓ Vertical compressive strains at the surface of the subgrade (εv)
- ✓ Horizontal tensile strains in the bottom of the cement-treated layer (ε), and
- ✓ Horizontal tensile strains in the bottom of the asphalt concrete layer (εt).

#### 2.4.1 Subgrade Soil

The aim of the design process is to protect, use, and improve the bearing capacity of the in-situ subgrade material so that the pavement is able to fulfill the service objective over the analysis period (TRH4, 1996).

The bearing capacity and quality of the subgrade roadbed fill is of prime importance in the selection of the appropriate pavement type and hence the overall life cycle strategy (TRH4, 1996). According to Cortes (2010) subgrade properties is a key input property in mechanistic empirical pavement design procedures. The support provided by the subgrade is generally regarded as one of the most important factors in determining pavement design thickness, composition and performance (Austroads, 2017).

Before applying the fatigue models, it is important to be aware of the subgrade's bearing capacity and whether external agents such as in-situ moisture can compromise the stability of the analyzed material. For example, according to Frost (2017) in-situ moisture, density, and porosity are some of the critical soil properties that affect the resilience of a modulus and the quality of the subgrade material (Forest, 2017).

Metcalf et al. (1999) indicated the inverted section is particularly attractive for use over a weak subgrade (Metcalf et al., 1999). However, there are many discussions about this subject around the world. According to Papadopoulos and Santamarina (2017), weak subgrades should be mechanically or chemically stabilized to prevent excessive bending in the cement-treated base.

Subgrade failure is decreased because cement-stabilized bases spread traffic loads over wide areas and can span weak subgrade locations (Adaska & Luhr, 2016). Cortes (2010), for example, estimated the mean resilient modulus to be 250 MPa with a standard deviation of 100 MPa, based on an extensive field and laboratory study conducted at test sections in the inverted pavement (Cortes, 2010).

According to Frost (2017), in 2016 the Georgia Tech team conducted a study in the same test sections covered in Cortes (2010). In this study, it was observed that the station with resilient modulus of the subgrade less than 100 MPa (classified as weak subgrade) presented high load cracking. The station with a resilient modulus of subgrade higher than 250 MPa (classified as strong subgrade) showed relatively better performance (Forest, 2017).

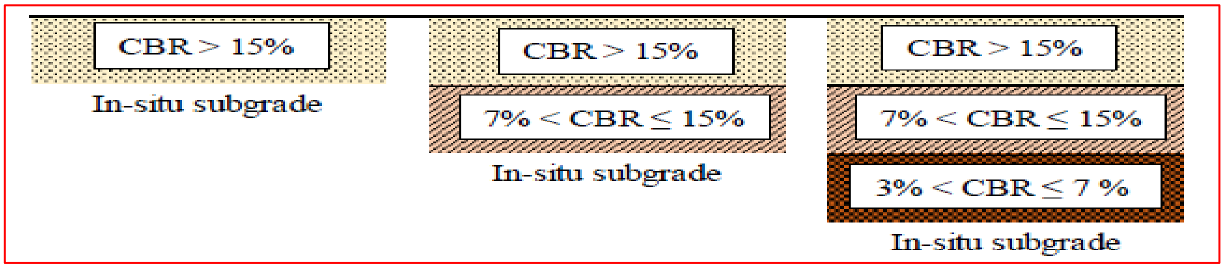


**Figure 2.3 Importing layers to obtain minimum subgrade strength (Adapted from SANRAL, 2014)**

According to De Almeida et al. (2019a) through sensitivity analyses and mechanistic simulations, concluded that the subgrade is considered weak if the resilient modulus is less than

50 MPa (De Almeida, 2021). According to Asutroads (2017), subgrades with CBR less than about 5 % may require treatment to avoid delays in construction and assist in the compaction of subsequent layers. For Ferri (2013) subgrade with resilient modulus below 40 MPa means a high risk of losses in the medium and long term (Ferri, 2013).

According to the bibliographic research developed, it was possible to select a series of prediction models (Table 2-4) for specific deformations at the top of the subgrade. Note that the fatigue models are expressed by Equation 2.1.

$$N = a \left(\frac{1}{\varepsilon v}\right) b \qquad [2.2]$$

Where:

N: Standard axles to set level of permanent deformation

εv: Vertical compressive strain at the top of a layer

a and b: Experimental regression coefficients (see Table 2-4)

### 2.4.2 Cement-Treated Base Materials

Cement-treated base (CTB) materials play a pivotal role in modern road construction, offering enhanced strength, stability, and durability. Comprising aggregates and cement, CTB materials are strategically used in various layers of road pavements, contributing to improved load-bearing capacity and overall structural resilience. A key component of inverted pavement systems is the strategic use of cement-treated base materials. These materials, composed of aggregates and cement, contribute to improved strength, stability, and load-bearing capacity.

Balbo (1993), when starting his research, believed that the failure of the cement-treated layer in Brazil was due to the lack of a design procedure in Brazil, and pioneered a fatigue model for cement-treated layers in Brazil (Equation 2.3). However, during his research, the author realized that the lack of knowledge about the mechanical behavior of the cement-treated layer aggravates the uncertainties and consequently causes failures in new projects.

According to Austroads (2017) the principal factors affecting the fatigue life of cemented materials include particle size distribution, particle shape, density, moisture content, mixing efficiency, and cracking pattern. Some of these factors are in turn dependent on binder type and content, etc. Therefore, due to the complexity of the variables involved in the success of the cement-treated layer and how its mechanical properties are influenced in different ways, Section 2.3 addresses the effects of varying the type and cement content, grain size, and type of aggregate, as well as the effects of variations in moisture content, curing time and compaction. In Section 2.4, the strength parameters of the cement-treated layer are addressed.

$$\text{Log10N}=17.137-19.608\text{SR} \quad [2.3]$$

Where:

N: Standard axles to set the fatigue life

SR: The relationship between the applied tensile strain (ε) and the tensile strain-at-break (εv) of the material

The Tensile Strain Relationship (SR) is another topic widely discussed among designers and scientists. For some researchers, the adoption of limiting strain criteria is essential for the success of the pavement structure. According to Balbo (2006), the relationship between tensile strain applied and tensile strain-at-break should be maintained at around 50 %. For modulus greater than 10000 MPa, Murphy et al. (1980) recommend limiting strain to 65 % of the strain-at-break.

The fatigue model proposed by Balbo (1993) is widely used in Brazil for both inverted and semi-rigid pavement. However, the main current instructions and guides in Brazil are no up to date and therefore recommend the fatigue model (Equation 2.4) developed by De Beer and other researchers from South Africa in 1989 (DER/SP, 2006a and DNIT, 2006a).

$$N=10^{7.19(1-SR/8)} \quad [2.4]$$

Where:

N: Standard axles to set the fatigue life

SR: Relationship between the applied tensile strain (ε) and the tensile strain-at-break (εv) of the material

In South Africa, cement-treated layers are analyzed as bound layers for two fatigue models, effective fatigue and crushing. The critical parameters for cemented material are given by:

- Maximum tensile strain (ε) at the bottom of the layer controlling the "effective fatigue life"; and
- Vertical compressive stress (εv) on top of the cemented layer controlling crushing life.

According to SANRAL (2014) the term "effective fatigue" is used to suggest typical fatigue cracking. Once a cemented material has reached the end of its effective fatigue life, it enters into a new phase wherein it behaves as an equivalent granular layer. The effective fatigue model for cemented materials is shown in Equation 2.5.

$$N = SF*10^{c(1-\varepsilon/d\varepsilon b)} \quad [2.5]$$

Where:

N: Effective fatigue life

ε: Horizontal tensile strain at bottom of layer (microstrain)

εb: Strain at break (microstrain)

c, d: Constants

SF: Shift Factor for crack propagation

Crushing life is analyzed in two conditions, namely crush initiation with roughly 2 mm deformation on top of the layer and advanced crushing with 10 mm deformation and extensive breakdown of the cemented material (Theyse et al., 1996). According to SANRAL (2014), crushing is not considered a terminal condition and hence it is not used in the critical layer calculation. However, it is an important check, as any crushing has a significant impact on the surfacing. The damage model for crush initiation and advanced crushing is given in Equation 2.6.

$$N=10^{a(1-\sigma v/bUSC)} \quad [2.6]$$

Where:

N: Standard axles to crack initiation or advanced crushing

εv: Vertical compressive stress at top of layer

USC: Unconfined compressive strength (KPa)

a, b: Constants

In Australia, according to the Guide to Pavement Technology Part 2 (Austroads, 2017), the fatigue model depends on the flexural strength and modulus (Equation 2.7).

$$Nf = \left(\frac{K}{\mu\varepsilon}\right)^{12} \quad [2.7]$$

Where:

$N$: Allowable number of repetitions of the load-induced tensile strain

$\mu\varepsilon$: Load-induced tensile strain at the base of the cemented material (microstrain)

K: Presumptive constant

### 2.4.3 Unbound Base Layer

The unbound aggregate base is the central component of the inverted pavement structure (TRH4, 1996 and Cortes and Santamarina, 2012). The knowledge about the mechanical properties of granular bases are key design inputs in both empirical pavement design methods as well as in mechanistic research.

The modulus of unbound granular materials must be appropriate for the range of stresses under which they are likely to operate. The modulus and small-strain stiffness of granular materials depend on stress history, state of stress, density, gradation, and moisture content (Uzan, 1985 and Austroads, 2017).

In Brazil, DER/SP (2006a) recommends an interval of moduli for the unbound base layer. However, the institution does not discriminate where it is placed or make any relation between the grading and elastic modulus. In Table 2-6 the moduli and Poisson's Ratio recommended by DER/SP (2006a) are shown, as well as the moduli and Poisson's Ratio adopted for the unbound base layer in inverted pavements in some publications.

**Table 2-6: Modulus and Poisson's Ratio for the unbound base layer in an inverted pavement in Brazil**

| Author/Organization | Modulus (MPa) | Poisson's Ratio |
|---|---|---|
| DER/SP (2006a) | 150 to 300 | 0.35 |
| Suzuki (1992) | 450 | 0.40 |
| Macêdo (1996) | 200 | - |
| Bernucci (2013) mentioned in Salvador and Motta (2015) | 300 | 0.35 |
| Alberto (2018) | 300 | 0.40 |

According to SANRAL (2014), in South Africa, unbound granular layers are assumed to accumulate permanent deformation, from shear deformation, within the layer. The resilient properties for unbound granular base are given in Table 2-6. The suggested ranges are shown, along with the values in brackets used in the development the catalogues in TRH4 (1996).

**Table 2-7: Modulus and Poisson's Ratio for the unbound base layer in an inverted pavement in South Africa (Adapted from SANRAL, 2014)**

| Material Code | Material Description | Modulus Over Cemented | Poisson's Ratio |
|---|---|---|---|
| G1 | High quality crushed stone | 250 to 1 000 (450) | 0.35 |
| G2 | Crushed stone | 200 to 800 (400) | 0.35 |
| G3 | Crushed stone | 200 to 800 (350) | 0.35 |
| G4 | Natural gravel (base quality) | 100 to 600 (300) | 0.35 |
| G5 | Natural gravel | 50 to 400 (250) | 0.35 |
| G6 | Natural gravel (subbase quality) | 50 to 200 (225) | 0.35 |

In Australia, Austroads (2017) suggests a guide when assigning maximum values to base quality crushed rock materials under asphalt surfacing when other, more reliable information is unavailable (Table 2-7).

**Table 2-8: Suggested vertical modulus of top sublayer of normal standard base material (Austroads, 2017)**

| Thickness of overlying bound material | Modulus of overlying bound material (MPa) | | | | |
|---|---|---|---|---|---|
| | 1 000 | 2 000 | 3 000 | 4 000 | 5 000 |
| 40 mm | 350 | 350 | 350 | 350 | 350 |
| 75 mm | 350 | 350 | 340 | 320 | 310 |
| 100 mm | 350 | 310 | 290 | 270 | 250 |
| 125 mm | 320 | 270 | 240 | 220 | 200 |
| 150 mm | 280 | 230 | 190 | 160 | 150 |
| 175 mm | 250 | 190 | 150 | 150 | 150 |
| 200 mm | 220 | 150 | 150 | 150 | 150 |
| 225 mm | 180 | 150 | 150 | 150 | 150 |
| ≥ 250 mm | 150 | 150 | 150 | 150 | 150 |

Lekarp et al. (2000) reinforce the importance of the particle size and shape, maximum grain size, load duration, and load frequency in the resilient response of the granular base. In

Brazil, the main standard organizations recommend normally four different types of grading of crushed stone classified from A to D (DERSA, 1997; DER/SP, 2005b; DNIT, 2009). DNIT (2006a) recommends the use of a grading crushed stone as a base layer between A to C, when the cumulative traffic is greater than 5 million ESALs. However, many designers have used and recommended the unbound base layer as a base in inverted pavement classified as B material. The B material recommended by each organization is quite similar, especially the maximum percentage passing in each sieve.

### 2.4.4 Asphalt Concrete

According to Cortes (2010), the asphalt layer's characterization is focused on determining elastic parameters, namely the elastic modulus and the Poisson's Ratio. For the design of new pavements, the (DER/SP, 2006a) recommends a range of different moduli for the asphalt layer. The variation of moduli is given in function the type of materials that includes the grading and the penetration grade bitumen. In Table 2-10 the moduli recommended by the (DER/SP, 2006a) and the moduli adopted for the asphalt layer in an inverted pavement in some publications are shown.

**Table 2-9: Modulus and Poisson's Ratio for the asphalt layer in Brazil**

| Author/Organization | Elastic Modulus (MPa) | Poisson's Ratio |
|---|---|---|
| DER/SP (2006a) | 2 000 to 4 000 | 0.30 |
| Suzuki (1992) | 8 000 | 0.30 |
| Macêdo (1996) | 3 500 | - |
| Bernucci (2013) mentioned in Salvador and Motta (2015) | 5 617 to 5 163 | 0.35 |
| Alberto (2018) | 3 500 | 0.35 |

According to SANRAL (2014), in South Africa, they generally use asphalt layers that are less than 50 mm thick, and failure of the asphalt layer is not necessarily a terminal condition for the pavement. For Cortes (2010) the use of thin asphalt concrete layers can lead to the development of new failure mechanisms, such as shear fatigue along the periphery of the loaded area. Where the asphalt thickness is less than 150 mm, the granular base layer(s) provides a substantial proportion of the load carrying capacity and both deformation and fatigue distress mechanisms are possible. Therefore, the asphalt and granular base materials must be of appropriate quality to ensure the intended service life results (Austroads, 2017).

The moduli frequently adopted in new designs in South Africa for thin continuously and gap-graded asphalt surfacing layers are shown in Table 2-9. The influences of the thickness and modulus of the asphalt layer on the inverted pavement behavior are discussed in Section 2.6.

**Table 2-10: Elastic moduli and Poisson's Ratio for asphalt materials used in SAMDM, 1996 (Adapted from SANRAL, 2014)**

| Asphalt Materials | Depth (d) Below surface (mm) | Modulus (MPa) | Poisson's Ratio |
|---|---|---|---|
| Gap graded asphalt surfacing | ≤ 50 | 3 000 | 0.44 |
| Continuously graded hot mix asphalt | ≤ 100 | 4 000 | 0.44 |
| | 100 < d ≤ 150 | 5 000 | 0.44 |
| | 150 < d ≤ 200 | 6 000 | 0.44 |
| | 200 < d ≤ 250 | 7 000 | 0.44 |

In Brazil, when designing new pavements, minimum asphalt layer thicknesses are recommended. The minimum thickness variation is given according to the traffic accumulated during the project period. Table 2-10 shows the minimum thicknesses of asphalt coating recommended according to the experience of the DER/SP (2006a) and DNIT (2006a).

**Table 2-11: Minimum asphalt layer thicknesses adopted in Brazil (Adapted from DER/SP, 2006a and DNIT, 2006a)**

| Cumulative equivalent traffic - ESALs | Asphalt surfacing Minimum thickness (mm) (DER/SP, 2006a) | Asphalt surfacing Minimum thickness (mm) (DNIT, 2006a) |
|---|---|---|
| ≤ 1 million | Asphalt surfacing | Asphalt surfacing |
| 1 million – 5 million | 50 mm | 50 mm |
| 5 million – 10 million | 75 mm | 75 mm |
| 10 million – 25 million | 100 mm | 100 mm |
| 25 million – 50 million | 125 mm | 125 mm |
| >50 million | 150 mm | 125 mm |

After knowing the minimum thickness required for the asphalt layer, fatigue analysis begins. In Brazil, the fatigue analysis of the asphalt layer may be done through different models.

DER/SP (2006a) recommends that the asphalt layer be analyzed using Equation 2.8, whose coefficients may be changed according to the fatigue models presented in Table 2-13.

$$N = \left(\frac{K}{\varepsilon t}\right)^{n} \quad [2.8]$$

Where:

N: Standard axles to set level of fatigue life

εt: Horizontal tensile strain at bottom of asphalt layer

K and n: Experimental regression coefficients

**Table 2-12: Fatigue models for asphalt concrete layer adopted in Brazil (Adapted from DER/SP, 2006a)**

| Author/Organization | Year | Coefficients | |
|---|---|---|---|
| | | a | b |
| FHWA | 1976 | 1.092E-06 | 3.512 |
| Asphalt Institute | 1976 | 2.961E-05 | 3.291 |
| Barker, Brabston & Chou | 1977 | 9.700E-10 | 4.030 |
| Pinto & Preussler – CAP 50-70 | 1980 | 2.850E-07 | 3.690 |

Many designers in Brazil prefer to use either fatigue model proposed by FHWA and the Asphalt Institute. The Asphalt Institute fatigue model presented by (DER/SP, 2006a) is an adjusted version, considering 13.5 % effective binder volume, 4 % air void content, and modulus of 3 000 MPa.

In South Africa, according to SANRAL (2014), the asphalt surfacing layers are only analyzed for fatigue. The fatigue model (Equation 2.9) is applicable for thin (< 50 mm) surfacing layers and thick (> 75 mm) asphalt bases.

$$Nf = 10^{\alpha(1-\log(\frac{\varepsilon t}{\beta})} \quad [2.9]$$

Where:

Nf: Fatigue life

α and β: Constants

εt: Horizontal tensile strain at bottom of asphalt layer

## 2.5. Pavement Design Background

Pavement design is the process of developing the most economical combination of pavement layers (in relation to both thickness and materials type) to suit the soil foundation and the traffic to be carried during design life. From the SANRAL (2013b) point of view, pavement design is to ensure that materials within the pavement layers are not overstressed at any time during these changes in the pavement's life. Over the years, in the pursuit of accurate simulation of pavement structure behavior under loading, various design methods have been developed. These design methods, on individual capacity, have been used to simulate pavement behavior based on some assumptions

At the outset, pavement designs were based on empirical methods that are back-dated to the development of the Public Roads soil classification system in the 1920s (Huang, 2004). Empirical methods are derived from experience in terms of field observation performance of in-service pavement or laboratory test sections. The purpose of laboratory methods is to subject a representative pavement material sample to an environment (consisting of simulated traffic loading and environmental conditioning) that closely simulates field conditions (Adu-Osei, 2000). These methods also define the interaction between pavement performance, traffic loads, and pavement thickness for a given set of paving materials, soil, location, and environmental conditions (Schwartz, 2007). Although the design of flexible pavements is still largely empirically based, these methods remain accurate only for the exact conditions for which they were developed, and perhaps invalid outside the range of variables used in its development.

This brought about various examples of empirical design methods developed with different location such as the American Association of State Highway and Transportation Officials (AASHTO) in the USA (1993), Road Note in the UK (Road Research Laboratory, 1970), Western Association of States Highway Officials (WASHO) in Malad and West Africa Compaction (WAC) in West Africa Countries (Fall, Ba, S., Sarr, Ba, M. and Ndiaye, 2011), to mention but a few.

Even though empirical methods tend to be simple and easy to use, these methods are associated with various limitations such as one climate condition, limited traffic, material type, and new construction only (i.e. cannot be used for rehabilitation). If these conditions change, the design is no longer valid.

Before the final introduction of the mechanistic-empirical design guide (MEDG) in the 21st century, other design methods aside, empirical methods were developed between 1940 and the 1960s which are: the limiting shear failure method, limiting deflection method, and regression method, all based on pavement performance and/or road test. However, these methods have various limitations and likewise do not satisfy all necessary requirements for an ideal design which makes them obsolete (Huang, 2004). Ultimately, pavement design methods differ from one to another yet, they are affected by the same factors which are: traffic and loading, structural models, materials, environment, and failure criteria. Nevertheless, a better approach to the design of flexible pavements is the mechanistic-empirical method.

## 2.5 Research gaps

Despite the potential advantages, there is a notable gap in the comprehensive understanding of the investigation of subgrade and performance analysis of cement-treated base materials within the context of inverted pavement systems such as: By addressing these research gaps, the present study aims to contribute a comprehensive understanding of the geotechnical aspects associated with inverted pavement systems using cement-treated base materials. The investigation strives to provide practical insights for optimizing design, construction, and performance in the realm of innovative road infrastructure. Table 2.14 below shows the research gap of the current study on the investigation of subgrade soil and performance characteristics of cement-treated base materials for road pavement enhancement.

**Table 2.13 Research gap**

| Researcher name | Title | Limitation/research gap |
|---|---|---|
| S. Loganayagan, Year- 2022 | Experimental Study on Practice of Cement Treated Subbase (CTSB) Layer in Flexible Pavement of National Highways in India | - Lack of generalizability to other types of pavement construction methods<br>- No comparison with alternative methods for sub-base construction<br>- Absence of long-term performance data for the cement-treated sub-base<br>- Limited discussion on the economic feasibility of implementing cement-treated sub-base in different regions |
| P. A. B. Rahane<br>Year-2022 | A Comparative Study of Cement-Treated Sub-Base and Granular Sub-Base | - Sample size not mentioned, Generalizability to other materials not discussed, Potential bias in the focus of the study, and Lack of suggestions for further research |
| E. Papadopoulos, J. Santamarina, Year-2019 | Inverted flexible pavement response and performance | The study suggests the need for additional large-scale field tests to assess the performance of inverted base pavement designs in various conditions relevant to the USA. |
| Y. Patil, Rahul Rayate, Year-2018 | Cement Treated Sub-Base For Bituminous Pavement | - Lack of pavement design guidelines for cement treated sub base<br>- Limited focus on rural and urban roads with light and medium traffic<br>- Potential lack of generalizability to roads with heavy traffic or different conditions |
| P. A. B. Rahane<br>Year- 2022 | A Comparative Study of Cement-Treated Sub-Base and Granular Sub-Base | - Sample size not mentioned, Generalizability to other materials not discussed, Potential bias in the focus of the study, and Lack of suggestions for further research |

# 3.0 Research Methodology

## 3.1 Description of the study area

Addis Ababa is located in the western margin of the Main Ethiopian Rift Valley. The study area (Figure 3.1), located at Addis Ababa Bole sub-city Megenagna-Imperial Junction-Bole Airport, is positioned at Easting = 477934.74, Northing = 994976.04, and an elevation of 2329.93 meters. This area serves as the starting point for the main road project, which originates near Megenagna and extends all the way to Bole Imperial Junction. Additionally, it encompasses another route originating from Gerji and concluding at the twenty-four area. These routes are integral to the transportation network and contribute significantly to the city's infrastructure and connectivity.

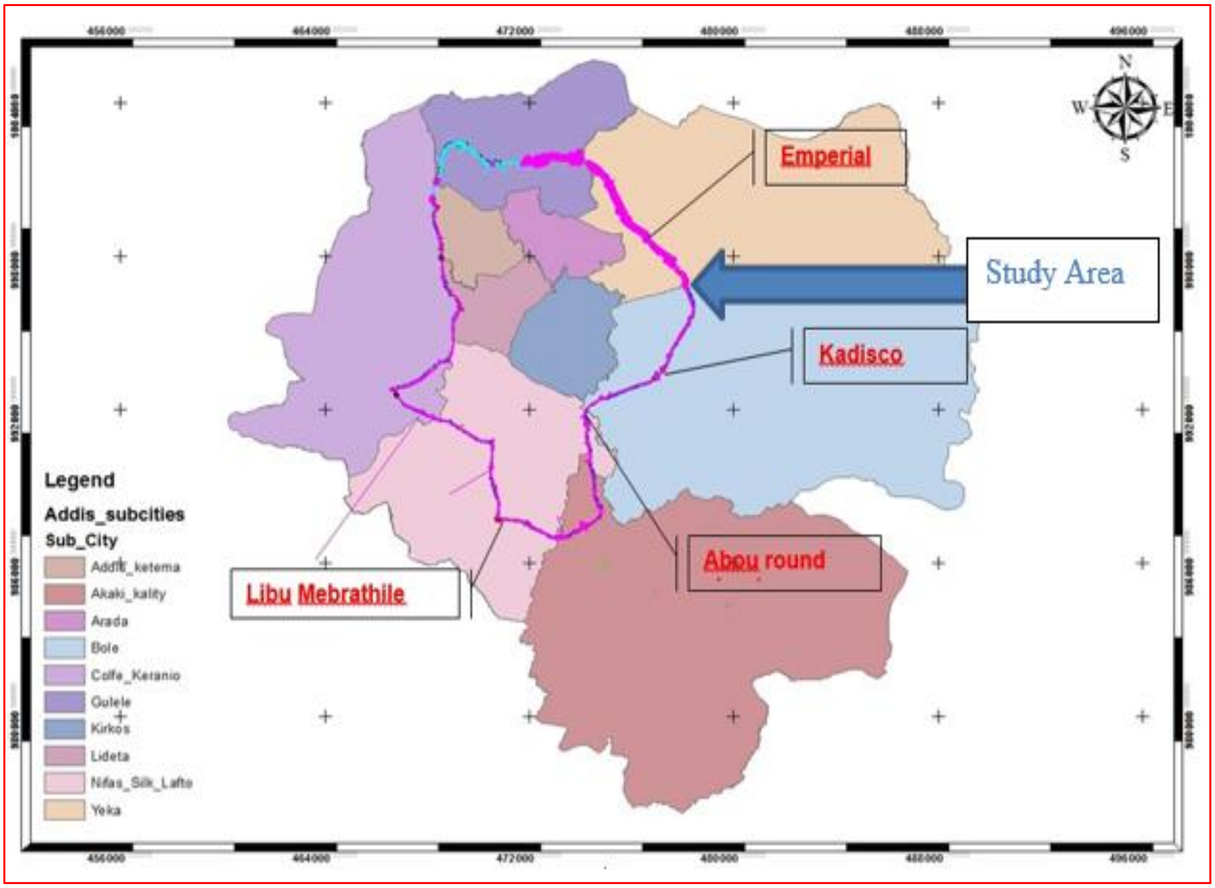


Figure 3.1 Location Map of the Study Area

## 3.2 Climate, Geology and Topography

### 3.2.1 Climate

Addis Ababa possesses a complex mix of highland climate zones, with temperature differences of up to 10 °C, depending on elevation and prevailing wind patterns. The high elevation leads to moderate temperatures year-round, and the city's position near the equator means that temperatures are very constant from month to month.

As part of the Ethiopian climate and based on the above classification; the city of Addis Ababa in general particularly falls within "Dega" and "Weina Dega" climatic zones, with altitudinal variation of from 2300 to 2500 meters a.s.l.

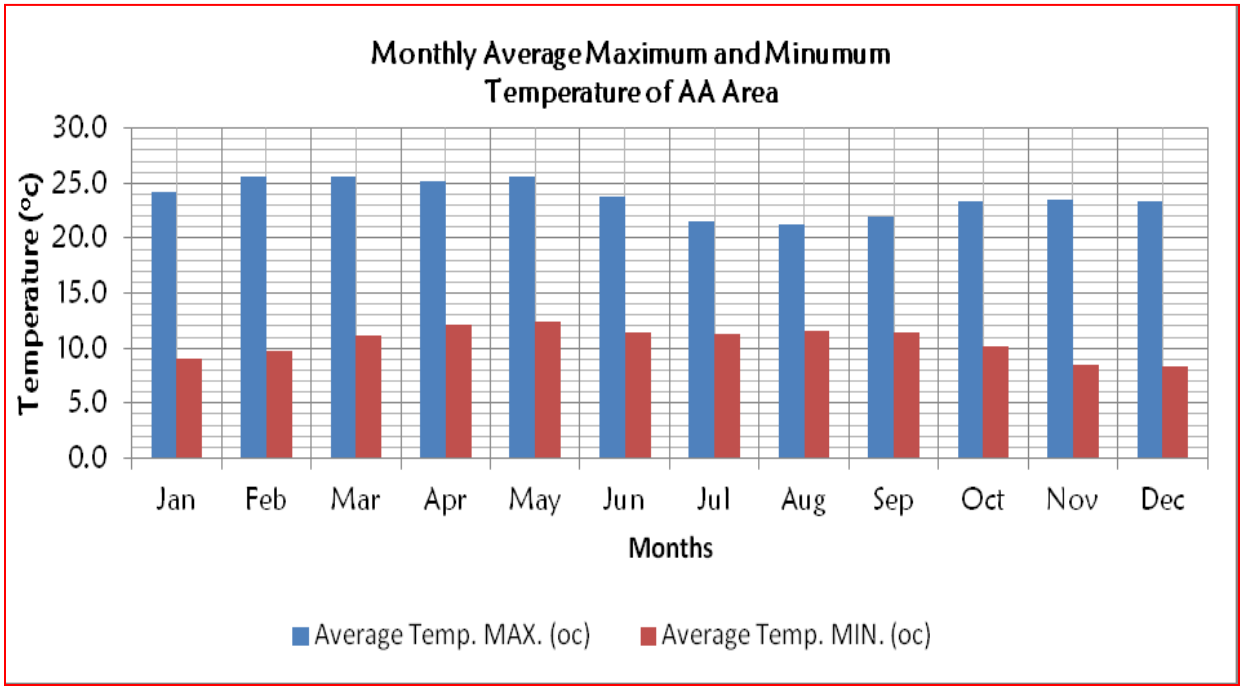


**Figure 3.2 Monthly Maximum and Minimum Temperature of Addis Ababa Area**

*Source: National Metrological Agency of Ethiopia; Addis Ababa City Observatory Station*

*(1981 – 2011 E.C)*

### 3.2.2 Temperature

Based on the rainfall data retrieved from Addis Ababa Observatory Station, the mean annual rainfall of Addis Ababa city varies between 600mm - 1600mm. Rainfall data that has been obtained is referred to estimate the amount of rainfall of the city in general and that of the project areas in particular.

The mean monthly rainfall varies in the range of 8.0mm – 288.6mm with major rainfall records in the months of June, July, August, and September and insignificant records from November to January.

According to the rainfall record, the mean annual rainfall measured is about 1158.1mm in which the areas receive about 74.2% of this rainfall from June to September. The following charts and tables show values and trends of measurements.

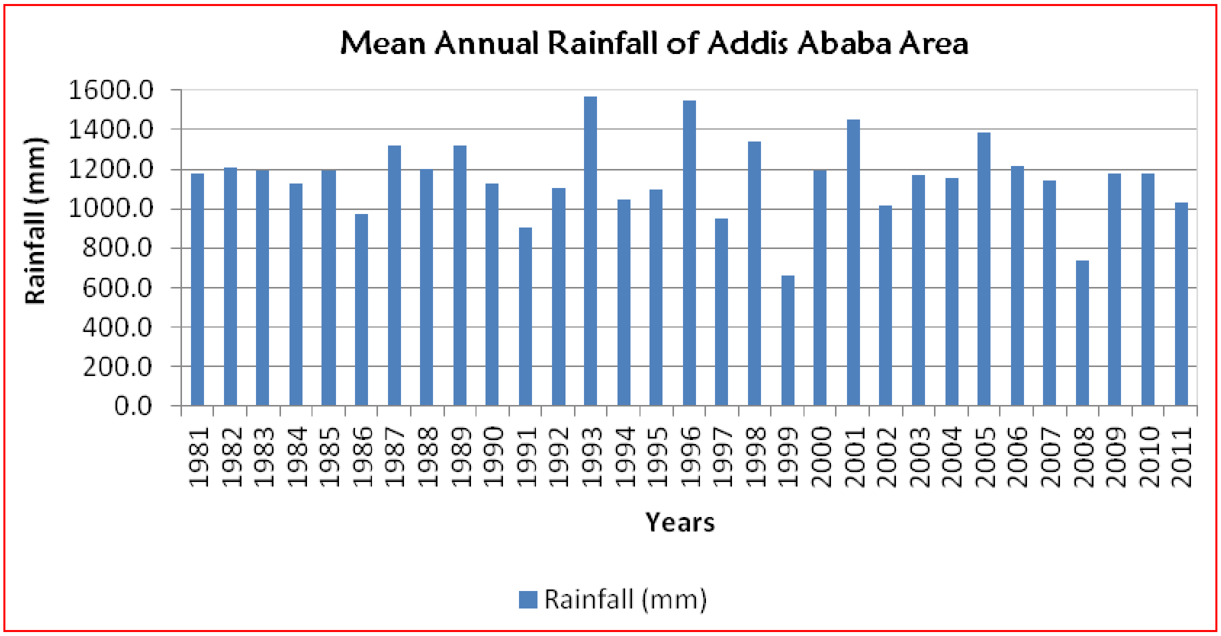


**Figure 3.3 Mean Annual Rainfall of Addis Ababa Area**

*Source: National Metrological Agency of Ethiopia; Addis Ababa City Observatory Station*

*(1981 E.C – 2011 E.C)*

### 3.2.3 Geology of the project area

Addis Ababa is situated within the central highland close to the rift margin where a thick succession of volcanic rocks predominate. From the geological map of Ethiopia (Mengsha et.al 1996), the regional geology of the city is dominated by extrusive volcanic rocks, which belong to the Ethiopian plateau and rift margin volcanic.

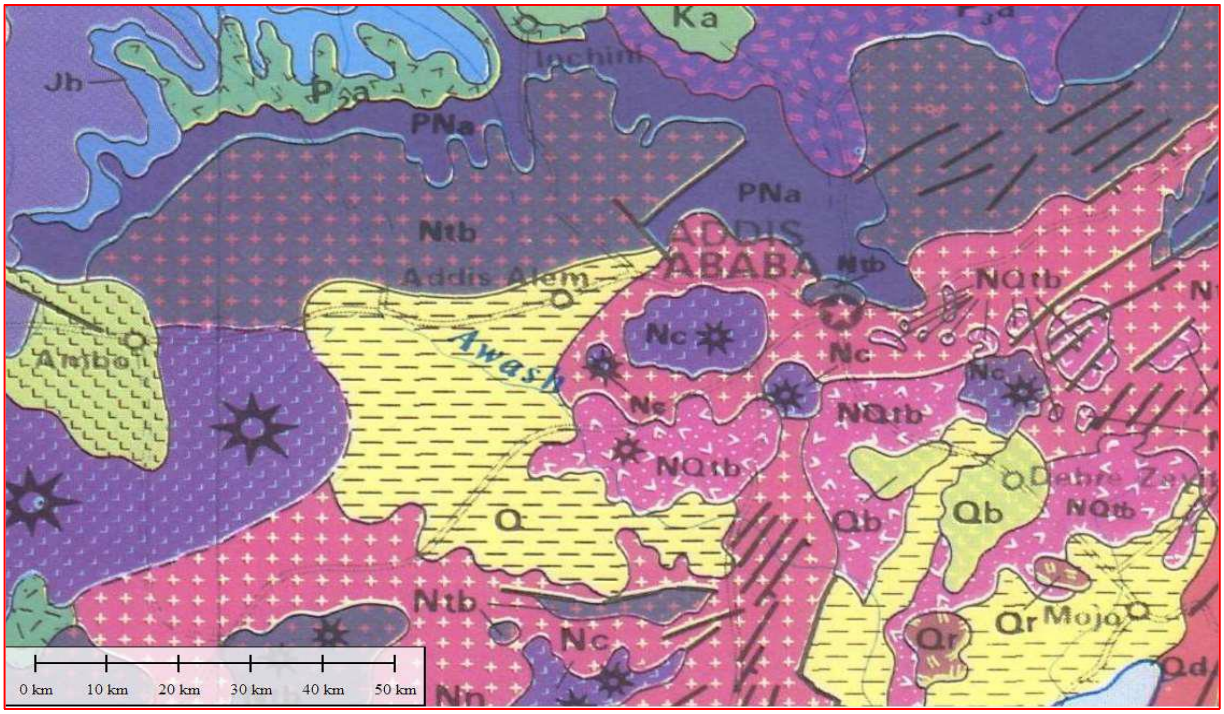


Bishoftu Formation: Alkaline basalt and trachyte.


Nazert series: ignimbrites, unwelded tuffs, ash flows, rhyolitic flows, domes, and trachyte.


Alajae Formation: transitional and sub-alkaline basalts with minor rhyolite and trachyte eruptive.


Chilalo Formation (Upper part): Alkaline basalt

Chilalo Formation (lower part): Trachyte, trashy–basalt, peralkaline, rhyolite with subordinate alkaline basalt.

**Figure 3.4: Geological formation of Addis Ababa City (Source: Geological map of Ethiopia, 1996 edition).**

The geological map of Ethiopia and literature which are written on the geology of Addis Ababa city (based on the geological map of Addis Ababa and its surroundings) have been referred to and reviewed in order to have a general understanding of the geological formations around corridors of the different road segments found in package 37 road design project before the commencement of the geotechnical investigation.

As per the Geological Map of Ethiopia (figure 2.3 above), 1996 edition, geological formations of the project corridors are classified into the following volcanic formations: -

a) NQtb=Bishoftu Formation: Alkaline basalt and trachyte.

b) Nn=Nazert Series: Ignimbrites, unwelded tuffs, ash flows, rhyolitic flows, domes, and trachyte.

c) PNa=Alajae Formation: transitional and sub-alkaline basalts with minor rhyolite and trachyte eruptive.

d) Ncb=Chilalo Formation (Upper part): Alkaline basalt

e) NC=Chilalo Formation (Lower part): Alkaline basalt Trachyte, trachy – basalt, paralkaline, rhyolite with sub – ordinate alkaline basalt.

### 3.2.4 Topography

The proposed research is located in the center of Addis Ababa, the capital city of Ethiopia. The topography of the project area is dominantly flat and rolling terrain.

## 3.3 Study Design

The study design is used to meet the objectives for the research to be done, important kinds of literature are revised to collect accepted theories and practices on cement-treated base material for inverted pavement systems. The current study design includes the following methods: Collection of Subgrade soil sample and the subgrade soil sample collected from megenagna-Imperial Junction-bole road, collection of crushed aggregate sample and the crushed aggregate sample collected from Bulbula quarry site, Preparation of samples for each laboratory test, laboratory investigation to determine the geotechnical properties of the Subgrade Soil, conducting laboratory investigation to determine the optimal application rate of cement and aggregate, to check the performance of the pavement fatigue and rutting criteria using PLAXIS-3D and IIT PAVE software to determine the stress, strain, and deflection for the pavement and to determine the economic feasibility of cement-treated base materials compared to conventional pavement.

### 3.3.1 Methodology Flow Chart

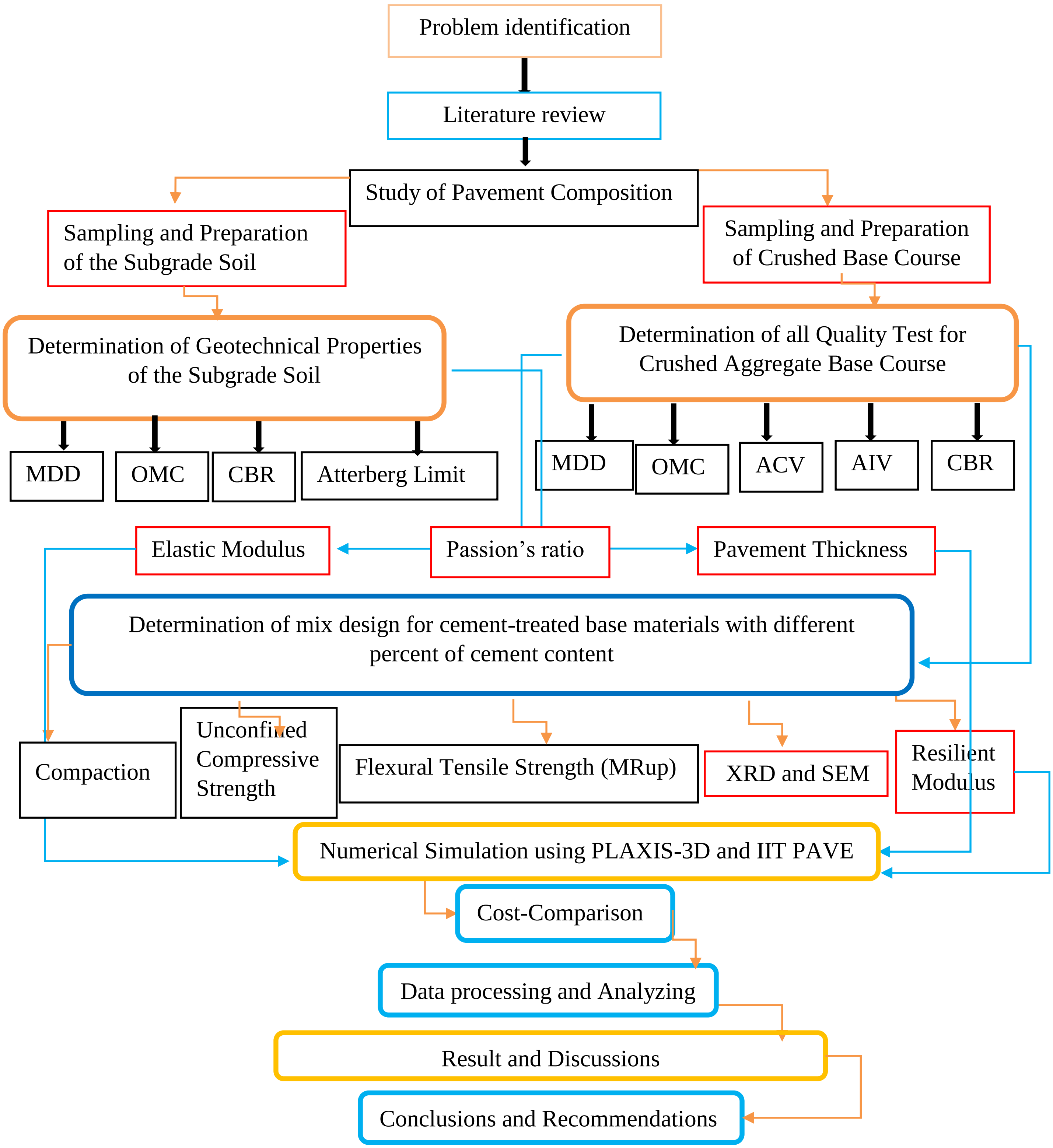


**Figure 3.5: Research Flow chart**

The Figure below it shows that the methodology process cycle of cement treated base (CTB) material

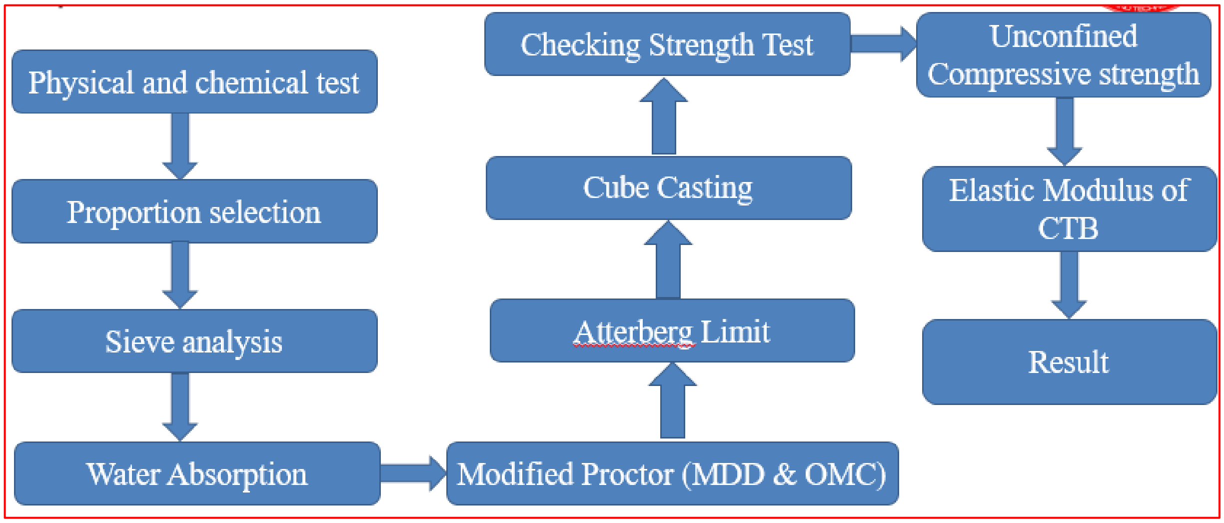


**Figure 3.6 Process Cycle of Cement Treated Base (CTB)**

### 3.3.2 Soil Extension Survey

To determine the physical properties and extent of the alignment soils, a detailed soil extension survey was conducted along the entire road section. The survey involved visual observations of key soil characteristics, such as color, texture, moisture content, and appearance, along the roadside, as well as from test pits that were excavated. The survey findings revealed that the majority of the soil along the intersection sections consists of dark to black, and medium to highly expansive clay soils, which are common soil types in Addis Ababa. These black clay soils were consistently encountered during the site investigation and were found to deepen as the test pits were advanced, continuing to a depth of more than 1.0 meters. This indicates that the expansive clay extends over a significant depth, which may have important implications for pavement design and stability

## 3.4 Sample Technique, Sample Size, and Sample Preparation

### 3.4.1 Sampling Technique

This study's sampling technique used is purposive sampling, which is a non-probability random sampling technique. To determine the engineering properties and to assess the suitability of the soils along the road alignment, representative disturbed samples were collected by digging test pits along the road alignment.

### 3.4.2 Sample Size

The sample soils have been excavated and sampled at a depth of 1.5m below the normal ground to obtain an expansive soil sample. The site was at Longitude 38° 48′ 10″, Latitude 9° 00′ 27″ for the first pit, Longitude 38° 48′.01″, Latitude 9° 00′ 09″ ′ for the second pit, Longitude 38° 47′ 54″, Latitude 8° 59′ 58″ for the third pit and Longitude 38° 47′ 47″, Latitude 8° 59′ ″ for the fourth pit. 4 samples of sub-grade materials were collected from the road alignment at variable intervals because the length of the road is too short and it is not possible to take sampling at regular intervals to assess the properties of the roadbed materials.

Test pits of approx. 1.0 m x 1.0 m size at staggered position are excavated up to a depth of 1.5m below the original surface of the road, and the lithological soil formations were properly logged. After collecting the samples, the sample tags are labeled and inserted into sample bags with the following information:

- ✓ The project name;
- ✓ GPS/Station of sampling;
- ✓ Depth of sampling;
- ✓ Type of material sampled and;
- ✓ The type of test required

After completing the logging and sampling, the test pits were backfilled, compacted, and leveled to their original level.

**Figure 3.7 Sampling of Subgrade Soil**

### 3.4.3 Soil Sample Preparation

After transporting the soil sample to the laboratory, breaking down large size particles to a manageable size was the first thing to do after transporting the sample to the laboratory. Sample preparation was done by the method stated in AASHTO T87- 86. Soil samples were air-dried by spreading the material out in trays in the laboratory and leaving it open to the air. According to the specified standard laboratory manual conducted by the American Society for Testing and Materials (ASTM) and the American Association of State of Highway and Transportation Officials (AASHTO) to determine the geotechnical properties of the subgrade soil, sieving of samples was carried out to prepare the specimen with the appropriate size required for each laboratory test.

### 3.4.4 Data Collection

An expansive soil sample has been collected from the pits manually using a pick axe, head pan, and shovel. Then, a disturbed sample was sampled at a depth of 1.5m below the normal ground surface. The researcher has used articles, previous literature, and different manuals as secondary data for comparison purposes with the results I have gotten from laboratory tests.

### 3.4.5 Study Variables

The study variables are plasticity index, plastic limit, and liquid limit from the Atterberg limit test, linear shrinkage limit test, particle size distribution i.e., sieve analysis, and optimum moisture content and maximum dry density from the proctor test, and California bearing ratio CBR test and resilient modulus MR from CBR test correlation formula.

## 3.5 Laboratory tests for the subgrade soil

Firstly, the collected soil sample was exposed to air, dried, and then pulverized into the required size before conducting the laboratory tests. Thereafter, the laboratory tests conducted on the air dried neat liquid limit, plastic limit, plasticity index, linear shrinkage, particle size distribution, classification of soils, compaction, CBR test, and Resilient Modulus MR conducted on the natural soil as per the American Society for Testing and Materials (ASTM). The table below it shows that laboratory tests and their standard reference to be used for the subgrade soil.

**Table 3-1 Laboratory tests and their standard reference to be used for subgrade soil**

| Laboratory tests | Standard references |
|---|---|
| Moisture content | ASTM D 2216 standard test methods for laboratory determination of water (moisture) content of soil and rock by mass moisture |
| Sieve analysis | ASTM D 6913-04 standard test methods for particle size distribution of soils using sieve analysis |
| Atterberg limits | ASTM D 4318 - Standard Test Method for Liquid Limit, Plastic Limit, and Plasticity Index of Soils. |
| Compaction | ASTM D 698 - Standard Test Methods for Laboratory Compaction Characteristics of Soil Using Standard Effort (12,400 ft-lbs./ft3 (600 KN-m/m3)) |
| UCS | ASTM D 2166 - Standard Test Method for Unconfined Compressive Strength of Cohesive Soil |
| CBR | ASTM D 1883-07 -Standard method for CBR (California bearing ratio) of laboratory compacted soil. |

### 3.5.1 Atterberg limit tests

Atterberg limit test have liquid and plastic limit tests which are carried out in accordance with (ASTM D-4318, 2010) and a soil specimen that is finer than the No. 40 (425 µm) sieve is used. The liquid and plastic limits of soil samples were measured by the combined method of liquid and plastic limits. According to ASTM-D4318, LL is the water content, in percent, of a soil at the arbitrary boundary between the semi-liquid and plastic states. This value was calculated using the Casagrande cup, which involves cutting a groove in the soil sample and raising and lowering the sample cup a predetermined number of times until the groove just about closes. The liquid limit is the soil moisture level at which this occurs. The graph shows the relationship between water content and blow count, and the liquid limit of the soil is defined as the water content that corresponds to the line's intersection with the 25-blow abscissa. Figure 3.8 it shows the atterberg limit test procedures.

**Figure 3.8 Atterberg limit test**

### 3.5.2 Particle Analysis Distribution

Grain size analysis divides soils into two distinctive groups, namely fine-grained and coarse grained soils. Soil particles coarser than 0.075mm, are generally termed as coarse-grained whereas soil particles finer than 0.075mm like clays and silts are termed as fine-grained. The particle size distributions can be done by using two methods: sieve analysis for particle sizes larger than 0.075mm (No. 200) in diameter, and the hydrometer analysis for particle sizes smaller than 0.075mm in diameter. The particle size distribution of the sample is attached in Annex-1.

#### 3.5.2.1 Sieve analysis

Sieve analysis is a method used to determine the grain size distribution of soils. Sieves are made of woven wires with square openings. In order to classify a soil for engineering purposes, one needs to know the distribution of the size of grains in a given soil mass. The particle size distribution is determined by (ASTM D-421, 1998). This enabled a continuous particle size distribution curve to be plotted from the size of the course (gravel) particles down to the finest (clay) size. A plot on a semi-logarithmic chart was then done of the percentage of material passing each sieve against the sieve sizes to give the grading. The figure 3.9 it shows that the particle size distribution or sieve size of crushed aggregate base materials.

**Figure 3. 1 Sieve analysis test**

### 3.5.3 Proctor test

The compaction test procedure is used to determine the maximum dry unit weight of compacted soils which can be used for specification of field compaction. The Proctor (Compaction) test is carried out by AASHTO T180 and helps to decrease compressibility, increase shear strength and bearing capacity, and sometimes decrease the permeability of soils for engineering construction (AASHTO T180).

The variation of maximum dry density and optimum moisture content for natural and treated soil samples are plotted, presented, and discussed in the next chapter, and the laboratory datasheet of compaction test results for the raw soil is tabulated in Annex-1.


**Figure 3. 10 Proctor test**

### 3.5.4 California Bearing Ratio (CBR) test

The California Bearing Ratio (CBR) test for subgrade soil involves collecting a representative soil sample, air-drying, and sieving it through a 19 mm sieve. Determine the Optimum Moisture Content (OMC) and Maximum Dry Density (MDD) using a Proctor test. Compact the soil in a CBR mold in three layers, achieving the MDD with a Proctor hammer.

For soaked samples, place the mold with a perforated base plate and filter paper in a soaking tank with surcharge weights for 96 hours. After soaking, position the mold in a loading machine, place a penetration piston on the sample, and apply a load at a constant penetration rate of 1.25 mm/min. Record the load at specified penetration intervals, calculate the CBR values for 2.5 mm and 5.0 mm penetrations using standard load values (1370 kg and 2055 kg, respectively), and report the higher value. Post-test, determine the sample's moisture content, and repeat the test for consistency. Follow ASTM D1883 or AASHTO T193 standards for accuracy and safety.

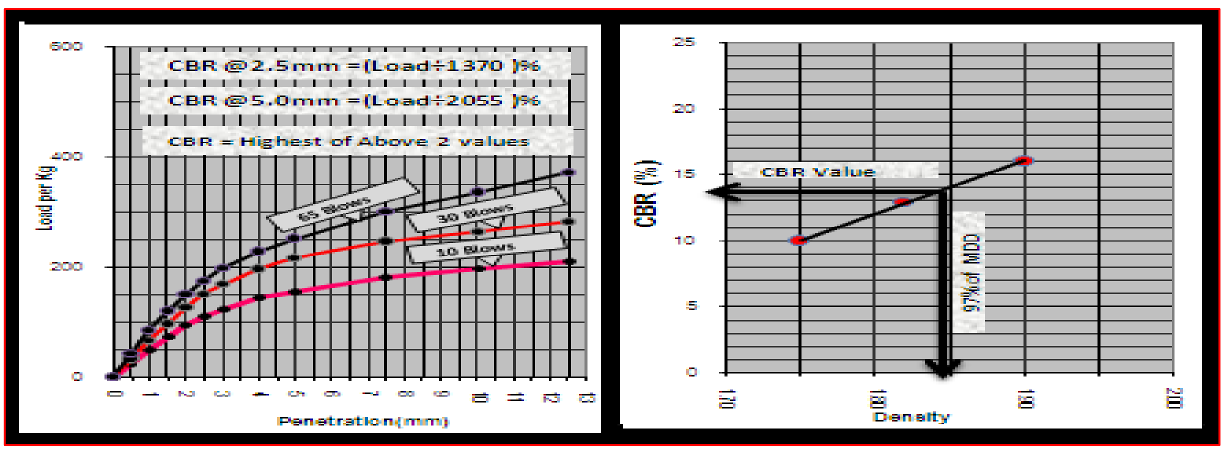


Figure 3.11 CBR Penetration

#### 3.5.4.1 CBR swell

The CBR swell of the soil was measured by placing the tripod with the dial indicator on the top marked point of the soaked CBR mold. The initial dial reading of the dial indicator on the soaked CBR mold was taken just after soaking the sample. At the end of 96 hours (4 days), the final dial reading of the dial indicator was taken and the swell percentage of the initial sample length was given by:

$$\text{CBR swell} = \frac{\text{change in length in mm during soaking}}{116.43\text{ mm}} * 100 \qquad [3.1]$$

### 3.7.5 Resilient Modulus (MR) test

Resilient modulus for the subgrade soil, which is measured taking into account only the elastic (or resilient) component of the deformation (or strain) of the specimen in a repeated load test is considered to be the appropriate input for linear elastic theory selected in these research for the analysis of flexible pavements. The resilient modulus of soils can be determined in the laboratory by conducting the repeated tri-axial test as per the procedure detailed in AASHTO T307-99[19]. Since these equipment are usually expensive, the following relationships may be used to estimate the resilient modulus of subgrade soil (MRS) from its CBR value.

$$MRS = 10.0 * CBR \text{ for } CBR \leq 5\ \% \qquad [3.2]$$

$$MRS = 17.6 * (CBR)^{0.64} \text{ for } CBR > 5\ \% \qquad [3.3]$$

Where,

MRS = Resilient modulus of subgrade soil (in MPa).

CBR = California bearing ratio of subgrade soil (%)

## 3.6 Crushed Base Course Material

### 3.6.1 Sampling for Crushed Base Course Material

Collect representative samples of crushed base materials from selected sites within the project area. The Crushed Base Course material was produced from the approved source at Bulbula quarry located at (E=474914, N=991426 and Elevation=2223m), during production, as per the requirements of the project, sampled, and all quality tests for the crushed test were determined frequently here in the project laboratories. Accordingly, the produced stockpile complies with the requirements and standards then to determine the mix design of cement-treated base materials. Ensure that the samples encompass variations in particle sizes, gradations, and mineralogical composition.

Figure 3.12 Sampling of Crushed Aggregate Base Course from Bulbula Crusher Site

### 3.6.2 Sample Preparation for Crushed Base Course Layer

Prepare the collected samples by air-drying them to remove excess moisture. Ensure that the samples are free from contaminants and adhere to standard testing procedures. Upon collection, reduce the bulk samples to a manageable size.

Figure 3.13 Sample Preparation for Crushed Aggregate Base Course

Use appropriate tools such as shovels, scoops, or sample splitters to obtain a representative portion for testing. Ensure that the reduced samples maintain the same characteristics as the original material. According to the specified standard laboratory manual conducted by the American Society for Testing and Materials (ASTM) and the American Association of State of

Highway and Transportation Officials (AASHTO) to determine the geotechnical properties of the crushed base course materials.

### 3.6.3 Laboratory Test for Unbound Crushed Base Course Material

**(a) Graded crushed stone (GB1)**

This material is produced by crushing fresh, quarried rock (GB1) and may be an all-in product, usually termed a 'crusher-run', or the material may be separated by screening and recombined to produce a desired particle size distribution, as per the specifications. The material shall be clean and free from organic matter, lumps of clay, or other deleterious substances. The material shall be of such a nature that it can be readily transported, spread, and compacted without segregation.

**(b) Grading**

The combined grading of the material shall be a smooth continuous curve falling within the grading limits shown in morth Table 400 when determined per the requirements of AASHTO T-27. The mass of material passing the 0.075mm sieve shall be determined in accordance with the requirements of AASHTO T-11. The nominal maximum particle size is 20 mm.

**Table 3.2 Grading limits for cement-treated Base**

| Sieve Size （mm） | 53 | 37.5 | 19 | 9.5 | 4.75 | 0.6 | 0.3 | 0.075 |
|---|---|---|---|---|---|---|---|---|
| Base | 100-100 | 95-100 | 45-100 | 35-100 | 25-100 | 8-65 | 5-40 | 0-10 |

**(c) Plasticity Index**

The fine fraction of a GB1 material shall be non-plastic or shall have a maximum Plasticity Index of 6 when determined in accordance with AASHTO T-90.

**(d) Californian Bearing Ratio (CBR)**

The in- situ dry density of the placed material should be a minimum of 98% of the maximum dry density obtained in the ASTM Test Method D 1557 (Heavy Compaction). The compacted thickness of each layer should not exceed 200 mm. Crushed stone base courses constructed with proper care with GB1 materials described above should have CBR values in excess of 100 percent.

**(e) Aggregate Crushing Value (ACV)**

Requirements expressed in terms of the results of the Aggregate Crushing Value (ACV) (British Standard 812, Part 110) may be used: the ACV should preferably be less than 25 and in any case less than 29. Other simpler tests e.g. the Aggregate Impact Test (British Standard 812, Part 112, 1990) may be used in quality control testing provided a relationship between the results of the chosen test and the Ten percent Fines Value (TFV) has been determined.

**(f) Mechanical Strength Requirements (TFVT)**

To ensure that the materials are sufficiently durable, they should satisfy the criteria given in Table 5200/2. These are the minimum percent fine value (TFV) (British Standard 812, Part 111) and limits on the maximum loss in strength following 24 hours of soaking in water. The likely moisture conditions in the pavement are taken into account in broad terms based on annual rainfall.

**Table 3.3 Mechanical Strength Requirements for the Aggregate Fraction of Crushed Stone Base Course Materials (GB1) as Defined by the Ten Percent Fines Test**

| Typical Annual Rainfall (mm) | Minimum 10% Fines Values (kN) | Minimum Ratio Wet/Dry Test (%) |
|---|---|---|
| >500 | 110 | 75 |
| <500 | 110 | 60 |

### 3.7 Cement Treated Crushed Base Course Layer (CTB)

Laboratory testing for crushed base course materials involves a comprehensive assessment of various geotechnical properties. The particle size distribution analysis determines the material's gradation and range of particle sizes, while Atterberg limits testing assesses its fine-grained characteristics and plasticity. The moisture-density relationship, evaluated through Proctor compaction tests, provides essential information for compaction efforts during construction. California Bearing Ratio (CBR) tests gauge the material's load-bearing capacity. Moisture content testing quantifies water content, and compaction tests assess achieved density. These tests were carried out in the laboratory.

On second phase Mix Design of CTB, Uniformity Coefficient, Sieve Analysis, Modified Proctor test MDD and OMC, Unconfined Compressive Strength Test, Indirect Tensile Strength Test, CBR Test, Resilience Modulus Test, X-ray Diffraction (XRD) and Scanning Electron Microscopy (SEM) of the cement treated base course samples were conducted.

**Table 3.4 Laboratory test for cement-treated base**

| Sr. no. | List of Experiments | Code Referred |
|---|---|---|
| 1 | Gradation of soil for Stabilization with cement for cement treated base (Selection of Proportion) | MORTH -Table 400-4 and ERA 2013 |
| 2 | Gradation of soil for Stabilization with cement for cement treated base (Sieve Analysis) | MORTH -Table 400-5 and ERA 2013 |
| **Physical Properties** | | |
| 3 | Modified Proctor ( Max. dry density) | IS 2720 (Part 8) |
| 4 | Modified Proctor (Optimum Moisture Content) | IS 2720 (Part 8) |
| 5 | Plasticity Index | IS 2720 (Part 5) |
| 6 | Plasticity Modulus | IS 2720 (Part 5) |
| 7 | Plasticity Product | IS 2720 (Part 5) |
| 8 | Uniformity Coefficient | IRC 84 page 12, clause 3.1.2 |
| 9 | Water absorption(20mm) | IS 2386 (Part 3) |
| 10 | Water absorption(10mm) | IS 2386 (Part 3) |
| 11 | Water absorption(Crushed dust) | IS 2386 (Part 3) |
| 12 | Compressive Strength (Cement 4% by wt. of mix) | IS 516 |
| 13 | Indirect Tensile Strength test | IS 5816 |

### 3.7.1 Mix Design of Cement Treated Base (CTB)

The mix design of Cement-Treated Base (CTB) is a crucial process in ensuring the material's effectiveness and durability for road construction and infrastructure projects. It involves determining the optimal proportions of soil, aggregate, cement, and water to meet specified performance criteria. The process begins with preliminary testing of the soil, aggregate, and cement to understand their properties, such as particle size distribution, water absorption, and setting times. Based on these properties, the appropriate proportions of soil and aggregate are selected to achieve the desired gradation and stability.

Cement content is then established, typically ranging from 3% to 8% by weight of the dry mix, depending on the required strength. The water content is adjusted to achieve the necessary moisture level for proper compaction, with a focus on maintaining an appropriate water-to-cement ratio. Multiple trial mixes are prepared with varying proportions to evaluate their performance through tests such as Proctor compaction, Unconfined Compressive Strength (UCS), Indirect Tensile Strength (ITS), and Flexural strength test.

The results from these tests are used to optimize the mix, balancing strength, workability, and cost. The final mix design is documented, specifying the exact proportions of soil, aggregate, cement, and water. Throughout the production process, regular quality control checks are conducted to ensure that the CTB mix maintains consistency with the designed proportions. This comprehensive approach ensures that the CTB material performs reliably and meets the necessary specifications for its intended application. The following listed points were first determined before the mix design of cement-treated base material

**Cement**: the strength grade of cement shall be 42.5, which is Ordinary Portland Cement (OPC) with high quality. The initial setting time shall be more than 3 hours, final setting time shall be more than 6 hours. Before and after entering the site, and sampling test must be carried out on the cement, including the varieties of cement, strength grade, stability, quantity, and delivery date. The cement can be used only after being checked and accepted. It is forbidden to use rapid-hardening cement and early-strength cement.

**Water**: Testing the quality of water used in Cement-Treated Base (CTB) materials is crucial to ensure that it does not adversely affect the performance and durability of the final product. According to ASTM standards, several tests are conducted to verify water quality. Visual inspection is the initial step, checking for clarity and the absence of visible impurities. The pH level is measured using ASTM D 4972, ensuring it falls between 6 and 8, which is essential for proper cement hydration. Chemical analyses, including tests for chlorides and sulfates as per

ASTM D 4327 and ASTM D 6691, determine if harmful substances are present at levels that could impact the mix's strength and durability. By adhering to these ASTM standards, the water used in CTB mixes can be confirmed to meet necessary quality requirements, ensuring that it contributes positively to the mix's performance and structural integrity.

#### 3.7.1.1 Selection of Proportion

Proportioning for Cement-Treated Base (CTB) using MoRTH Table 400-4 involves a systematic process to determine the correct mix of materials, including crushed base course, stone dust, and cement. The process begins with the selection of appropriate materials: crushed base course should be well-graded, free from organic matter and deleterious substances; stone dust should be fine aggregate derived from crushing stones, passing through the 4.75 mm sieve; and cement should conform to IS: 12269, typically Ordinary Portland Cement (OPC) or another specified type. Representative samples of crushed base course, stone dust, and cement are then collected, ensuring they are clean, dry, and free from impurities.

Initial mix proportions are selected based on research from MoRTH Table 400-4, which provides a range for starting laboratory trials. For instance, typical proportions by weight might include 25% from 25mm-14mm, 35% from 14mm-4.5mm coarse crushed aggregate base course and 40% below 4.75mm fine aggregate or stone dust, and 2-6% cement. Laboratory trials are conducted by mixing different proportions within these specified ranges and testing for desired properties. The mixing procedure involves batching the materials by weighing the required amounts of crushed base course, stone dust, and cement, followed by thorough dry mixing of crushed base course, and stone dust. Cement is then added to the dry mix, ensuring uniform distribution, and water is gradually added to achieve the desired moisture content, which can be determined using the Proctor test (ASTM D698 or ASTM D1557).

Once mixed, the material undergoes various tests. Compaction tests determine the maximum dry density (MDD) and optimum moisture content (OMC). Strength tests, such as unconfined compressive strength (UCS) (ASTM D1633), California Bearing Ratio (CBR) (ASTM D1883), and indirect tensile strength (ITS) (ASTM D6931), are conducted on prepared samples. Durability is assessed through wet-dry and freeze-thaw cycle tests. Based on the test results, mix proportions are adjusted to meet the required strength, durability, and compaction characteristics. The process is iterated until the desired properties are achieved.

#### 3.7.1.2 Sieve Analysis for Cement-Treated Base (CTB)

The sieve analysis for Cement-Treated Base (CTB) materials, conducted by ASTM C136/C136M standards, is a fundamental test used to determine the particle size distribution of aggregates. This analysis ensures that the CTB aggregate gradation meets specified criteria, essential for optimal performance in road pavement construction.

**Sample Collection and Preparation**

First, a representative sample of the CTB material is collected from the field or a laboratory-prepared mix. This sample is then dried in an oven at a temperature of 110°C ± 5°C until it reaches a constant weight. This step ensures that any moisture present in the sample does not affect the results of the sieve analysis. Once dried, the total weight of the sample is measured accurately using a balance, and this weight is recorded.

**Sieve Setup**

The sieves are then arranged in descending order of opening size, with the coarsest sieve on top and a pan at the bottom to collect the finest particles. The standard set of sieves includes various sizes such as 37.5 mm, 25 mm, 19 mm, 12.5 mm, 9.5 mm, 4.75 mm, 2.36 mm, 1.18 mm, 0.600 mm, 0.300 mm, 0.150 mm, and 0.075 mm. This arrangement allows for a thorough separation of the sample into different size fractions.

**Sieve Shaking**

The prepared sample is then placed on the top sieve of the stack. The entire sieve stack is secured in a mechanical sieve shaker, which facilitates the sieving process by shaking the sieves for a specified duration, typically between 10 to 15 minutes. This shaking action ensures that the particles are adequately separated and passed through the sieves based on their sizes.

**Weighing the Sieved Fractions**

After the sieving process, each sieve is carefully removed from the stack. The material retained on each sieve, as well as the material collected in the pan, is weighed individually. These weights are meticulously recorded. This step is crucial as it provides the data needed to determine the distribution of particle sizes within the sample.

**Calculating the Percentage of Passing**

The next step involves calculating the cumulative weight of material retained on each sieve.

**Plotting the Gradation Curve**

The results of the sieve analysis are then plotted on a semi-logarithmic graph, with the sieve sizes on the x-axis (log scale) and the percentage passing on the y-axis. This gradation curve visually represents the particle size distribution of the aggregate and helps in comparing it against specified gradation limits for CTB materials.

### 3.7.1.3 Modified Proctor Test

Compacted specimens must be examined for moisture content and density in compliance with ASTM D 558 CTB. Samples from each sublet must be obtained and utilized to construct laboratory test specimens that accurately reflect the individual sublets. To assess whether to accept a lot based on density, an average density for the lot were calculated using the density findings for each sublease that makes up the lot. ASTM D 1556, ASTM D 2167, or ASTM D 6938 research must be followed when conducting a density test within each subdivision in the field. In line with ASTM D 3665's research, a random selection process were determine the test site.

One of the key elements affecting the CTAB's strength is the dry density of the compacted soil. Water is necessary for addition in order to reach the highest density and facilitate cement hydration. Regardless of the type of mixer used, the mixing design must adhere to (AASHTO T134).

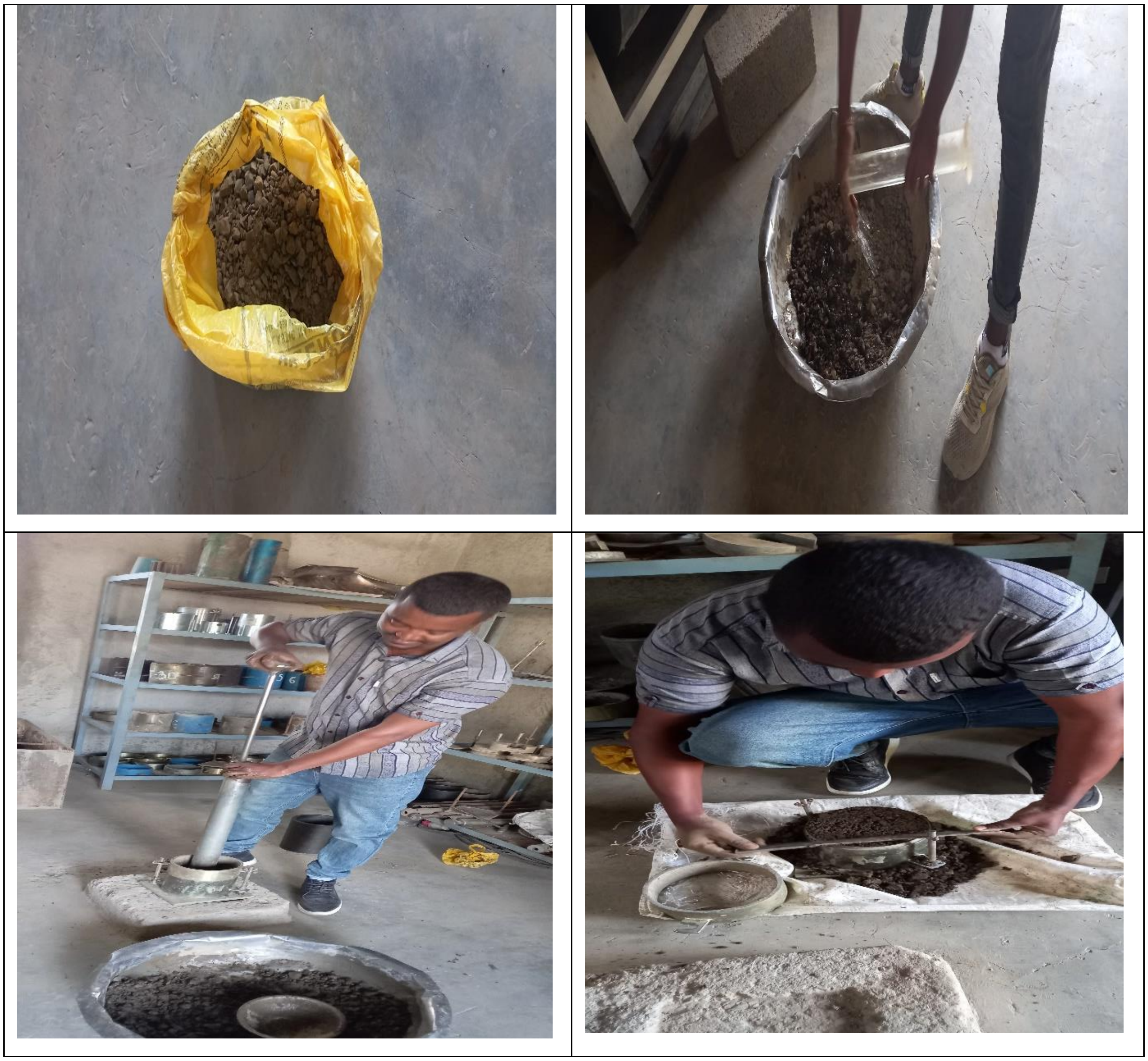

**Figure 3.14 Modified Proctor Test to determine MDD and OMC**

The process must be continued until the cement and water are distributed evenly throughout the aggregate to prevent the formation of cement balls when water is added and a mixture with a uniform appearance is achieved. Cement and aggregate were divided into weight-based portions; five kilograms of aggregate and four percent of the weight of the cement aggregate were measured. Subsequently, establish the moisture-density curve to ascertain the optimal dampness material and maximum. (AASHTO T134-70) states that a homogenous mixture can be obtained by combining 6 kg of base aggregate with cement and water at 2%, 4%, 6%, 8% and 10% of the base dry weight.

**3.7.1.5 Atterberg limit**

Determining the Liquid Limit (LL), Plastic Limit (PL), and Plasticity Index (PI) of soil is essential for understanding its behavior and suitability in engineering applications, as specified under IS 2720 (Part 5).

The **Liquid Limit** is assessed using Casagrande's device, which measures the water content at which the soil transitions from a plastic to a liquid state. To perform this test, a soil sample is prepared by air-drying and pulverizing it to pass through a 425 µm sieve. The soil is then mixed with distilled water until it becomes pliable. A portion of this mixture is placed in the liquid limit device's cup, and a groove is cut in the soil using a grooving tool. The device is operated to make the cup drop and close the groove. Water is gradually added until the soil mixture closes the groove after 25 blows, indicating the Liquid Limit. The water content at this point is measured and recorded as the Liquid Limit (LL).

The **Plastic Limit** is determined by rolling a soil sample into a thread on a glass plate until it starts to crumble, indicating the transition from a semi-solid to a plastic state. To perform this test, the soil sample is mixed with water to achieve a pliable consistency and then rolled into a thread of 3 mm diameter. When the thread begins to crumble, the water content is measured. This water content is recorded as the Plastic Limit (PL), representing the moisture content at which the soil begins to lose its plasticity.

Finally, the **Plasticity Index** is calculated to assess the range of moisture content over which the soil remains plastic. It is determined by subtracting the Plastic Limit (PL) from the Liquid Limit (LL). The formula used is PI = LL - PL. This index provides valuable information about the soil's plasticity and is crucial for understanding how the soil were behave under varying moisture conditions

**3.7.1.6 Uniformity Coefficient (UC)**

One important measure for evaluating the gradation of aggregates in road construction, particularly cement-treated base (CTB) materials, is the Uniformity Coefficient (UC). The UC, as defined in IRC: 84, is computed by dividing the aggregate's 60% finer particle size by its 10%

finer particle size. A greater UC denotes a well-graded aggregate with a broad range of particle sizes, which typically results in better compaction and stability. This ratio aids in determining the range of particle sizes in the aggregate. In order to conduct the test, the sizes that correspond to 10% and 60% passing are determined by sieve analysis applied to a representative sample of the aggregate.

A soil or aggregate sample is passed through a number of standard sieves to determine the particle size distribution, which is then used to calculate the Uniformity Coefficient. The values of (D60) and (D10) can be found by graphing the cumulative percent passing against sieve sizes on a semi-logarithmic graph. Next, the formula is used to determine the UC.

$$(UC) = \frac{(D60)}{(D10)} \quad [3.4]$$

A high uniformity coefficient denotes a wide range of particle sizes, indicating a well-graded material, which is often preferred in construction for improved stability and compaction. On the other hand, a low uniformity coefficient indicates a more homogeneous distribution of particle sizes, which could cause problems with stability and compaction. All things considered, the Uniformity Coefficient is a crucial criterion for assessing a material's fitness for use in engineering and construction.

#### 3.7.1.7 Water Absorption

For materials like aggregates and soils, water absorption is an important characteristic because it shows how well they can absorb water, which affects how they behave in engineering and building applications. A sample of the material is first dried in an oven at 105–110°C until it reaches a consistent weight in order to calculate the water absorption. It is noted what this dry weight is. After that, the sample is immersed in water for a predetermined amount of time usually 24 hours to guarantee complete saturation. The sample is taken out after soaking, the surface wetness is carefully wiped off, and the wet weight is calculated. The following formula is used to determine the water absorption percentage:

Where the weights of the dry sample (W Dry) and the saturated sample (W Wet) are indicated. Greater porosity and a larger capacity for water uptake are indicated by a high water absorption percentage, which may have an impact on the material's strength and durability. On the other hand, a low percentage of water absorption denotes less porosity and improved stability under different moisture levels. The water absorption of an aggregate, for instance, would be determined as 8% if it weighed 500 g while it was dry and 540 g after soaking. Comprehending the process of water absorption facilitates the assessment of a material's appropriateness for diverse building uses and the forecasting of its behavior in various environmental scenarios.

The ASTM C127 for coarse aggregates and ASTM C128 for fine aggregates contain the technique details for aggregates. An oven heated to 105–110°C is used to dry a representative sample of the aggregate until it reaches a consistent weight, denoted as (W dry). After that, the sample is submerged in water containing coarse particles for a full day, and fine particles using a more exact technique. The aggregate is surface-dried after soaking, weighed once again to determine (W wet), and the water absorption is computed using the following formula:

$$\text{Water Absorption (\%)} = \frac{(\text{W wet} - \text{W dry})}{(\text{W dry})}100 \qquad [3.5]$$

**3.7.1.8 Compressive Strength test**

The ASTM C39 compressive strength test for Cement-Treated Base (CTB) materials is a crucial procedure for evaluating the CTB mix's strength and appropriateness for use in construction. The CTB mix, which consists of soil, aggregate, and a predetermined weight proportion of cement, is prepared first in the process. After that, the mixture is crushed into conventional molds, usually in three layers, and each layer is uniformly compacted using a vibrating table or tamping rod. Once the surface has been levelled, the specimens are covered to stop moisture loss and are allowed to set for a full day.

When the first setting period is over, the specimens are demolded and put in a curing tank that is kept at 27 ± 2°C. They stay in the curing tank for the prescribed amount of time—usually 7, and 28 days to ensure optimal cure. Upon completion of the curing period, the specimens are taken out, left to dry on the surface, and subsequently put through a compression testing equipment. To guarantee uniform load application, the specimens are centered in the machine. The load is delivered at a steady rate until the specimens fail. A record of the specimen's maximum load is kept.

The compressive strength is calculated using the formula: Compressive Strength (MPa) = P/A, Where P is the maximum load in Newton and A is the cross-sectional area of the specimen in square millimeters.

**Figure 3.15 Compressive strength test procedure for compaction, demolding and curing of CTB**

This test provides vital information on the strength characteristics of the CTB material, ensuring it meets the necessary standards and is suitable for its intended use in road construction and other infrastructure projects.

#### 3.7.1.9 Unconfined Compressive Strength (UCS) test

The Unconfined Compressive Strength (UCS) test for Cement-Treated Base (CTB) materials is essential for evaluating their strength under unconfined conditions, providing a measure of the maximum axial compressive stress that a cylindrical CTB specimen can withstand. Procedure for Unconfined Compressive Strength Test According to ASTM D 1633.

The CTB material shall have a minimum Unconfined Compressive Strength (UCS) of 4.5 to 7 MPa as per IRC: SP: 89 in 7/28 days. While the conventional cement stabilized material should attain this strength in seven days, granular materials and soil-aggregate mixture stabilized with lime, pozzolanic stabilizers, lime-fly ash etc., should meet the above strength requirement in 28 days since the strength gain in such materials is a slow process (IRC:37-2018, n.d.).

To conduct this test, a CTB mix is prepared by thoroughly blending soil, aggregate, and a specified percentage of cement by weight, with the appropriate amount of water added to achieve the desired consistency. The mixture is then compacted into cylindrical molds in layers, using a tamping rod or vibrating table to ensure uniform compaction, and the surface is leveled before being covered to prevent moisture loss.

After 24 hours, the specimens are removed from the molds and placed in a curing tank maintained at 27 ± 2°C, where they remain for a specified curing period, typically 7, 14, or 28 days. Once the curing period is complete, the specimens are taken out, surface-dried, and placed in a compression testing machine. The machine is set to apply load at a constant rate until the specimens fail, and the maximum load applied is recorded. The UCS is then calculated using the formula: UCS (MPa) = P/A. Where P is the maximum load in Newton, and A is the cross-sectional area in square millimeters. This test provides crucial data on the strength characteristics of CTB materials, ensuring they meet the required standards and are suitable for their intended use in construction and infrastructure projects.

**Figure 3.16 Unconfined Compressive stregth test procedure for CTB**

#### 3.7.1.10 Indirect Tensile Strength (ITS) test

The Indirect Tensile Strength (ITS) test for Cement-Treated Base (CTB) materials, following ASTM standards, is used to evaluate the tensile strength of the material under conditions that simulate indirect tensile stresses. This test is typically conducted according to ASTM D 6931, which provides a standardized method for assessing the tensile strength of asphalt mixtures but can be adapted for CTB materials.

To conduct this test, a CTB mix is prepared by thoroughly blending aggregate, and a specified percentage of cement by weight, with the appropriate amount of water added to achieve the desired consistency. The mixture is compacted into cylindrical molds in layers, using a tamping rod or vibrating table to ensure uniform compaction, and the surface is leveled before being covered to prevent moisture loss. After 24 hours, the specimens are removed from the molds and placed in a curing tank maintained at 27 ± 2°C, where they remain for a specified curing period, typically 7, and 28 days. Once the curing period is complete, the specimens are taken out, surface-dried, and placed horizontally between loading strips in a compression testing machine, ensuring the specimen is centered for even load application across the diameter. The load is applied at a constant rate until the specimen fails, and the maximum load applied is recorded.

The ITS is calculated using the formula:

$$\text{ITS (MPa)} = 2P/\pi DL \qquad [3.6]$$

Where P is the maximum load in Newton,

L is the length of the specimen in millimeters, and

D is the diameter of the specimen in millimeters.

This test provides vital information about the tensile strength of CTB materials, ensuring they meet the necessary standards and are suitable for use in construction and infrastructure projects.

**Figure 3.17 Indirect Tensile Stregth test procedure for CTB**

#### 3.7.1.11 Flexural Strength (Modulus of Rupture) Test

The flexural strength test for Cement-Treated Base (CTB) materials, following ASTM standards, is a key procedure for evaluating the material's ability to withstand bending stresses. This test is typically conducted according to ASTM C293 or ASTM C1609, which provide standardized methods for assessing the flexural properties of concrete and similar materials.

The modulus of rupture (MRUP) or flexural strength of the CTB material is required to carry out the fatigue damage analysis of the cement-treated base. The values of modulus of rupture (MPa) for cementitious bases may be taken as 20 percent of the 28-day UCS value (MPa) (IRC:37-2018, n.d.). A relationship between UCS, Indirect Tensile Strength (ITS) and Flexural Strength, if developed for the materials being used in a project, were be useful for quality control since ITS is easy to determine on the cores taken from the field. Flexural Strength is approximately 1.5 times the ITS value for cement bound aggregates (IRC:37-2018, n.d.). Subject to the following limiting (maximum) values:

**Table 3.5 values of modulus of rupture (MPa) for cementitious bases**

| | |
|---|---|
| Cementitious stabilized aggregates | 1.40 MPa |
| Lime-fly ash-soil | 1.05 MPa |
| Soil-Cement | 0.7 MPa |

To begin the test, a CTB mix is prepared by blending soil, aggregate, and a specified percentage of cement by weight, with water added to achieve the desired consistency. The mixture is then compacted into beam molds, which are usually sized at 100 mm x 100 mm x 500 mm or 150 mm x 150 mm x 700 mm, depending on the specific ASTM standard being followed. The compaction process involves filling the mold in layers, each layer being uniformly compacted using a tamping rod or vibrating table, and leveling the surface to ensure an even finish. After molding, the specimens are covered to prevent moisture loss during the initial curing period of 24 hours. After this initial curing, the specimens are demolded and placed in a curing tank at a controlled temperature of 27 ± 2°C, as specified by ASTM standards. They remain in the curing tank for a period typically ranging from 7 to 28 days, depending on the requirements of the project.


**Figure 3.18 Flexural Stregth (Modulus of Rupture) test procedure for CTB**

Upon completion of the curing period, the specimens are removed from the curing tank and allowed to air-dry before testing. For the flexural strength test, the beam specimens are positioned in the flexural testing machine according to ASTM research, with supports placed at the specified span length. The load is then applied at a constant rate until the specimen fails. The maximum load applied is recorded during this process.

#### 3.7.1.12 Resilience Modulus for Cement Treated Base

ASTM D 7369 offers a standardized procedure for assessing the resilience of cement-treated base (CTB) materials under repeated loading circumstances, which can be used to calculate their robust modulus. The process starts with the preparation of cylindrical CTB material samples, which are then compressed using a standard compaction method to a predetermined density and moisture content. The samples undergo a specified curing period to guarantee that the cement is completely hydrated.

Calculating the elastic modulus of ECTB from the 28-day Unconfined Compressive Strength (UCS) of CTB material can be done using equation 3.10. The strength of cementitious layers increases over time, and pavements with CTB layers that are 7/28 day unconfined may be analyzed using an elastic modulus of 5000 MPa (IRC:37-2018, n.d.).

$$ECTB = 1000 * UCS \qquad [3.7]$$

Where,

UCS = 28-day unconfined compressive strength (MPa) of the cementitious granular material. It should be ensured that the average laboratory strength value should be more than 1.5 times the required (design) field strength.

ECTB = Elastic modulus (MPa) of 28-day cured CTB material

Curing of cemented bases shall be done for a minimum period of seven days before the commencement of the construction of the next upper layer to achieve the required strength as described in IRC: SP:89 (IRC:37-2018, n.d.), and curing should start immediately by spraying bitumen emulsion/wet jute mat or periodical mist spray of water without flooding or other methods.

#### 3.7.1.13 Poisson's ratio

Poisson's ratio is a critical property for evaluating the elastic behavior of Cement-Treated Base (CTB) materials in road construction. To calculate the Poisson ratio of CTB represents the ratio of lateral strain to axial strain when the material is subjected to uniaxial stress. To determine Poisson's ratio, cylindrical samples of CTB material are first compacted to a specified density and moisture content, and then cured to allow the cement to fully hydrate. During testing, a uniaxial compression machine applies incremental loads to the samples while measuring both axial and transverse strains using strain gauges.

Poisson's ratio is calculated by dividing the transverse strain by the axial strain, providing insight into how the material deforms laterally relative to its length under stress. Typically, Poisson's ratio for CTB materials ranges from 0.2 to 0.4, indicating their ability to deform in response to applied loads. This property is essential for predicting the material's performance under real-world traffic conditions and for designing pavements that can effectively distribute and withstand stresses, ensuring the long-term durability and stability of road infrastructures.

### 3.8 Crack Relief Layer

A crack relief layer, also known as a stress-relief or interlayer, is a crucial component in pavement design aimed at mitigating reflective cracking in asphalt overlays. Reflective cracking occurs when existing cracks in the underlying pavement surface propagate upward into a new overlay, potentially leading to reduced pavement performance and increased maintenance needs. The primary purpose of a crack relief layer is to interrupt the path of these cracks, effectively preventing their migration into the new pavement layer. By doing so, it helps to absorb and dissipate the stresses caused by traffic loads and environmental conditions, enhancing the overall durability and performance of the pavement.

In the case of pavements with CTB, a crack relief layer, provided between the bituminous layer and the cementitious base, delays the reflection of crack from the CTB layer into the bituminous layer. The crack relief layer may consist of dense graded crushed aggregates of 100 mm thickness conforming to MoRTH (IRC:37-2018, n.d.). Specifications for Wet Mix Macadam (WMM) or the Stress Absorbing Membrane Interlayer (SAMI) of elastomeric modified binder applied at the rate of 10 – 12 kg/10 m2 covered with 0.1 m3 of 11.2 mm aggregates. For the pavement analysis, the SAMI layer is not considered as a structural layer, i.e., it shall not be included in the pavement composition for pavement analysis.

Design considerations for a crack relief layer include its thickness, which varies depending on the chosen material and specific pavement conditions, and proper placement to ensure effectiveness. The material must be compatible with both the existing pavement and the new overlay to ensure optimal bonding and performance. Environmental factors such as temperature fluctuations and moisture conditions, as well as traffic load considerations, also play a role in material selection and design.

### 3.8.1 Resilient Modulus

The resilient modulus of a well-graded granular layer depends upon the gradation and the confinement pressure to which it is subjected to under the application of wheel load. A typical value of 450 MPa is used for the sandwiched aggregate layer for the analysis of pavement. The granular crack relief layer shall be compacted to 100% of the modified Proctor compaction maximum density(IRC:37-2018, 2018).

## 3.9 Design Principles and Performance Criteria

### 3.9.1 Design Principles

The principle behind pavement design is to build pavements that, over the course of their intended service life, were operate and perform structurally adequately. Roughness from variations in surface profile, bituminous and cementitious material-bound layer cracking, rutting (permanent or plastic deformation) of unbound/unmodified or partially modified subgrade, granular layers, and bituminous layers are the main indicators of the functional and structural performance of pavements.

The explanation of pavement performance is provided by performance models, which can be classified as (a) purely empirical (based only on historical data) or (b) mechanistic-empirical (mechanistic parameters, such as stresses, strains, and deflections, that are calculated according to a particular theory and methodology and that explain the performance of the pavement in terms of them). When it comes to designing bituminous pavements, the majority of modern pavement design techniques use the mechanistic-empirical solution. These approaches identify a critical mechanistic parameter for each of the chosen structural distresses and control it during the design phase to a reasonable (limited) value. From the performance models, the limiting values of these important mechanistic parameters are found(Li et al., 2011).

The design of flexible pavements under IRC: 37 continues to follow the mechanistic-empirical design approach that was employed in the second and third versions. In "linear elastic layered theory," which models the pavement as a multi-layer system, the pavement is analyzed. Since all of the upper levels are presumed to be finite in thickness and infinite in horizontal extent, the lowest layer, known as the subgrade or foundation, is regarded as semi-infinite. Inputs for the pavement that are needed to calculate the stresses, strains, and deflections caused by a load applied at the pavement's surface include elastic modulus, Poisson's ratio, and each layer's thickness. A revised version of FPAVE software called IITPAVE was created(IRC:37-2018, n.d.)

The vertical compressive strain on top of the subgrade is considered in these research to be the critical mechanistic parameter for controlling subgrade rutting. Horizontal tensile strain at the bottom of the bottom bituminous layer is taken as the causative mechanistic parameter which has to be limited to control bottom-up cracking in bituminous layers. Similarly, to ensure that the Cement Treated Bases (CTB) do not fail by fatigue cracking, tensile strain and tensile stress at the bottom of the CTB are considered to be the critical parameters to control(IRC:37-2018, n.d.).

Another significant problem with bituminous pavements is rutting, which is brought about by cumulative plastic (permanent) distortion in these layers as a result of repetitive application of traffic loads. Because the bituminous mix becomes less stiff at higher temperatures and because a larger percentage of plastic (irrecoverable) deformation occurs when pavement temperatures are higher and loading conditions are heavier, these factors can lead to the early development of unacceptable levels of rut depth in bituminous mixes. The two main issues to be considered are moisture damage to mixtures and brittle cracking caused by excessive age hardening of bitumen in the upper layers. By combining the mixed design into the structural design and taking these distresses into account,

The structural study of a multi-layered pavement that is subject to traffic loading forms the basis of the design processes. The design is predicated on the requirement that strains at three crucial points not beyond specific thresholds.

These limiting strains, shown in Fig. 3.19, are as follows:

- ✓ Vertical compressive strains at the surface of the subgrade (εv)
- ✓ Horizontal tensile strains in the bottom of the cement-treated layer (ε), and
- ✓ Horizontal tensile strains in the bottom of the asphalt concrete layer (εt).

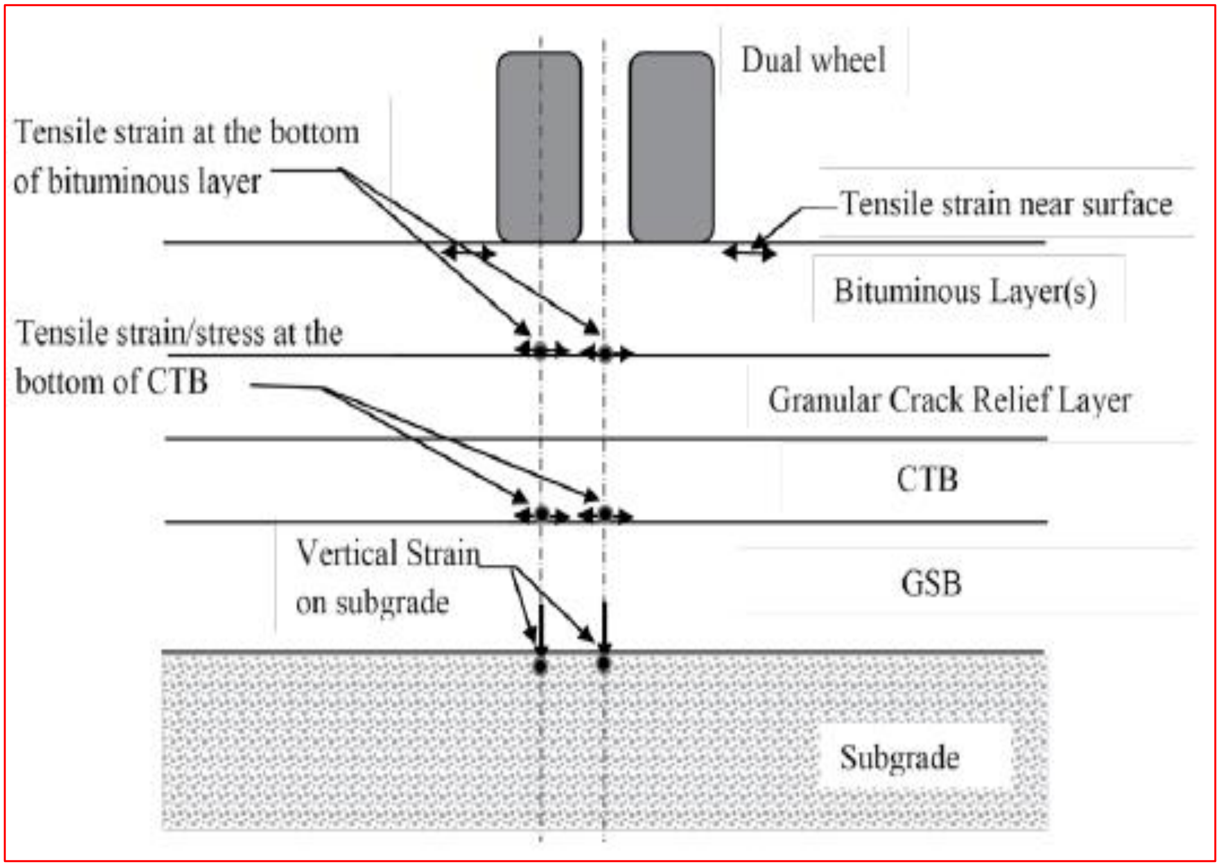


**Figure 3.19 Compressive and tensile strains at different layers**

The research recommends that pavement sections be chosen so that they satisfy the limiting stresses and strains prescribed by the performance models adopted in the research for subgrade rutting, bottom-up cracking of bituminous layer, and fatigue cracking of cement-treated bases. This were ensure that bituminous pavements perform satisfactorily and that the magnitudes of distress remain within acceptable levels during the service life period. Incorporating the mix of design elements that significantly impact pavement performance into the design process has resulted in the research suggesting further measures.

### 3.9.2 Analysis of Flexible Pavements

The pavement has been regarded as a linear elastic layered system to compute the stresses, strains, and deflections in this study. In this study, pavement analysis and design were conducted using IITPAVE software, which was created for the analysis of linear elastic layered systems. According to IRC37-2018, a mechanistic-empirical approach is used in the design of flexible pavement. When modeling pavements as a multi-layered system, the linear elastic theory is employed. First, traffic census data, CBR test results, and other geotechnical tests are used to establish the design traffic. After that, a trail composition is chosen in accordance with past performance or Code rules. IITPAVE software is used to determine the maximum strains at crucial places. The inputs are the thickness of each layer, the elastic modulus, and the Poisson's ratio. To analyze the CTB layer for a dual wheel configuration, a design load of 20KN is applied with 0.80MPa tire pressure. When dealing with a granular layer, a tire pressure of 0.56 MPa is taken into account. The maximum strain values are compared with the limiting strain values obtained from the performance criteria mentioned in the code.

## 3.10 Numerical Modeling

Numerical modeling refers to the use of mathematical models and computational algorithms to simulate physical systems and predict their behavior under various conditions. In the context of geotechnical and pavement engineering, numerical modeling involves using specialized software, such as PLAXIS 3D, to simulate and analyze the behavior of soil-structure systems, including pavements, under applied loads. This allows engineers to predict how materials (such as soil, asphalt, or cement-treated base) respond to external forces like traffic loads, environmental conditions, and construction processes. Numerical modeling is essential for optimizing pavement designs, evaluating performance, and reducing costs in road construction projects

### 3.10.1 Basic Geotechnical Properties for Numerical Modeling

The general properties required for simulating the soil material as per the Mohr-Coulomb model mainly include: bulk unit weight ($\gamma$, $kN/m^3$), saturated unit weight ($\gamma_{sat}$, $kN/m^3$), the at-rest coefficient of horizontal soil stress ($K_o$)…etc.

The bulk unit weight ($\gamma_{unsat}$, kN/m3) of the cohesive soil has been calculated (Eq. 3.1) by using the index property correlation recommended by (Carter, M. and Bentley S. P, 2016). Table A-2 in the appendix

$$\gamma unsat = \gamma d(1 + w) \quad [3.8]$$

$$Ko = 1 - Sin\varphi' \quad [3.9]$$

For a saturated state the degree of saturation S = 100%

$$eS = wGs \quad [3.10]$$

$$\gamma sat = \left(\frac{Gs+e}{1+e}\right) * \gamma w \quad [3.11]$$

### 3.10.2 Shear Strength Characteristics Parameters

The strength characteristics required for simulating the soil material as per the Mohr-Coulomb model mainly include effective cohesion (c'', kN/m$^2$), effective angle of internal friction (ϕ'', $^o$), and initial angle of dilatancy (ψ, $^o$). The relationship between the effective shear strength parameter (φ'') and plasticity index (PI) for remolded clays has been established by (Carter, M. and Bentley S. P., 2016).

$$\varphi'' = 0.085\text{PI}^{1.4} - 0.75\text{PI} + 31.9 \quad [3.12]$$

The other shear strength parameter effective cohesion value (c‟) had empirically correlated to effective friction angle (ϕ‟), as recommended by (Burt G. Look, 2007).

### 3.10.3 Elastic Properties of Materials or Stiffness Characteristics

The elastic deformation parameters of the soil material required as per Mohr Coulomb model include: Young's modulus (E) and Poisson's ratio (ν). The stiffness parameter (Young's modules, E) has been correlated with the California bearing ratio (CBR) value based on the poison's ratio (Elsa Eka Putri, et. al, 2012).

$$E = 863.83\ \text{CBR(kPa)}, \text{v} = 0.0 \quad [3.13]$$

$$E = 840.53\ \text{CBR(kPa)}, \text{v} = 0.3 \quad [3.14]$$

$$E = 751.00\ \text{CBR(kPa)}, \text{v} = 0.4 \quad [3.15]$$

### 3.10.4 PLAXIS-3D

PLAXIS 3D is a powerful finite element analysis (FEA) software used in geotechnical engineering to simulate the behavior of soil-structure interactions under various loading conditions. It is particularly useful for modeling complex pavement systems, such as flexible pavement and inverted pavement, which are subjected to traffic loads, environmental influences, and other dynamic forces. Below is a guide on how to use PLAXIS 3D for modeling flexible and inverted pavement systems, along with key considerations and steps for simulation.

#### 3.10.4.1 Numerical Modeling Overview of Flexible Pavement and Inverted Pavement

##### 3.10.4.1.1 Flexible Pavement

In a flexible pavement system**,** which typically consists of an asphalt surface layer, a granular base, a subbase, a capping, and a subgrade, PLAXIS 3D can be used to simulate the mechanical behavior of each layer under traffic loads. The asphalt layer, modeled with linear elastic or viscoelastic material properties, absorbs the direct traffic load and serves as the primary load-carrying component.

The granular base, represented using models such as Mohr-Coulomb acts to distribute the load and transfer stresses to the subgrade. The subgrade itself is typically modeled using Mohr-Coulomb based on its geotechnical properties. Traffic loading is applied as a vertical, uniform load (usually 80 kN per axle), and boundary conditions are defined to allow for free vertical movement at the top while restricting lateral displacement at the edges.

The staged construction process in PLAXIS 3D allows for the sequential activation of pavement layers, followed by load application in separate phases to observe the performance under realistic conditions. Static and cyclic loading analyses can be performed to evaluate stress distribution, settlement, and deformation under single or repeated traffic loads.

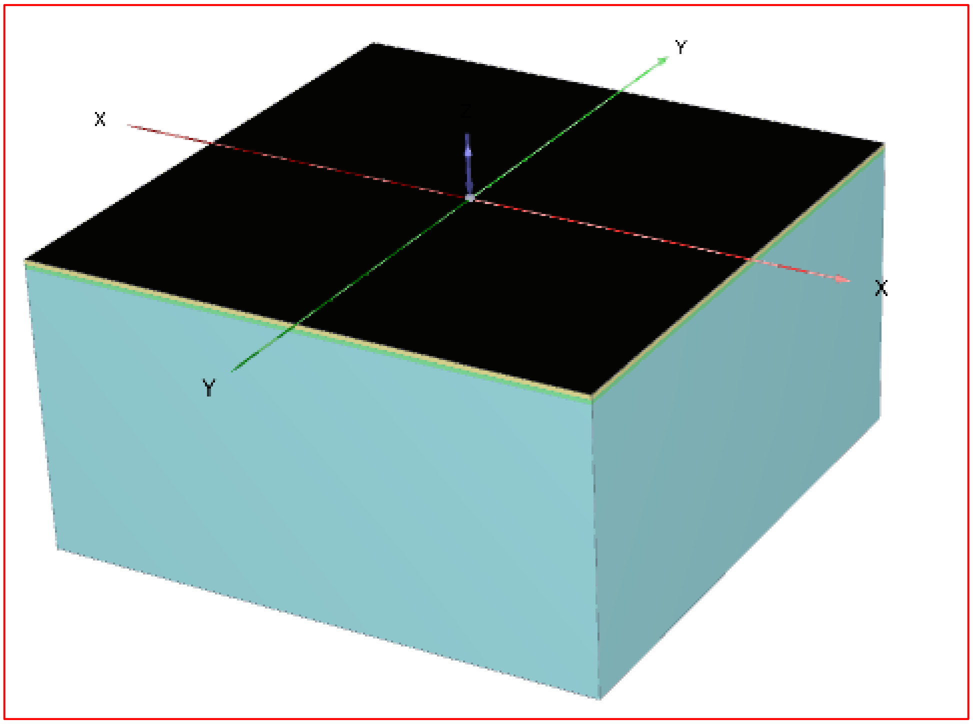


Figure 3.20 Modeling for Conventional Pavement

#### 3.10.4.1.2 Setting up a PLAXIS 3D Model for Flexible Pavement

Setting up a PLAXIS 3D model for flexible pavement involves defining the geometry, assigning material properties, and applying appropriate loading and boundary conditions to simulate the real-world behavior of the pavement system under traffic loads. First, the geometry of the pavement structure is established, which typically includes a surface asphalt layer, granular base, and subgrade. The asphalt layer, which forms the top surface, is modeled using linear elastic or viscoelastic material properties, depending on whether time-dependent behavior (such as rutting) is to be considered. The granular base layer, positioned beneath the asphalt, is modeled with a Mohr-Coulomb or Hardening Soil model to represent the material's stress-dependent behavior. The subgrade, representing the soil foundation, is usually modeled with a Mohr-Coulomb or Hardening Soil model to capture its plasticity and stress-dependent characteristics.

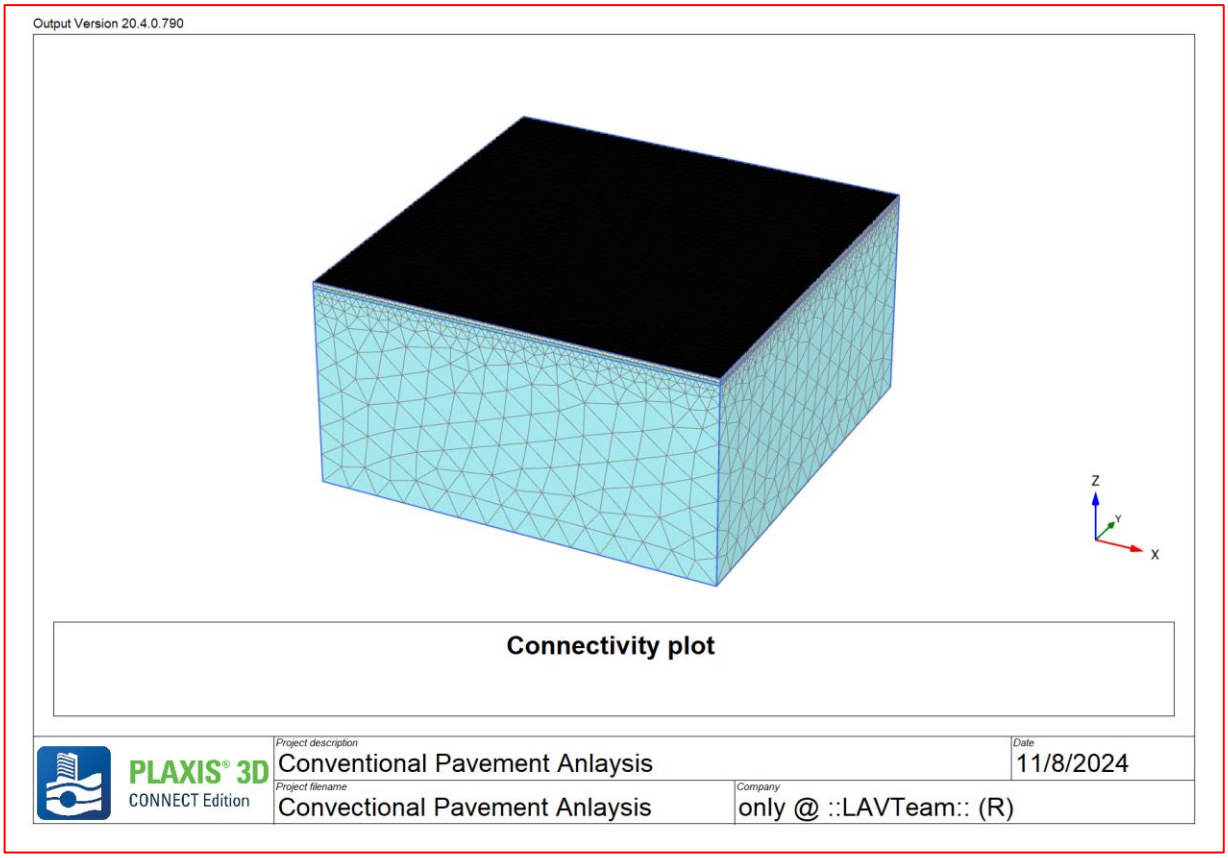


**Figure 3.21 Mesh generation for Conventional Pavement**

Next, the material properties for each layer, such as Elastic Modulus, Poisson's ratio, friction angle, cohesion, and density, are defined based on laboratory test results or standard pavement design values. For the granular base and subgrade, properties like shear strength and stiffness are critical for simulating load distribution and settlement accurately. Once the material properties are set, appropriate boundary conditions are applied. The top surface is left free to allow for vertical displacement under traffic loads, while the lateral boundaries are typically pinned to restrict horizontal movement, ensuring the pavement system behaves as it would in the field. The bottom boundary is generally fixed to prevent any vertical displacement, simulating a rigid foundation beneath the subgrade.

After the geometry and material properties are defined, traffic loading is applied. This is typically done using a static load, representing an axle load (e.g., 80 kN) applied over the surface of the asphalt layer. If a more dynamic, long-term analysis is required, cyclic loading can be applied to simulate repeated traffic loads and evaluate potential fatigue effects. In staged construction, the pavement layers are progressively activated, starting from the subgrade, followed by the granular base and asphalt layers, which allows for a more realistic simulation of construction sequences. After construction and loading phases are defined, the static analysis is run to assess stress distribution, settlement, and deformation under traffic loading. The results from this analysis provide valuable insights into the pavement's performance, including its ability to distribute loads, resist permanent deformation, and ensure long-term durability.

## Table 3.1: Materials Input Parameters for PLAXIS 3D Software

| TYPES OF MATERIAL | PLASTIC INDEX PI | Φ ANGLE OF INTERNAL FRICTION | AVERAGE Φ | C COHESION | CALIFORNIA BEARING RATIO (CBR) | ELASTICITY MODULUS VOID RATIO = 0 | ELASTICITY MODULUSE @v=0.3 | ELASTICITY MODULUSE @v=0.35 | AVERAGE ELASTICITY MODULUSE @v=0.35 | ELASTICITY MODULUSE @ v=0.4 | SPECIFIC GRAVITY (GS) | WATER CONTENT (w) | Dry Density γdry | VOID RATIO e=w*GS | UNIT WEIGHT OF WATER | SATURATED UNIT WEIGHT γsat=(GS+e)/(1+e) | UNSATURATED UNIT WEIGHT γunsat=γd(1+w) | γsat average | γunsat average |
|---|---|---|---|---|---|---|---|---|---|---|---|---|---|---|---|---|---|---|---|
| SUBGRADE SOIL | 28.00 | 19.92 | 19.24 | 9.62 | 2.00 | 1.73 | 1.68 | 1.59 | 1.39 | 1.50 | 2.50 | 19.70 | 1.64 | 0.49 | 1,000.00 | 20.05 | 19.63 | 20.20 | 18.96 |
| | 36.00 | 17.73 | | | 1.00 | 0.86 | 0.84 | 0.80 | | 0.75 | 2.53 | 22.40 | 1.47 | 0.57 | 1,000.00 | 19.77 | 17.99 | | |
| | 32.00 | 18.78 | | | 1.00 | 0.86 | 0.84 | 0.80 | | 0.75 | 2.52 | 16.00 | 1.57 | 0.40 | 1,000.00 | 20.83 | 18.21 | | |
| | 26.00 | 20.54 | | | 3.00 | 2.59 | 2.52 | 2.39 | | 2.25 | 2.50 | 19.00 | 1.68 | 0.48 | 1,000.00 | 20.17 | 19.99 | | |
| FILL MATERIAL | 20.26 | 22.44 | 24.02 | 14.02 | 25.00 | 21.60 | 21.01 | 19.89 | 21.09 | 18.78 | 2.67 | 12.00 | 1.85 | 0.32 | 1,000.00 | 22.65 | 20.72 | 22.47 | 20.71 |
| | 12.06 | 25.63 | | | 27.00 | 23.32 | 22.69 | 21.49 | | 20.28 | 2.67 | 12.50 | 1.84 | 0.33 | 1,000.00 | 22.52 | 20.70 | | |
| | 15.68 | 24.15 | | | 26.00 | 22.46 | 21.85 | 20.69 | | 19.53 | 2.67 | 13.40 | 1.83 | 0.36 | 1,000.00 | 22.30 | 20.75 | | |
| | 16.46 | 23.85 | | | 28.00 | 24.19 | 23.53 | 22.28 | | 21.03 | 2.67 | 13.00 | 1.83 | 0.35 | 1,000.00 | 22.40 | 20.68 | | |
| SUBBASE MATERIAL | 11.00 | 26.09 | 25.66 | 21.50 | 41.00 | 35.42 | 34.46 | 32.63 | 34.22 | 30.79 | 2.66 | 9.80 | 1.92 | 0.26 | 1,000.00 | 23.17 | 21.08 | 23.13 | 20.83 |
| | 12.00 | 25.66 | | | 44.00 | 38.01 | 36.98 | 35.01 | | 33.04 | 2.66 | 9.00 | 1.90 | 0.24 | 1,000.00 | 23.39 | 20.71 | | |
| | 12.00 | 25.66 | | | 45.00 | 38.87 | 37.82 | 35.81 | | 33.80 | 2.66 | 10.00 | 1.89 | 0.27 | 1,000.00 | 23.11 | 20.79 | | |
| | 13.00 | 25.23 | | | 42.00 | 36.28 | 35.30 | 33.42 | | 31.54 | 2.66 | 11.00 | 1.87 | 0.29 | 1,000.00 | 22.84 | 20.76 | | |
| BASE COURSE MATERIAL | 0.00 | 31.90 | 31.90 | 0.00 | 116.00 | 100.20 | 97.50 | 92.31 | 92.31 | 87.12 | 2.80 | 9.00 | 2.11 | 0.25 | 1,000.00 | 24.38 | 23.00 | 24.38 | 23.00 |
| | 0.00 | 31.90 | | | 116.00 | 100.20 | 97.50 | 92.31 | | 87.12 | 2.80 | 9.00 | 2.11 | 0.25 | 1,000.00 | 24.38 | 23.00 | | |
| | 0.00 | 31.90 | | | 116.00 | 100.20 | 97.50 | 92.31 | | 87.12 | 2.80 | 9.00 | 2.11 | 0.25 | 1,000.00 | 24.38 | 23.00 | | |
| | 0.00 | 31.90 | | | 116.00 | 100.20 | 97.50 | 92.31 | | 87.12 | 2.80 | 9.00 | 2.11 | 0.25 | 1,000.00 | 24.38 | 23.00 | | |
| CTB | 0.00 | 31.90 | 31.90 | 0.00 | | | 0.00 | 5,220.00 | 5,220.00 | 5,220.00 | 2.80 | 9.00 | 2.11 | 0.25 | 1,000.00 | 24.38 | 23.00 | 24.38 | 22.52 |
| | 0.00 | 31.90 | | | | | 0.00 | 5,220.00 | | 5,220.00 | 2.80 | 9.00 | 2.11 | 0.25 | 1,000.00 | 24.38 | 23.00 | | |
| | 0.00 | 31.90 | | | | | 0.00 | 5,220.00 | | 5,220.00 | 2.80 | 9.00 | 2.11 | 0.25 | 1,000.00 | 24.38 | 23.00 | | |
| | 0.00 | 31.90 | | | | | 0.00 | 5,220.00 | | 5,220.00 | 2.80 | 9.00 | 2.11 | 0.25 | 1,000.00 | 24.38 | 21.10 | | |

#### 3.10.4.1.3 Inverted Pavement

In contrast, an **inverted pavement system** features a **cement-treated base (CTB)** layer placed above the subgrade, with a granular interlayer between the CTB and the subgrade. This unique configuration aims to improve load distribution and reduce rutting by transferring stresses more evenly across the pavement layers. In PLAXIS 3D, the **CTB layer** is typically modeled with linear elastic or Mohr-Coulomb material properties to reflect its enhanced load-carrying capacity. The granular interlayer is modeled similarly to the granular base in a flexible pavement, but its role in supporting the CTB and distributing loads is emphasized. The subgrade in the inverted system is modeled in the same way as in the conventional flexible pavement, but its performance is improved due to the load redistribution provided by the CTB. As in the flexible pavement model, traffic loads are applied to the surface layer, and boundary conditions are defined to prevent excessive displacement. The analysis focuses on understanding the performance of the CTB layer in terms of stress distribution, deformation, and its impact on the subgrade.

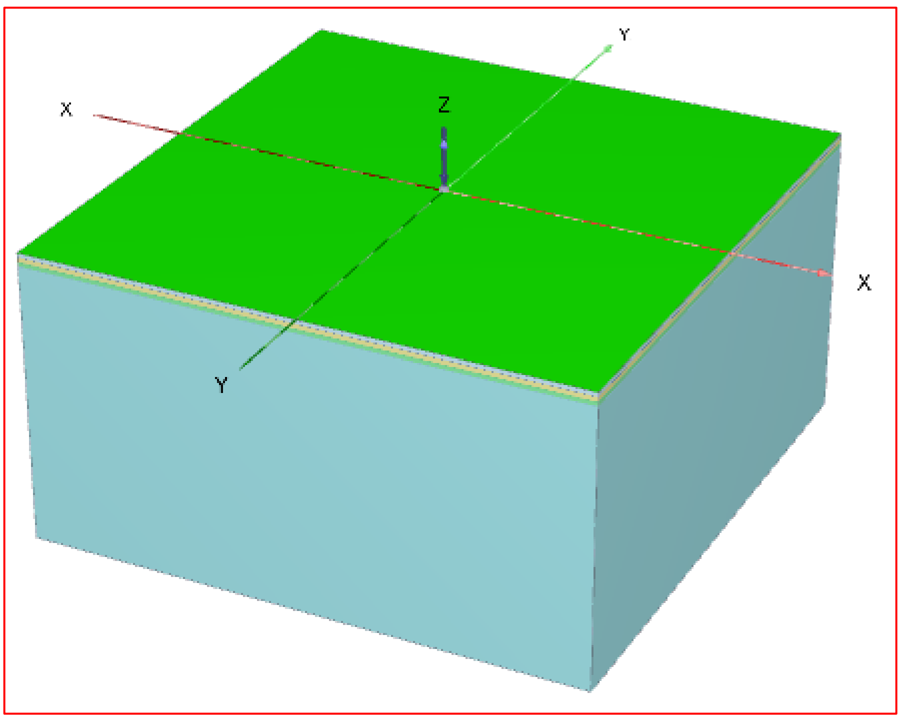


**Figure 3.22 Modeling for Inverted Pavement**

#### 3.10.4.1.4 Setting up a PLAXIS 3D Model for Inverted Pavement

Setting up a PLAXIS 3D model for an inverted pavement system requires defining the geometry, material properties, loading conditions, and boundary conditions to simulate the unique structure and behavior of this type of pavement. Inverted pavements typically feature a cement-treated base (CTB) layer placed on top of the subgrade, with a granular interlayer between the CTB and subgrade, and a traditional asphalt surface layer on top.

First, the geometry of the pavement system is created, which involves defining the asphalt surface layer, cement-treated base (CTB) layer, granular interlayer, and subgrade. The asphalt layer is modeled similarly to flexible pavements, usually with a linear elastic or viscoelastic material model to simulate its behavior under traffic loads. The CTB layer, which is one of the distinguishing features of inverted pavements, is modeled using a linear elastic or Mohr-Coulomb model. The CTB layer, being cement-stabilized, is much stiffer than the granular base and plays a crucial role in distributing loads to the subgrade and reducing rutting. The granular interlayer, placed between the CTB and subgrade, is modeled with similar properties to the granular base in a conventional pavement but with a slightly different stiffness to reflect its function in stress distribution. The subgrade is typically modeled using a Mohr-Coulomb or Hardening Soil model, depending on the soil properties, to represent the soil’s response under the applied loads.

Once the geometry is set, material properties must be assigned to each layer. The asphalt layer should have properties such as Elastic Modulus, Poisson’s ratio, and density to reflect its elasticity and strength. The CTB layer requires properties such as Young’s Modulus, Poisson’s ratio, and shear strength to represent the cement-stabilized material. The granular interlayer is assigned similar properties to the base material in a flexible pavement, including friction angle and cohesion, but with a focus on its role in improving load distribution. For the subgrade, modulus of elasticity, friction angle, cohesion, and Poisson’s ratio are defined based on geotechnical test data or standard values for the region.

Next, the boundary conditions are defined to simulate realistic behavior. The top surface is left free to allow for vertical displacement under load, while the lateral boundaries are typically pinned to prevent horizontal movement. The bottom boundary is usually fixed to prevent vertical displacement, simulating an immovable foundation below the subgrade. For more realistic behavior, the subgrade's bottom layer can be modeled with free-field conditions (if applicable) to allow for natural settlement beneath the pavement.

Once the geometry, material properties, and boundary conditions are set, traffic loading is applied to the asphalt surface. A typical static load, such as an 80 kN axle load, is applied, simulating the impact of a heavy vehicle's wheel load. For more detailed analysis, cyclic loading can be applied to simulate the effects of repeated traffic loads over time, which is especially important for evaluating long-term pavement performance and fatigue. The model can be constructed in staged construction, where each layer is progressively activated during the analysis, beginning with the subgrade and working up to the asphalt layer. This staged approach ensures that the material behavior during construction and load application is accurately captured.

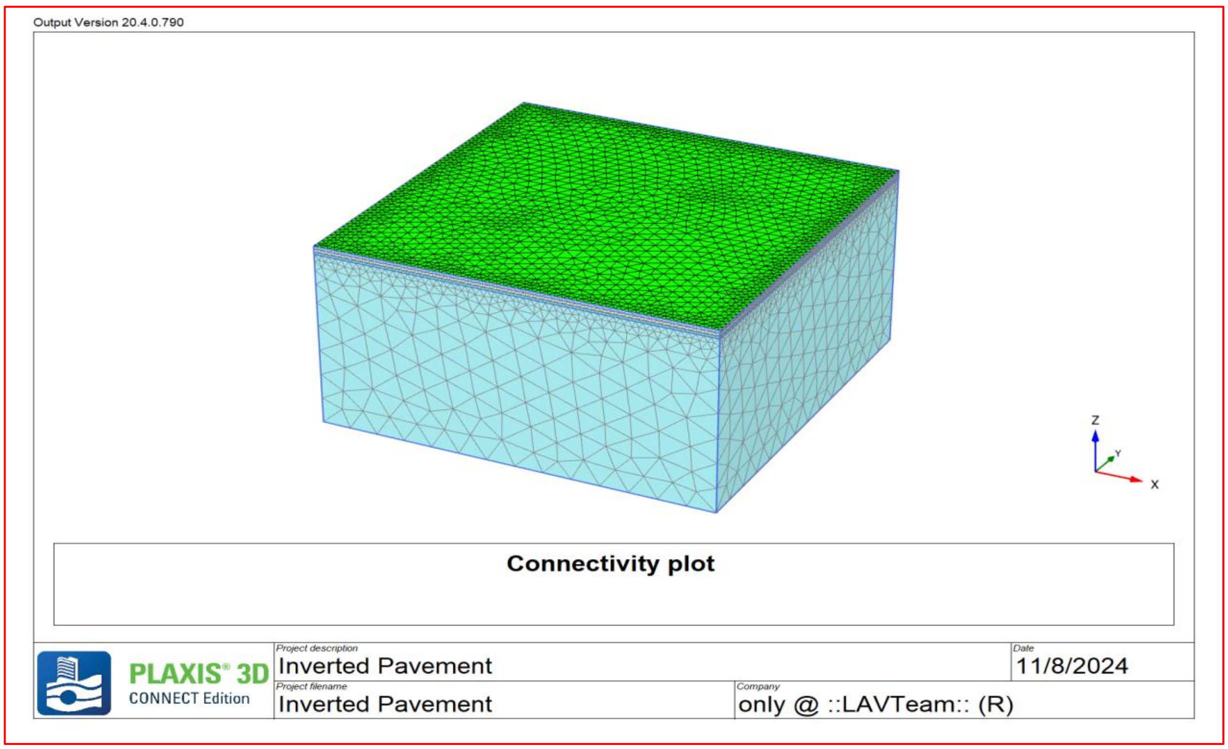


**Figure 3.23 Mesh generation for Inverted Pavement**

Finally, after construction and load application, a static analysis or cyclic analysis is run to evaluate the pavement's stress distribution, deformation, rutting potential, and settlement under traffic loading. The model provides insights into the load distribution through the CTB layer and how well the inverted pavement system reduces stress concentrations on the subgrade. The analysis can also highlight the fatigue performance of the pavement and predict how the system will behave over time, making it easier to assess the effectiveness of the inverted pavement design, especially in areas with weak subgrades or heavy traffic.

Through this process, PLAXIS 3D enables a detailed evaluation of the inverted pavement system's performance under realistic loading conditions, offering valuable information to optimize the design for durability, cost-efficiency, and long-term sustainability.

### 3.10.5 IITPAVE Software

IITPAVE is a software tool developed by the Indian Institute of Technology for the analysis and design of flexible pavement structures. This software assists engineers and designers in evaluating the structural performance of pavement layers under various loading conditions, ensuring optimal design and longevity of the pavement. IITPAVE employs a layered elastic analysis approach to model the pavement structure, considering each layer's material properties such as elastic modulus, Poisson's ratio, and thickness. Users input these parameters along with traffic load characteristics, including the magnitude and distribution of axle loads. The software's user-friendly interface allows for easy input of data, and the model setup includes defining geometric dimensions and boundary conditions to simulate real-world constraints.

Once the input data is prepared and the model is set up, the analysis is executed to calculate the stresses, strains, and deflections within the pavement layers. The results provide insight into the distribution of these factors, identifying high-stress concentrations and potential failure points. The deflection profile is reviewed to ensure that the pavement can accommodate anticipated loads without excessive deformation. The software also evaluates the pavement's resistance to fatigue cracking and rutting, which are key indicators of long-term performance.

Based on the analysis, users can optimize the pavement design by selecting appropriate materials and adjusting the thickness of each layer to balance cost and performance. This iterative process ensures that the pavement structure is both robust and economical. IITPAVE also facilitates the generation of detailed reports, including graphical representations of stress, strain, and deflection distributions, which are essential for documenting the design process and validating decisions.

IITPAVE is used not only for designing new pavements but also for pavement rehabilitation, performance evaluation, and research and development. It helps in designing overlays and rehabilitation measures for existing pavements, addressing issues such as cracking and rutting, and serves as a valuable tool for academic and industry research, facilitating the development of new materials and pavement designs. By incorporating IITPAVE into the pavement design process, engineers can ensure that pavements are durable, cost-effective, and capable of withstanding the demands of traffic and environmental conditions.

To use IITPAVE, start by downloading and installing the software from the official source. Once installed, open the application and create a new project by selecting "New Project" from the File menu, and enter the project name and details. Next, define the pavement layers by navigating to the "Layer" tab, where you can specify the thickness, material properties (such as modulus of elasticity and Poisson’s ratio), and type of each layer (e.g., asphalt concrete, CTB, granular base, or subgrade).

After defining the layers, move to the "Load" tab to set the traffic loading conditions, including the load magnitude, contact area, and load position on the pavement surface. In the "Boundary" tab, set the boundary conditions by defining the constraints and conditions at the edges of the pavement model. With all inputs defined, go to the "Run" tab and click "Run Analysis" to perform the pavement analysis. The software were then compute the stresses, strains, and deflections within the pavement system.

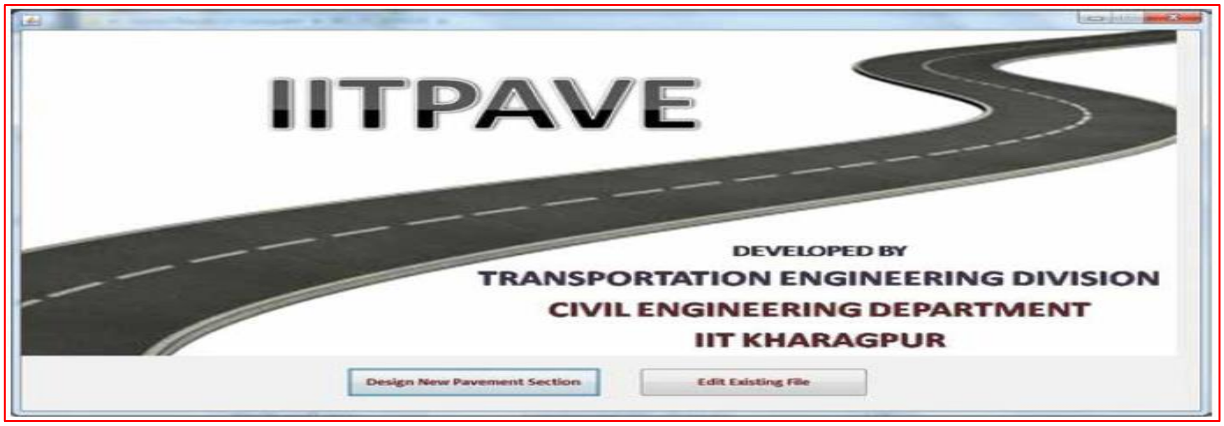


**Figure 3.24 Screenshot of IITPAVE start screen**

Once the analysis is complete, view the results in the "Results" tab, where you can access graphical and tabular data on stresses, strains, and deflections. Analyze these results to evaluate the pavement system's performance under the specified loading conditions. Save the project and export the results as needed for documentation and presentation. To ensure accuracy, use precise input data for layer properties, load conditions, and boundary conditions, and maintain detailed documentation of each project, including inputs, assumptions, and analysis results. Understanding how to interpret the results were help in making informed decisions about pavement design and performance, contributing to the development of durable and efficient road structures.

#### 3.10.5.1 Design Lane and Lane Distribution Factor

The design lane (direction) of a road is the lane (direction) with the heaviest traffic load for which the pavement is designed, and mainly depends on the volume of traffic and the axle load damaging effect; and a lane distribution factor is the factor used to consider the overlap of the traffic in using traffic lanes, and is dependent on the number of lanes of the road. While determining the design lane distribution factor, number of lanes of the road project is first determined. it can be noted that the number of lanes for most of the road segments is three for each direction. According to AASHTO Pavement design Manual, for roads with such number of lanes, a distribution factor between 60% - 80% is considered. Considering the average value a distribution factor of 70% is recommended.

### 3.10.5.2 Design Traffic in terms of cumulative number of ESA (CESA)

Based on the cumulative traffic volume for each class of vehicles in one direction over the design period and the corresponding equivalency factors, the cumulative number of equivalent standard axles over the design period is determined using the formula given below. The design period for the analysis is 20 years from the year 2023.

CESA = EF*(0.7*AADT*365*((1+i) n - 1)/i),

Where i is the growth rate

**Table 3.6 Cumulative number of ESA and Traffic Class (Source from AACRA)**

| Megenagna-Imperial-Bole | | | | | | | | | | |
|---|---|---|---|---|---|---|---|---|---|---|
| Year | Cummulative ESA | | | | | Total AADT | Number of ESA | Traffic Class | Cummulative Number of ESA | Traffic Class |
| | Cars and Taxi | LGV | Medium | Heavy | Truck-Trailer | | | | | |
| 2023 | | 745,516.00 | 104,614.00 | 1,173,382.00 | 740,608.00 | 2,764,120.00 | 2,764,120.00 | T4 | 74,629,855.00 | T10 |
| 2024 | | 804,411.00 | 113,611.00 | 1,274,293.00 | 815,410.00 | 5,771,845.00 | 5,771,845.00 | T5 | | |
| 2025 | | 867,960.00 | 123,381.00 | 1,383,882.00 | 897,766.00 | 3,272,989.00 | 9,044,834.00 | T6 | | |
| 2026 | | 936,529.00 | 133,992.00 | 1,502,896.00 | 988,440.00 | 3,561,857.00 | 12,606,691.00 | T7 | | |
| 2027 | | 1,010,515.00 | 145,515.00 | 1,632,145.00 | 1,088,273.00 | 3,876,448.00 | 16,483,139.00 | T7 | | |
| 2028 | | 1,010,515.00 | 145,515.00 | 1,632,145.00 | 1,088,273.00 | 3,876,448.00 | 20,359,587.00 | T8 | | |
| 2029 | | 1,010,515.00 | 145,515.00 | 1,632,145.00 | 1,088,273.00 | 3,876,448.00 | 24,238,034.00 | T8 | | |
| 2030 | | 1,010,515.00 | 145,515.00 | 1,632,145.00 | 1,088,273.00 | 3,876,448.00 | 28,112,482.00 | T8 | | |
| 2031 | | 1,010,515.00 | 145,515.00 | 1,632,145.00 | 1,088,273.00 | 3,876,448.00 | 31,988,930.00 | T9 | | |
| 2032 | | 1,010,515.00 | 145,515.00 | 1,632,145.00 | 1,088,273.00 | 3,876,448.00 | 35,865,378.00 | T9 | | |
| 2033 | | 1,010,515.00 | 145,515.00 | 1,632,145.00 | 1,088,273.00 | 3,876,448.00 | 39,741,825.00 | T9 | | |
| 2034 | | 1,010,515.00 | 145,515.00 | 1,632,145.00 | 1,088,273.00 | 3,876,448.00 | 43,618,273.00 | T9 | | |
| 2035 | | 1,010,515.00 | 145,515.00 | 1,632,145.00 | 1,088,273.00 | 3,876,448.00 | 47,494,721.00 | T9 | | |
| 2036 | | 1,010,515.00 | 145,515.00 | 1,632,145.00 | 1,088,273.00 | 3,876,448.00 | 51,371,169.00 | T10 | | |
| 2037 | | 1,010,515.00 | 145,515.00 | 1,632,145.00 | 1,088,273.00 | 3,876,448.00 | 55,247,616.00 | T10 | | |
| 2038 | | 1,010,515.00 | 145,515.00 | 1,632,145.00 | 1,088,273.00 | 3,876,448.00 | 59,124,064.00 | T10 | | |
| 2039 | | 1,010,515.00 | 145,515.00 | 1,632,145.00 | 1,088,273.00 | 3,876,448.00 | 63,000,512.00 | T10 | | |
| 2040 | | 1,010,515.00 | 145,515.00 | 1,632,145.00 | 1,088,273.00 | 3,876,448.00 | 66,876,960.00 | T10 | | |
| 2041 | | 1,010,515.00 | 145,515.00 | 1,632,145.00 | 1,088,273.00 | 3,876,448.00 | 70,753,407.00 | T10 | | |
| 2042 | | 1,010,515.00 | 145,515.00 | 1,632,145.00 | 1,088,273.00 | 3,876,448.00 | 74,629,855.00 | T10 | | |

Design Traffic Classes According to the sub-grade and traffic class the cumulative number of ESA is 75 million and the traffic classification is T10 for the sections of the Megenagna-Imperial -Bole roads. Whereas the subgrade class is S3 for the whole section of the road. Hence, the road is designed using ERA Pavement Design Manual, 2013, Chart D1 for traffic class T10 to meet the desired pavement surfacing type in accordance to the traffic class to carry the traffic loading on each road segment in the design period. Table 3.7 it show that traffic classification using ERA 2013 PDM.

Table 3.7 Traffic classification using ERA 2013 PDM

| Road Section | Traffic Loading | Subgrade | | Pavement Layer Thicknesses (mm) | | | | | ERA-2013 (PDM) |
|---|---|---|---|---|---|---|---|---|---|
| | Traffic Class | Design Subgrade CBR at 93% MDD | Subgrade Class | HMA | DBM | Base course | Subbase | Improved Subgrade | |
| Megenagna-Imperial-Bole Airport | T-10 | 5 | S-3 | 90 | 220 | _ | 175 | 150 | Chart D1 |

Table 3.8 it shows that the pavement design of the original design chart D1 and the research design including structural numbers. The following table provides the basis for converting SN in to actual thicknesses of surfacing, base and sub base:

**Table 3.8 the following table provides the basis for converting SN in to actual thicknesses of surfacing, base and sub base:**

| Layer | Coefficient | Correction | Factored | Orginal Design | Research CTB |
|---|---|---|---|---|---|
| **Asphalt AC** | 0.4 | 1.00 | 0.4 | 90 | 125 |
| **Crack Relief Layer** | 0.145 | 1.00 | 0.145 | 0 | 150 |
| **CTB** | 0.233 | 1.00 | 0.233 | 0 | 225 |
| **DBM** | 0.4 | 1.00 | 0.4 | 220 | 0 |
| **Subbase** | 0.13 | 1.00 | 0.13 | 175 | 175 |
| **Capping** | 0.08 | 1.00 | 0.08 | 150 | 150 |
| Structural Number (SN)= a1D1 + a2D2m2 + a3D3m3 | | | | 6.25 | 6.26 |
| al, a2, a3 = layer coefficients representative of surface, base, and sub base courses, respectively | | | | | |
| D1, D2, D3 = actual thicknesses (in inches) of surface, base, and sub base courses, respectively, and | | | | | |
| m2, m3 = drainage coefficients for base and sub base layers, respectively (which are 0.8 and 0.6 for AA weather condition) | | | | | |

### 3.10.5.3 Determination of effective CBR/Resilient Modulus of soil subgrade

CBR test have been carried on 4 days soaked soil sample on various spots along the road stretch. The design CBR is taken the 90th percentile subgrade CBR value. The design CBR value is 6%. Hence resilient modulus of the subgrade were determined from the formulae given below.

$$M_{RS} = 10.0 * CBR \quad \text{for } CBR \leq 5\,\%$$

$$M_{RS} = 17.6 * (CBR)^{0.64} \quad \text{for } CBR > 5\,\%$$

Where

MRS = Resilient Modulus of subgrade soil in MPa

CBR= California bearing ratio (in percent) of subgrade soil.

Here for 7% CBR value, Resilient Modulus of subgrade soil is 61.15 MPa. The subgrade is improved by borrow material layer whose CBR value is 20%. The resilient modulus of existing borrow material layer is 119.72 MPa. Therefore effective CBR is to be determined using IITPAVE software. The poisson's ratio of subgrade soil is taken as 0.35. From IITPAVE software, maximum surface deflection is obtained as 1.44 mm.

```
No. of layers              2
E values (MPa)          119.70   61.15
Mu values                 0.350.35
thicknesses (mm)        500.00
single wheel load (N) 40000.00
tyre pressure (MPa)       0.56
Single Wheel
  Z        R       SigmaZ       SigmaT      SigmaR      TaoRZ       DispZ       epZ         epT         epR
  0.00     0.00-0.5525E+00-0.4860E+00-0.4860E+00 0.0000E+00 0.1443E+01-0.1774E-02-0.1023E-02-0.1024E-02
```

**Figure 3. 25 IITPAVE Software maximum surface deflection**

Now using the maximum surface deflection, the resilient modulus of the equivalent single layer is determined from the formula given below.

$$M_{RS} = \frac{2(1-\mu^2)pa}{\delta}$$

Where

p = contact pressure = 0.56 MPa

a = radius of circular contact area, which can be calculated using the load applied (40,000 N) and the contact pressure ‘p’ (0.56 MPa) = 150.8 mm

μ = Poisson’s ratio

δ = Maximum surface deflection

From the above formula, resilient modulus of the equivalent single layer is obtained as 102.92MPa but the maximum resilient modulus for subgrade is 100 MPa according to IRC. Therefore take value 100 MPa were be used in design. The corresponding effective CBR value is 15.8%.

#### 3.10.5.4 Design and Analysis of Cement Treated Base.

Initially the following compositions are considered.

- ✓ 125mm thick bituminous course comprising of bituminous concrete and dense bituminous macadam with VG40 grade bitumen.
- ✓ 150mm granular crack relief layer.
- ✓ 225mm cement treated base course
- ✓ 175mm cement treated sub-base course.
- ✓ Subgrade

The elastic properties of different layers are as follows in table 3.9.

**Table 3.9 Elastic properties of different layers**

| Material Type | Elastic/Resilient Modulus (MPa) | Poisson’s Ratio |
|---|---|---|
| Bituminous layer with VG40 or Modified Bitumen | 3000 or tested value (whichever is less) | 0.35 |
| Crack Relief Layer (Granular interlayer) | 450 | 0.35 |
| Cement treated base | 5000 | 0.25 |
| Subbase | 300 for natural gravel | 0.35 |
| | 350 for crushed aggregates | 0.35 |
| Subgrade Use Eq. 3.1 or 3.2 | MRS = 10.0 * CBR for CBR $\leq$ 5 % | 0.35 |
| | MRS = 17.6 * $(CBR)^{0.64}$ for CBR > 5 % | 0.35 |

### 3.10.5.5 Performance Criteria

The following performance criteria are used in this research for the design of bituminous pavements

#### 3.10.5.5.1 Subgrade rutting criteria

According to this research, a critical or failure rutting situation is defined as an average rut depth of 20 mm or higher, measured along the wheel paths. Equations 3.1 and 3.2, for 80% and 90% reliability levels, respectively, provide the equivalent number of standard axle load (80 kN) repetitions that the pavement can support before the critical average rut depth of 20 mm or higher occurs. The rutting performance model was first created using performance data from the MoRTH R-6 Research Scheme. Later, using additional performance data gathered for the MoRTH R-56 Research Scheme, two distinct models for two distinct dependability levels were created (IRC:37-2018, n.d.)

$NR = 4.1656 \times 10\text{-}08\ [1/\varepsilon v]^{4.5337}$ (for 80 % reliability)

$NR = 1.4100 \times 10\text{-}08\ [1/\varepsilon v]^{4.5337}$ (for 90 % reliability)

Where, NR= subgrade rutting life (cumulative equivalent number of 80 kN standard axle loads that can be served by the pavement before the critical rut depth of 20 mm or more occurs)

εv = vertical compressive strain at the top of the subgrade calculated using linear elastic layered theory by applying standard axle load at the surface of the selected pavement system

IITPAVE software is used in this research for the analysis of pavements. For the computation of stresses, strains, and deflections in the pavement, thicknesses and elastic properties (elastic modulus and Poisson’s ratio) of different layers are the main inputs.

$NR = 1.4100 \times 10\text{-}08\ [1/\varepsilon v]^{4.5337}$ (for 90 % reliability)

$74{,}629{,}855 = 1.4100 * 10\wedge^{-8} (1/\ \varepsilon v)^{4.5337}$

Allowable vertical strain εv=0.00034

Substitute NR with design traffic to obtain allowable vertical strain εv. εv allowable = 0.000331

Now find the maximum vertical compressive strain using IITPAVE software. εv= 0.000112 which is less than the allowable strain. Hence safe.

**3.10.5.5.2 Fatigue cracking criteria for bituminous layer**

Following performance models are used for fatigue cracking check for bituminous layer for different percentage of reliability. Here 90% reliability is considered since the design traffic is more than 20msa.

The critical or failure condition is fatigue cracking, which manifests as related cracks and occupies a total area in the road section under consideration that is at least 20% greater than the paved surface area of the section. Equations 3.3 and 3.4, for the 80% and 90% reliability levels, respectively, indicate the corresponding number of standard axle (80 kN) load repetitions that the pavement can tolerate before the critical condition of the cracked surface area of 20% or greater occurs. The fatigue performance models in Equations 3.3 and 3.4 were developed with the MoRTH R-56 methodology(IRC:37-2018, 2018).

$$N_f = 1.6064*C*10^{-04}\,[1/\varepsilon_t]^{3.89}*\,[1/M_{Rm}]^{0.854} \quad \text{(for 80 \% reliability)}$$

$$N_f = 0.5161*C*10^{-04}\,[1/\varepsilon_t]^{3.89}*\,[1/M_{Rm}]^{0.854} \quad \text{(for 90 \% reliability)}$$

Where

$$C = 10^{M}, \quad \text{and} \quad M = 4.84\left(\frac{Vbe}{Va+Vbe} - 0.69\right)$$

Va = percent volume of air void in the mix used in the bottom bituminous layer

Vbe = percent volume of effective bitumen in the mix used in the bottom bituminous layer

Nf = fatigue life of bituminous layer (cumulative equivalent number of 80 KN standard axle loads that can be served by the pavement before the critical cracked area of 20 % or more of paved surface area occurs)

εt = maximum horizontal tensile strain at the bottom of the bottom bituminous layer (DBM) calculated using linear elastic layered theory by applying standard axle load at the surface of the selected pavement system

MRm = resilient modulus (MPa) of the bituminous mix used in the bottom bituminous layer, selected as per the recommendations made in this research.

Here as per the guidelines given in the code (12.3,page no 37), for flexible pavement with CTB , Va and Vbe are taken as 3.5% and 11.5% respectively and factor C were be 2.35. Resilient modulus for above equation is 3000 MPa. Substituting Nf as the design traffic to obtain allowable tensile strain at the bottom of the bituminous layer.

$$N_f = 0.5161 * C * 10^{-04} [1/\varepsilon_t]^{3.89} * [1/M_{Rm}]^{0.854} \quad \text{(for 90 \% reliability)}$$

#### 3.10.5.5.3 Fatigue Performance Models for Cement Treated Base (CTB)

In the case of pavements with a CTB layer, a fatigue performance check for the CTB layer should be carried out as per equation 3.5 (based on cumulative standard axle load repetitions estimated using vehicle damage factors), and as per equations 3.6 and 3.7 (cumulative fatigue damage analysis) using axle load spectrum data. It may be noted that ‘cement treated’ refers to stabilization by different types of cementitious materials such as cement, lime, fly ash, or a combination thereof. The terms, ‘cement treated’ and ‘cementitious’, have been used interchangeably in this research. Equation 3.5 is based on the Australian experience (Rivki et al., n.d.) whereas equation 3.6 is as per the recommendations of the Mechanistic-Empirical Pavement Design Guide (IRC:37-2018, 2018).

To calculate the tensile strain (εt) value at the bottom of the CTB layer, pavement analysis using IITPAVE with a contact stress of 0.8 MPa on the pavement surface must be performed. Equation 3.5 yields several standard axle loads that must not be less than the design traffic when the computed tensile strain value is substituted along with other inputs.

$$N = RF \left[ \frac{\left(\frac{113000}{E^{0.804}} + 191\right)}{\varepsilon_t} \right]^{12}$$

Where,

RF = reliability factor for cementitious materials for failure against fatigue

= 1 for Expressways, National Highways, state highways, Urban Roads, and other categories of roads if the design traffic is more than 10 MSA

= 2 for all other cases

N = number of standard axle load repetitions that the CTB can sustain

E = elastic modulus of CTB material (MPa)

$\varepsilon t$ = tensile strain at the bottom of the CTB layer (micro strain)

Here RF is taken as 1 for design traffic more than 10 MSA, E is taken as 5000 MPa and limiting tensile strain is obtained by substituting the N with design traffic.

### 3.11 Cost Comparison

A comprehensive cost comparison between Cement-Treated Base (CTB) and Dense Bituminous Macadam (DBM) involves evaluating initial and long-term costs, including materials, construction, maintenance, and lifecycle expenses. For initial costs, CTB consists of aggregates, cement, and water, while DBM comprises aggregates, bitumen, and filler materials. The construction process for CTB involves mixing aggregates with cement and water, spreading, compacting, and curing, requiring specialized equipment and skilled labor. DBM construction involves heating and mixing aggregates with bitumen, spreading, and compacting using pavers, also requiring specialized equipment and skilled labor.

In terms of maintenance costs, CTB has a lower frequency of maintenance due to its high durability, typically involving minor repairs and occasional sealing. Conversely, DBM has a higher frequency of maintenance due to its susceptibility to water damage and deformation, requiring regular crack sealing, surface dressing, and periodic resurfacing. The lifespan of CTB is generally longer, lasting around 20-30 years or more, while DBM lasts about 10-20 years depending on traffic and environmental conditions.

CTB offers high load-bearing capacity and better resistance to water damage and temperature variations, resulting in lower long-term maintenance costs. DBM, while providing good initial flexibility and load-bearing capacity, is prone to damage from environmental factors, leading to higher long-term maintenance costs.

The cost comparison were offer valuable insights into the economic viability of utilizing cement-treated base materials compared to conventional alternatives, facilitating informed decision-making in pavement construction practices.

### 3.12 Data Processing and Analysis

The laboratory test results of both Subgrade Soil and Cement-treated crushing aggregate base courses were primary data sources. In processing and analysis, a literature review of research papers and data from laboratory results were analyzed to come up with an output. Laboratory results were checked for accuracy and were compared to the output with the available standard specifications. Finally, the organization and presenting the results of the analysis were done in accordance with the research objective.

### 3.13 Ethical Consideration

Samples that were used for this experiment have to be collected from a specified location after permission has been given by the local authority.

# 4. Results and Discussions

## 4.1 Laboratory Test Result, Data Analysis and Interpretation

The data analysis and interpretation are based on field investigation works and laboratory tests, which help to assess and determine the engineering property of subgrade and construction materials to be used for the construction of roads. During the fieldwork, sampling of subgrade and construction materials was undertaken, and the samples were carried to the central laboratory for pertinent tests that can help to define the type and quality of the respective materials.

The tests are conducted, and the results are analyzed with respect to ERA Pavement Design Manual 2013, ERA Standard Technical Specification 2013, AASHTO Standard Specification for Transportation Materials and Methods of Sampling and Testing, Part I and Part II, Latest edition, and ERA 2011 Design Standard for Low Volume Roads and other pertinent manuals. The analysis and interpretation of the test results are discussed in detail in the subsequent sections.

### 4.1.1 Subgrade Soil Analysis.

The subgrade soil was investigated by visual observation, pit excavation, and sampling of representative soil layers from the test pits. As mentioned above, samples of sub-grade materials were collected from the road alignment at every required interval to assess the properties of the roadbed materials. Classification tests (sieve analysis, Atterberg limits, and natural moisture content), modified proctor, three-point CBR, and swell tests were conducted. The test results are summarized and presented in Appendix III.

### 4.1.2 Plasticity Analysis

An indication as to the nature of the soil along the route may be given by the variation in the Plasticity Index (PI). The PI is influenced by the type and proportion of clay minerals present within the material, and high PI values are often an indication of the expansiveness of the soil.

The variation of PI and Liquid limit along the project road is presented in the figure below. It can be seen from the figure that the values of PI range from 32 to 36% for most of the samples, while that of the Liquid limit range from 54 to 69%, for research road alignment. The PI and the

LL test results indicate that the soil has a plastic nature, and confirm that the material has expansiveness behavior.

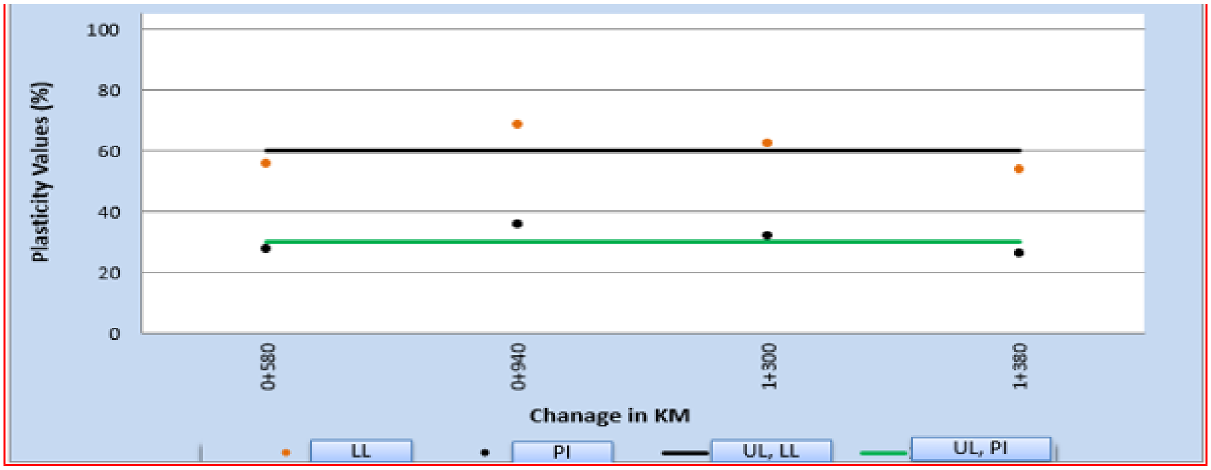


**Figure 4.1 – Plasticity Distribution of the project**

The plasticity of soil can also be expressed in terms of the plasticity chart shown below. The plasticity chart helps to classify the type of soils based on their plasticity characteristics (i.e. Atterberg Limits and Indices of soils). Generally, materials falling above the A-Line are classified as clays, and below the A-Line are classified as silts.

As can be noted from the graphs below, the majority of soils along the research road alignment fall above the A-Line in group CH, and it is described as high plasticity clay soil. The plasticity chart of sub-grade soil is presented in Figure below.

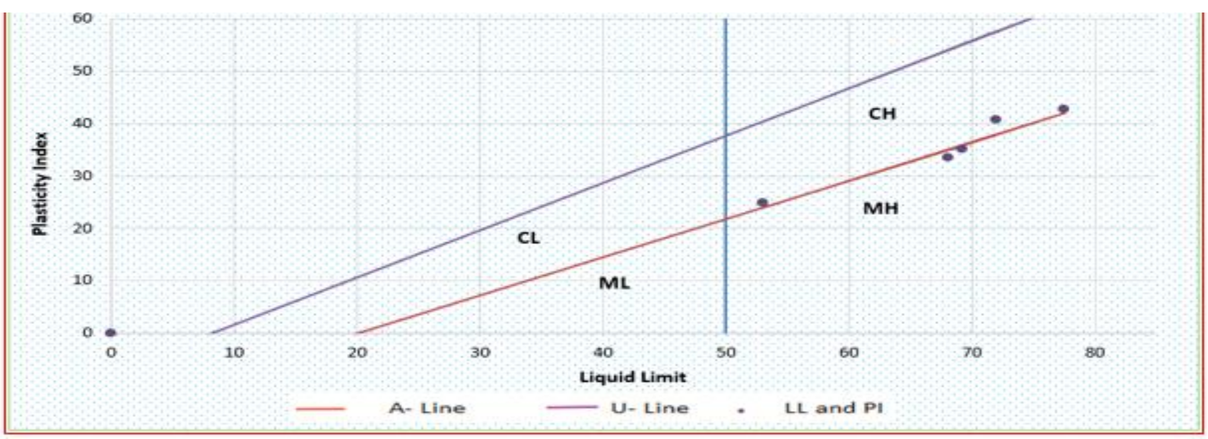


**Figure 4-2. Plasticity Chart for Sub-grade Samples**

### 4.1.3 Subgrade Soil Classification

The AASHTO soil classification reveals that the subgrade materials along the VIP road alignment are mainly classified as A-7-6 and A-7-5 soil groups. Out of the two groups, A-7-6 comprises 75% of the subgrade material (the largest proportion), followed by A-7-5, which constitutes 25%. The composition of the subgrade soil materials for the road alignment is summarized in the figure below.

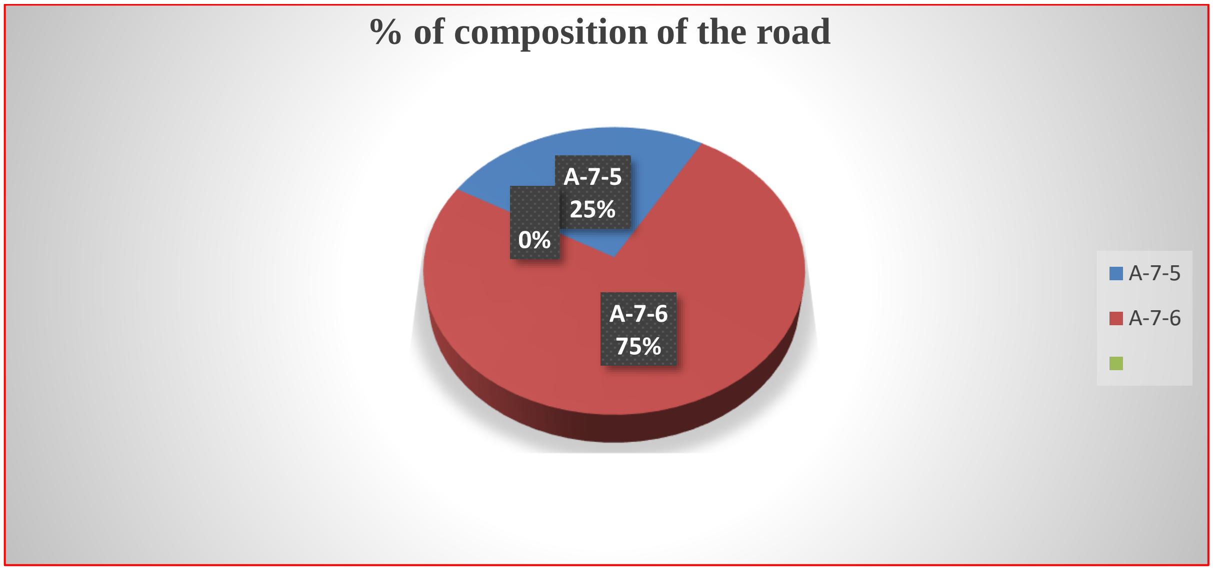


Figure 4.3 – %age compositions of sub-grade soil for the road section

### 4.1.3 Subgrade Strength Analysis

#### 4.1.3.1 Compaction

Soil samples obtained from test pits have been compacted in the laboratory at various moisture contents to derive a dry density versus moisture content relationship. Compaction tests were carried out at required intervals. Compaction was carried out by AASHTO T180 (4.5 kg hammer or heavy hammer). The Maximum Dry Density (MDD) obtained from these tests is summarized in below.

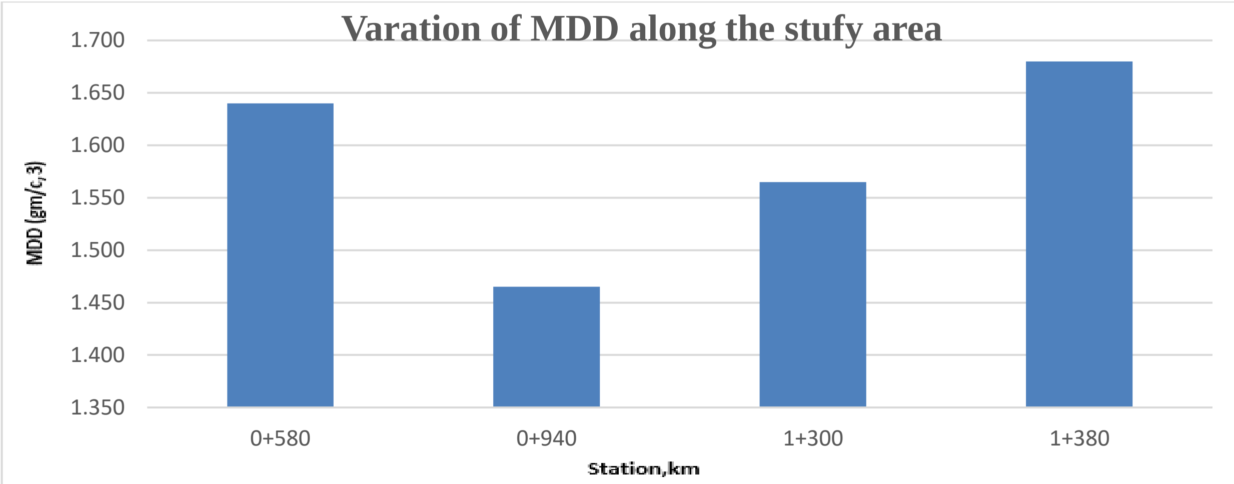


**Figure 4.4 – Variation of MDD along the study area**

The MDD value along the road alignment ranges between 1.47 g/cm$^3$ and 1.68 g/cm$^{3.}$ This indicates that the expected strength of the subgrade soil is relatively low to medium.

The optimum moisture content (OMC) along the road alignment varies from 16% to 22.4%. The values of optimal moisture content (OMC) obtained from the compaction tests are presented in Figure below.

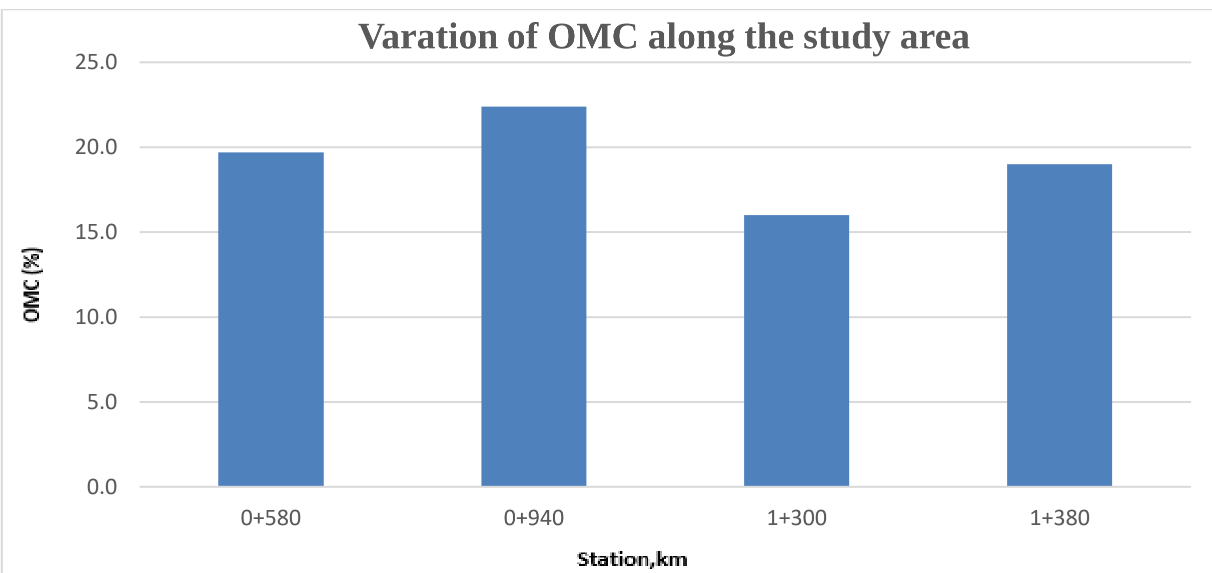


**Figure 4.5 – Variation of OMC for the study area**

#### 4.1.4 California Bearing Ratio (CBR) and Swell Values

Soaked CBR tests were carried out on disturbed soil samples recovered from trial pits along the road alignment to determine the shear strength of the sub-grade material. Three-point CBRs were undertaken per AASHTO T-193 to note the variation of strength with increasing compaction effort. The CBR values at 93% of MDD are plotted in Figure below.

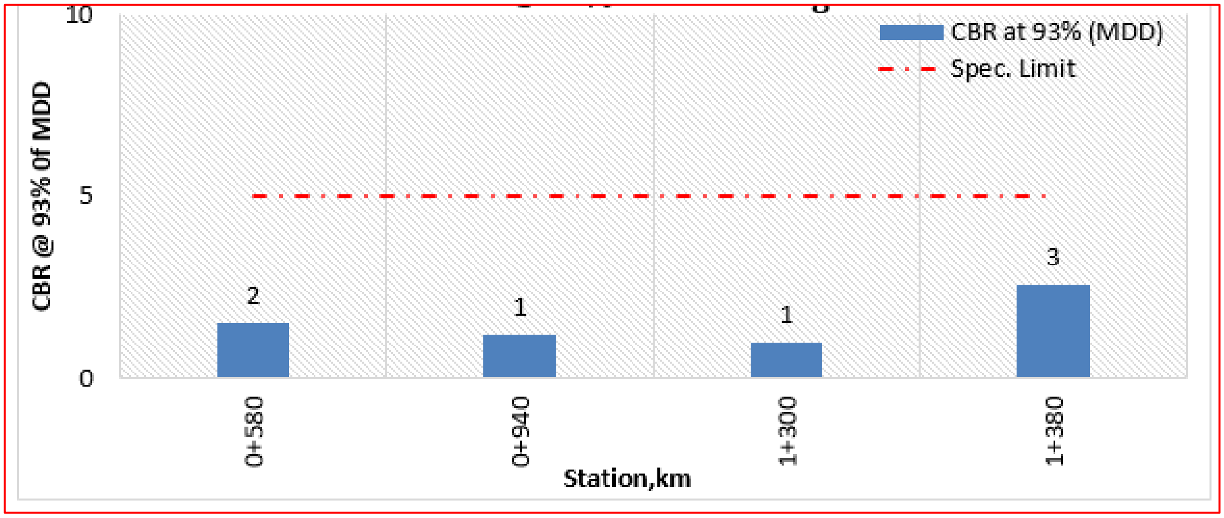


Figure 4.6 – CBR Value of the study area

As can be seen from the above figure, the CBR values @ 93% of MDD along the road alignment vary between 1% and 3%. This implies that the sections of the roads have a subgrade class of S1 to S2, as per the ERA subgrade class.

The swell value of the samples is also determined along with the CBR value to evaluate the potential heaving of the subgrade soils. Accordingly, 100% of the swell value of both alignment soils is greater than 3%. The variation of the CBR-Swell value for the project road is presented in the figure below.

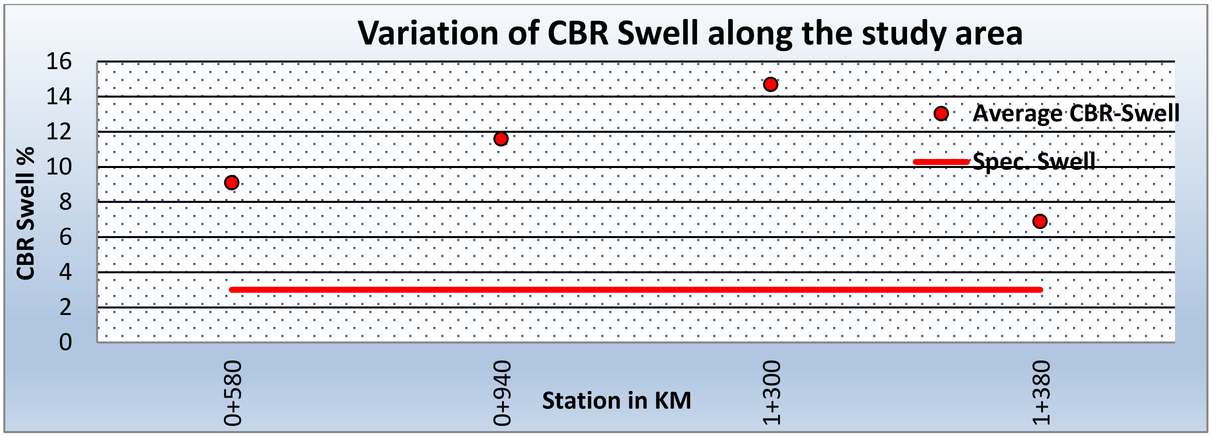


**Figure 4.7. Variation of CBR-Swell for the study area**

## 4.2 Subgrade Soil Data Interpretation

As mentioned above, representative samples of sub-grade materials were collected from the road alignment at reasonable intervals to assess the properties of the roadbed materials. Classification tests (sieve analysis and atterberg limits), modified proctor, three-point CBR, and swell tests were conducted on all samples collected from the project. The test results are summarized and presented in Annex I.

The classification analysis reveals that the subgrade materials along the road alignment are mainly classified as A-7-6 and A-7-5 soil groups. Out of the two groups, A-7-6 comprises 75% of the subgrade material (the largest proportion), followed by A-7-5, which constitutes 25%. The research road CBR values at 93% of the maximum dry density of the A-7-6 subgrade materials group tested for CBR are 1%. The group index of the material varies between 3 and 31. Materials found within this group usually exhibit poor subgrade strength. The physical description of the soil type in this group is dark grey silty clay soil. The AASHTO classification, M145-91, classifies this type of material as clay material and rates it as a poor subgrade. All the CBR test results for this group of materials show a poor CBR value for the subgrade strength rating as per the AASHTO classification.

100% of the materials in this group have a percent swell greater than 3%, which is an indication of expansive soil as per the criteria set in ERA specification 2014 section 4103.

67% of the test results for the liquid limit and plastic limit are less than 60% and 30%, respectively. This indicates that the majority of the soil in this group is not sensitive to moisture change along the road project where A-7-6 material exists.

The second soil group found in the road section is A-7-5. The group comprises 25% of the tested samples. Out of the samples in this group of materials tested for CBR, 100% are 1%, which can be rated as poor subgrade material. The group index is 41. The physical description of the soil type in this group is predominantly light to dark brown silty clay soil. The AASHTO classification, M145-91, classifies this type of material as clay soil material, and it is a poor subgrade. The CBR value and the Group Index of this soil group are in agreement with the AASHTO classification.

The swell test results reveal that 100% of the samples have a swell value greater than 3%, which indicates that the majority of the group is expansive material.

100% of the test results for liquid limit and plasticity index (PI) are greater than or equal to 60% and 30%, respectively. The LL and PI test results for this soil group indicate that the majority of the soil samples in this group are high in plasticity, which confirms that the soils have expansive behavior.

### 4.3 Results and Discussion for Cement-Treated Base (CTB)

The results and conclusions of the study that was carried out were be explained in this chapter. This chapter discusses the OMC-MDD relationship, durability performance, unconfined compressive strength test for different mixtures, and the resilient modulus of the base layer treated with cement.

#### 4.3.1 Particle Size Distribution:

The sieve analysis verified that the CTB aggregates satisfied the necessary grading requirements, guaranteeing a well-graded mix that is necessary for stability and compaction. Particle sizes in the aggregate mix should range from fine to coarse. In doing so, a dense packing of the particles were be ensured, reducing voids and supplying a robust interlocking framework. Table 4.1 it shows the particle size distribution for cement treated base material.

**Table 4.1 Particle size distribution for cement treated base material**

| No of sample | | 1 | | | 2 | | Grading Modulas | PP | As per MORT&H Table 400-4 | |
|---|---|---|---|---|---|---|---|---|---|---|
| Dry sample weight (g) | | 3514.2 | | | 3242.2 | | | | | |
| After wash dry sample (g) | | 3201.5 | | | 3025.3 | | 2.54 | | | |
| Inch | Sieve Size(mm) | Mass of Retained Sample (g) | Cumulative Passing ( g ) | Cumulative Passing (%) | Mass of Retained Sample (g) | Cumulative Passing ( g ) | Cumulative Passing (%) | Average Passing (%) | LOWER | UPPER |
| 1 1/4 | 53 | 0.0 | 3514.2 | 100.0 | 0.0 | 3242.2 | 100.0 | 100.0 | 100.0 | 100.0 |
| 1.06 | 37.5 | 0.0 | 3514.2 | 100.0 | 0.0 | 3242.2 | 100.0 | 100.0 | 95.0 | 100.0 |
| 3/4 | 19 | 1000.3 | 2513.9 | 71.5 | 1000.2 | 2242.0 | 69.2 | 70.3 | 45.0 | 100.0 |
| 3/8 | 9.5 | 400.0 | 2113.9 | 60.2 | 400.0 | 1842.0 | 56.8 | 58.5 | 35.0 | 100.0 |
| NO 4 | 4.75 | 750.0 | 1363.9 | 38.8 | 750.0 | 1092.0 | 33.7 | 36.2 | 25.0 | 100.0 |
| NO 8 | 0.6 | 500.0 | 863.9 | 24.6 | 500.0 | 592.0 | 18.3 | 21.4 | 8.0 | 65.0 |
| NO 30 | 0.3 | 250.0 | 613.9 | 17.5 | 50.0 | 542.0 | 16.7 | 17.1 | 5.0 | 40.0 |
| NO 200 | 0.075 | 300.0 | 313.9 | 8.9 | 325.0 | 217.0 | 6.7 | 7.8 | 0.0 | 10.0 |
| pan | | 1.2 | 0.0 | | 0.1 | | | | | |
| Wash loose | | 312.7 | | | 216.9 | | | | | |
| Total | | 3514.2 | | | 3242.2 | | | | | |

### 4.3.2 Blending for CTB

The blending of different aggregate sizes was required to obtain the desired composition for cement treated base material CTB. Table 4.2 it shows that the combined grading for cement treated base material.

**Table 4.2 combined grading for cement treated base CTB material**

| COMBINED GRADING AND MIX PROPORTION | | | | | | | | | | |
|---|---|---|---|---|---|---|---|---|---|---|
| TEST METHOD: AASHTO T 27 | | | | | | | | | | |
| Standard mm | Cum.Percent Passing | | | MIX Proportion,% | | | After Blending | | As per MORT&H Table 400-4 | |
| | 14-25mm | 5-14mm | Crush sand (0-5mm) | 14-25mm | 5-14mm | Crushed Sand | Cum.Passing,% | Ideal Limit | LOWER LIMIT | UPPER LIMIT |
| | | | | 35 | 25 | 40 | | | | |
| 53 | 100.0 | 100.0 | 100.0 | 35.0 | 25.0 | 40.0 | 100 | 100 | 100.0 | 100.0 |
| 37.5 | 100.0 | 100.0 | 100.0 | 35.0 | 25.0 | 40.0 | 100.0 | 98 | 95.0 | 100.0 |
| 19 | 73.3 | 100.0 | 100.0 | 25.7 | 25.0 | 40.0 | 90.7 | 73 | 45.0 | 100.0 |
| 9.5 | 1.4 | 82.3 | 99.9 | 0.5 | 20.6 | 40.0 | 61.0 | 68 | 35.0 | 100.0 |
| 4.75 | 1.3 | 27.5 | 97.8 | 0.5 | 6.9 | 39.1 | 46.5 | 63 | 25.0 | 100.0 |
| 0.6 | 1.3 | 5.0 | 74.4 | 0.5 | 1.3 | 29.8 | 31.5 | 37 | 8.0 | 65.0 |
| 0.3 | 1.3 | 3.0 | 41.0 | 0.5 | 0.8 | 16.4 | 17.6 | 23 | 5.0 | 40.0 |
| 0.075 | 1.3 | 2.5 | 7.5 | 0.5 | 0.6 | 3.0 | 4.1 | 5 | 0.0 | 10.0 |

The figure 4.9 it shows that the grading chart for cement treated base material.

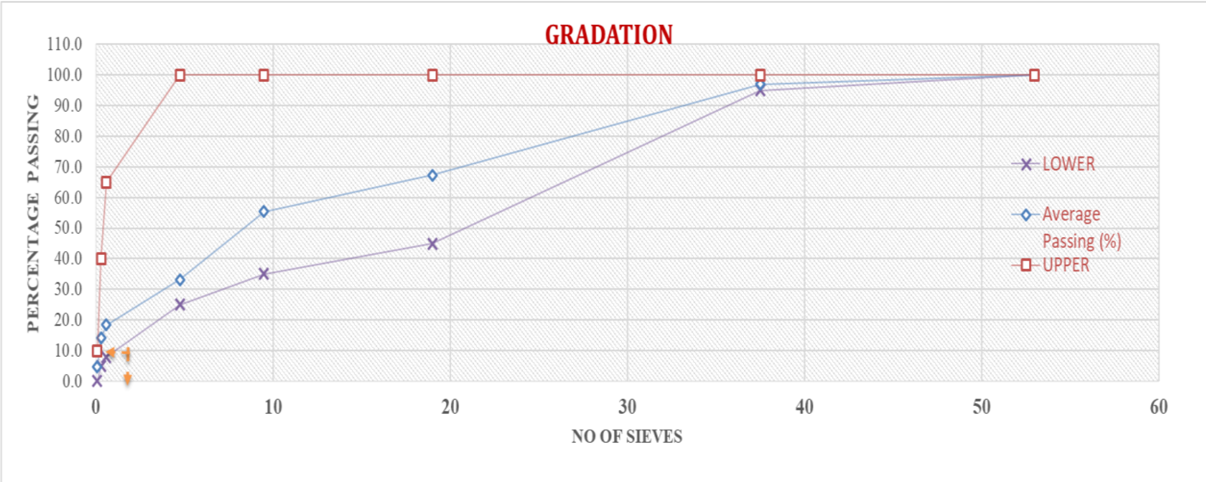


**Figure 4.9 Gradation chart for cement treated base material**

The uniformity coefficient (Cu) and coefficient of curvature (Cc) values were within acceptable ranges as per IRC 84, indicating a well-graded mix. Cu=D60/D10

Cu=13/0.4=32.5 Ok

The figure 4.10 it shows that the uniformity coefficient for the cement treated base material and the value 32.5 should be more than >5 as per MORT&H. Therefore the result satisfied the required specification.

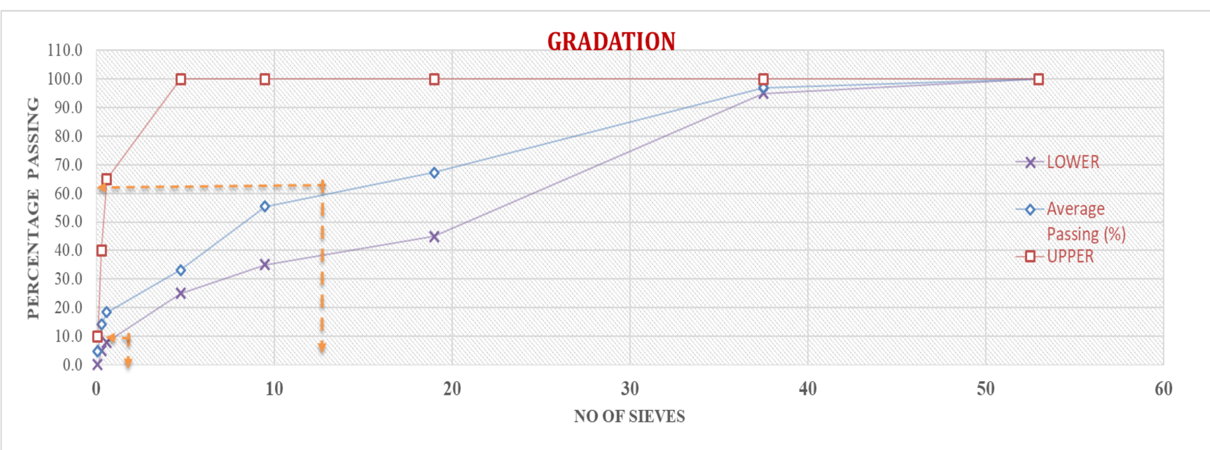


**Figure 4.10 Coefficient of Uniformity (CU) for cement treated base material**

### 4.3.3 Atterberg Limits:

The liquid limit, plastic limit, and plasticity index were determined according to IS 2720 (Part 5). The results indicated that the materials exhibited none plasticity or NP, which is desirable for a stable base layer.

### 4.3.4 Modified Proctor Test

The Modified Proctor Test, performed in accordance with IS 2720 (Part 8), revealed that the maximum dry density (MDD) of the CTB mix was 2.14 g/cm³ at an optimum moisture content (OMC) of 6.8%. The inclusion of cement increased the MDD by approximately 5%, indicating improved compaction potential.

The Modified Proctor Test was used to assess the compaction properties of the CTB mixture in order to calculate the Maximum Dry Density (MDD) and Optimum Moisture Content (OMC). In this test, five layers of the CTB mixture were compacted in a mold, and each layer was subjected to 56 blows from a 450 mm-dropped, 4.5 kg rammer. To determine the link between moisture and density, this process was repeated for varying moisture contents. In compliance with IS 2720 (Part 8), the dry density of each compacted sample was determined and plotted against moisture content, with the peak of the curve representing the MDD and the accompanying OMC. The figure 4.11 it shows the moisture density relation and from the graph the maximum dry density is 2.14 and the optimum moisture content is 6.8.

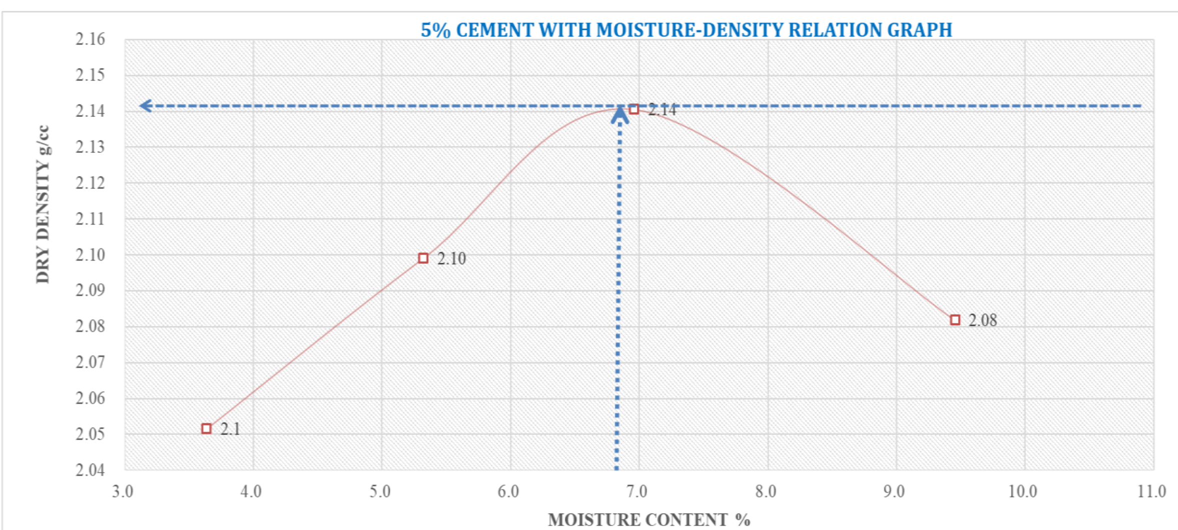


**Figure 4.11 Moisture-density relation graph**

### 4.3.5 Unconfined Compressive strength (UCS)

The suggestion from MORT&H states that cubes must be cast for each of the three sets needed after the Optimum Moisture Content (OMC) regarding the percentage of cement is established. For seven days, these cubes are exposed to moist curing. Each set's compressive strength is determined following the curing time. The acquired compressive strength values are multiplied by 0.75 to determine the Unconfined Compressive Strength (UCS). This procedure guarantees that the compressive strength data are accurately used to determine the UCS in accordance with the prescribed parameters. Now, it was determined that the cement content from the graph is 5.0% in accordance with the graphical form and need of the goal UCS, which is 5.22 N.mm2. The figure below it shows the unconfined compressive strength and the cement content for the cement treated base materials.

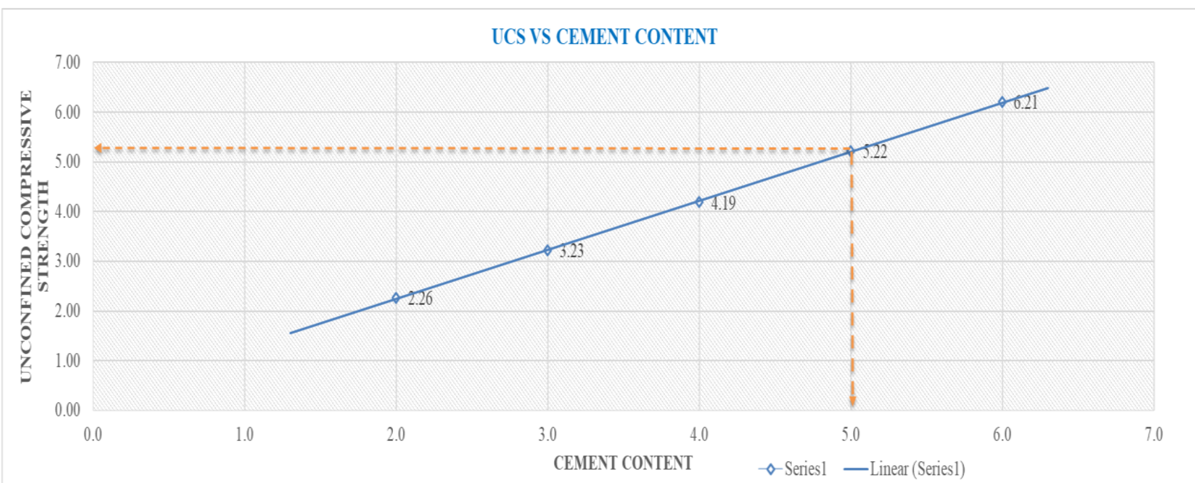


Figure 4.12 Unconfined compressive strength vs cement content graph

The following summary provides an overview of the various tests conducted to evaluate the properties of Cement-Treated Base (CTB) material, focusing on Atterberg Limits, Compaction, and Unconfined Compressive Strength (UCS).

To summarize, the testing carried out on the Cement-Treated Base (CTB) material yields extensive information regarding its mechanical and physical characteristics. The soil's plasticity is evaluated by the Atterberg Limits test, which affects workability and compaction behavior.

The compaction test finds the best conditions for reaching maximum density, vital for maintaining the integrity and endurance of the pavement construction.

The CTB mixture's strength is finally confirmed by the UCS test, which also verifies that it satisfies the necessary requirements for load-bearing capability. By combining these tests, we can make sure that the CTB is a solid and dependable foundation layer that is appropriate for usage in road pavement systems.

### 4.3.6 X-ray Diffraction (XRD) and Scanning Electron Microscopy (SEM) Analysis of Cement-Treated Base (CTB)

This section presents and discusses the results of X-ray Diffraction (XRD) and Scanning Electron Microscopy (SEM) analyses conducted on Cement-Treated Base (CTB) samples. These analyses provide insights into the mineralogical composition, crystalline phases, and microstructural characteristics of CTB, which are essential in understanding its mechanical behavior and durability.

#### 4.3.6.1 X-ray Diffraction (XRD) Analysis

The XRD analysis was performed to identify the crystalline phases present in the CTB samples. The diffraction pattern revealed that the dominant phases in the CTB mix included calcium silicate hydrates (C-S-H), calcium hydroxide (portlandite), and unhydrated cement particles. These phases are indicative of successful cement hydration and contribute to the overall strength and stability of the CTB.

- ✓ Calcium Silicate Hydrate (C-S-H) The presence of C-S-H, the primary binding phase in cement hydration, was confirmed by characteristic diffraction peaks. This phase is responsible for the development of compressive strength in CTB, contributing to the material's stiffness and resistance to deformation.
- ✓ Calcium Hydroxide (Portlandite) Portlandite, a byproduct of the hydration reaction, was also identified. While portlandite contributes to early strength, its presence in large amounts can be indicative of incomplete hydration, which may affect long-term durability.
- ✓ Unhydrated Cement Particles Minor peaks corresponding to unhydrated cement particles were observed, which suggests that not all cement reacted during the hydration process.

This is typical in cement-treated materials, where complete hydration may not occur due to factors such as water content or curing conditions.

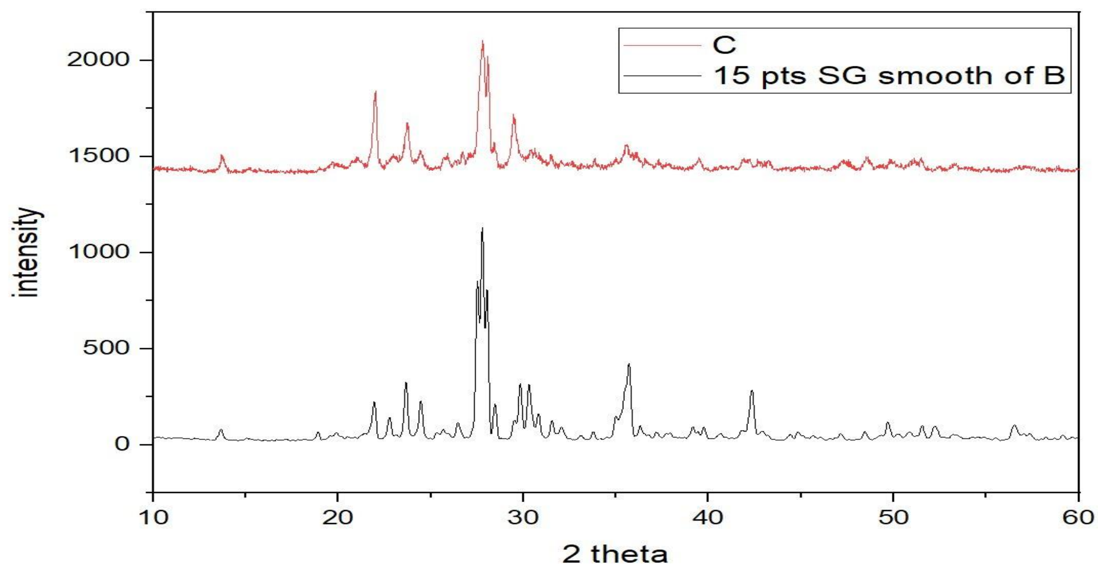


**Figure 4.13 XRD for CTB and Control Sample**

The XRD graph shows two curves representing different materials:

- C (Red Curve): - This represents the XRD pattern for the Cement-Treated Base (CTB) sample.
- 15 Points SG Smooth of B (Black Curve): - This represents the XRD pattern for the control sample (likely untreated or reference material).

Interpretation:

- ✓ Comparison of Peaks:- Both the CTB (red curve) and control (black curve) show distinct peaks at various 2θ angles. The positions of these peaks indicate the presence of crystalline phases in both samples.
- ✓ Intensity: - The red curve (CTB) shows higher overall intensities than the black curve (control) at certain peak positions, suggesting that the CTB has a greater concentration of certain crystalline phases, possibly due to the cement hydration process.
- ✓ Differences in Crystalline Phases: - The CTB sample (red curve) appears to have additional peaks or more intense peaks compared to the control sample. This difference is likely due to the formation of cement hydration products like calcium silicate hydrates

(C-S-H) and calcium hydroxide (portlandite) in the CTB. The control sample (black curve) likely represents the base material without cement treatment, showing fewer or less intense peaks, which could correspond to natural minerals in the untreated soil or aggregates.

- ✓ Significance of Peaks:
  - Cement Hydration Products: - In the CTB sample, the peaks could represent phases like C-S-H (which contributes to strength) and portlandite. The presence of these phases is typical in cement-treated materials and is responsible for the improved mechanical properties of the CTB.
  - Control Sample: - The control sample's peaks may correspond to naturally occurring minerals, and the absence of cement hydration phases suggests that this material lacks the cement-induced crystalline structure seen in the CTB.

The XRD analysis indicates that the CTB sample has undergone significant changes in its crystalline structure compared to the control, likely due to cement hydration. The higher intensity peaks in the CTB sample reflect the formation of cementitious phases that contribute to the material's strength and durability. In contrast, the control sample shows fewer and less intense peaks, indicating the absence of these cement-induced phases.

The XRD results confirm that the cement hydration process in the CTB samples proceeded as expected, leading to the formation of key cementitious phases that contribute to the material's mechanical performance. The balance between hydrated and unhydrated phases suggests a well-designed mix, with sufficient cement content to ensure strength while minimizing the risk of excessive brittleness.

#### 4.3.6.2 Scanning Electron Microscopy (SEM) Analysis

The SEM analysis was conducted to observe the microstructure of the CTB samples, focusing on the morphology of the hydration products, the distribution of cement particles, and the development of the pore structure. SEM images provided visual evidence of the microstructural characteristics that contribute to the material's performance.

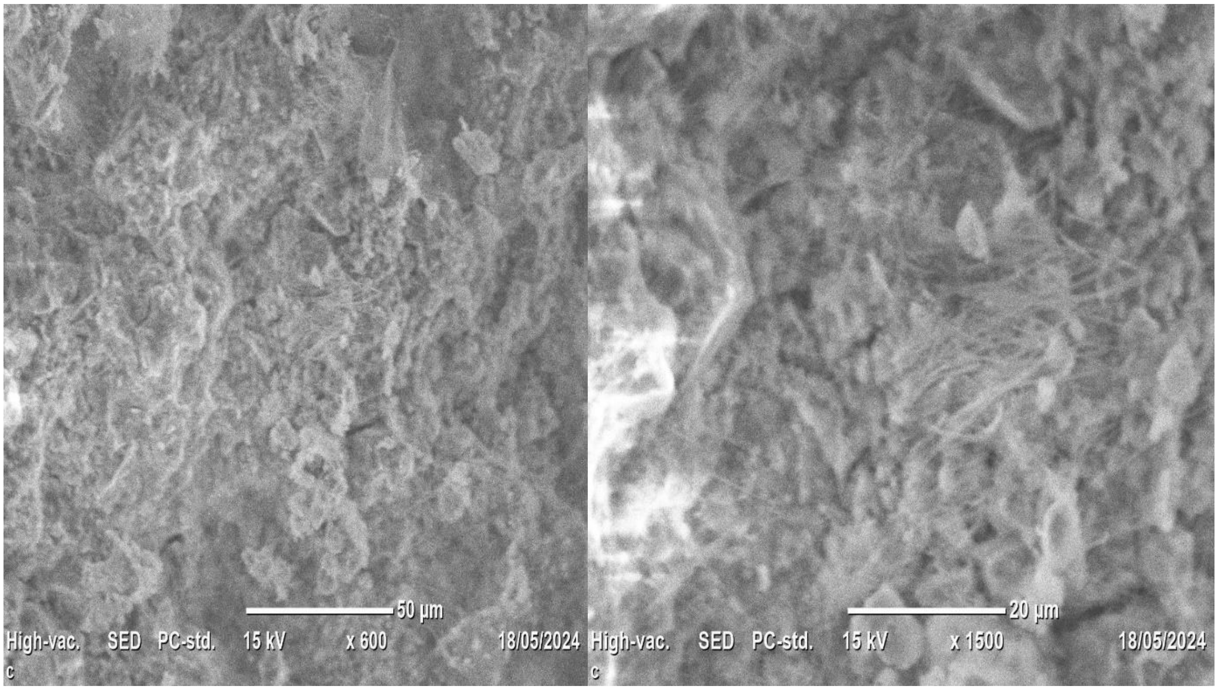


**Figure 4.14 SEM Image for CTB**

Microstructural Observation: - The SEM images revealed a dense matrix of hydration products, with C-S-H gels forming a continuous network that bonds the aggregate particles together. This dense microstructure is critical for the material's compressive strength and its resistance to cracking under load.

Pore Structure: - Pores were observed in the CTB microstructure, but they were relatively small and uniformly distributed. The low porosity is a positive indicator, as it reduces the potential for water ingress and subsequent durability issues, such as freeze-thaw damage or chemical attack.

Crack Propagation: - SEM analysis also allowed for the observation of micro-cracks within the matrix. These cracks were found to be minimal and confined to areas around unhydrated cement particles, suggesting that the overall integrity of the material was not compromised. The limited presence of micro-cracks indicates that the CTB mix was effective in resisting shrinkage and thermal stresses during curing.

### 4.3.7 Discussion for XRD and SEM

The combined XRD and SEM analyses provide valuable insights into the microstructural and mineralogical properties of the CTB samples, which directly influence their mechanical performance and durability.

- ✓ Strength Development: - The formation of C-S-H phases, as revealed by XRD, is critical for the strength development in CTB. The dense microstructure observed in SEM images supports the conclusion that the cement content and hydration process were optimized to produce a material with high compressive strength and resistance to deformation.
- ✓ Durability Considerations: - The low porosity and minimal presence of micro-cracks observed in SEM suggest that the CTB mix is likely to exhibit good long-term durability. However, the presence of un-hydrated cement particles and portlandite indicates that proper curing and mix design is essential to prevent potential durability issues, such as carbonation or leaching over time.
- ✓ Microstructural Integrity: - The SEM analysis also highlights the importance of achieving a well-distributed pore structure and minimizing micro-cracks. These microstructural features are key to ensuring that the CTB can withstand repeated loading and environmental exposure without significant degradation.

Overall, the XRD and SEM results confirm that the CTB mix used in this study exhibits the desired mineralogical and microstructural characteristics necessary for strong and durable pavement performance. These findings support the suitability of CTB as a cost-effective and resilient alternative to conventional pavement materials in Ethiopian road construction. Proper mix design and curing practices are critical to maximizing the benefits of CTB, ensuring that it meets the demands of heavy traffic and challenging environmental conditions.

### 4.3.6 Resilience Modulus for CTB

The 28-day Unconfined Compressive Strength (UCS) of the material can be used to estimate the resilient modulus (MR) of cement-treated base (CTB). This estimate is essential to the design and study of pavement constructions as well as to comprehend the elastic behavior of CTB under traffic loads. A useful and effective technique for determining the elastic modulus of CTB is frequently provided by the relationship between the UCS and the MR.

Empirical correlations are usually used to estimate the elastic modulus (E) from the 28-day UCS of CTB. These correlations offer a trustworthy way to translate UCS measurements into estimations of the elastic modulus. They are the result of comprehensive laboratory testing and statistical analysis. The strength of cementitious layers increases over time, and pavements with

CTB layers that have 7/28 day unconfined compression strength values ranging from 4.5 to 7 MPa may be analyzed using an elastic modulus of 5000 MPa.

Finally, it can be observed that empirical correlations allow for an efficient estimation of the cement-treated base's (CTB) elastic modulus from the 28-day Unconfined Compressive Strength (UCS). The design and study of robust and effective pavement constructions are made easier by this method, which offers a useful way to assess the elastic properties of CTB. Through the application of these correlations, engineers can guarantee that the pavement functions well under traffic loads, preserving its structural soundness and lengthening its lifespan.

### 4.4 Discussion for cement-treated base material

Effectiveness of Cement Stabilization were the marked improvements in UCS, CBR, resilient modulus, and ITS values underscore the effectiveness of cement stabilization in enhancing the mechanical properties of base materials. The increased compressive and tensile strengths contribute to a more robust and durable pavement structure, capable of withstanding heavy traffic loads and adverse environmental conditions.

Compaction Characteristics were the improved MDD and optimized OMC indicate that cement-treated base materials can achieve higher densities, leading to a more stable and well-compacted base layer. This is crucial for minimizing settlements and ensuring the longevity of the pavement.

Enhanced Load-Bearing Capacity were the high CBR values demonstrate that CTB significantly enhances the load-bearing capacity of the pavement base, reducing the risk of rutting and deformation. This makes CTB particularly suitable for heavy-duty pavements and high-traffic areas.

Economic Viability were the cost analysis reveals that CTB is not only technically superior but also economically advantageous compared to traditional DBM. The lower initial construction costs, combined with reduced maintenance requirements, make CTB a cost-effective solution for road pavement construction.

Environmental and Practical Benefits were using locally available materials for CTB construction reduces the environmental impact associated with transporting aggregates over long distances. Additionally, the improved performance characteristics of CTB contribute to longer pavement life, reducing the frequency of repairs and associated environmental footprint.

### 4.5 Numerical Modeling PLAXIS 3D result and discussion

In a PLAXIS 3D analysis of an inverted pavement system, the results and discussion focus on interpreting how the cement-treated base (CTB), granular interlayer, and subgrade layers interact under load and how this configuration compares to conventional flexible pavement in terms of deformation, stress distribution, and fatigue resistance. The main results often include deformation contours, stress distribution patterns, and fatigue analysis, providing insights into the pavement's performance.

1. Deformation and Settlement Analysis

Inverted pavement systems typically exhibit reduced deformation and settlement compared to conventional flexible pavements. The deformation contour results from PLAXIS 3D demonstrate that the cement-treated base (CTB) layer significantly restricts downward movement, distributing loads more evenly across the subgrade. The CTB's stiffness allows it to bear a large portion of the applied stress, which results in less overall deformation, especially in the subgrade.

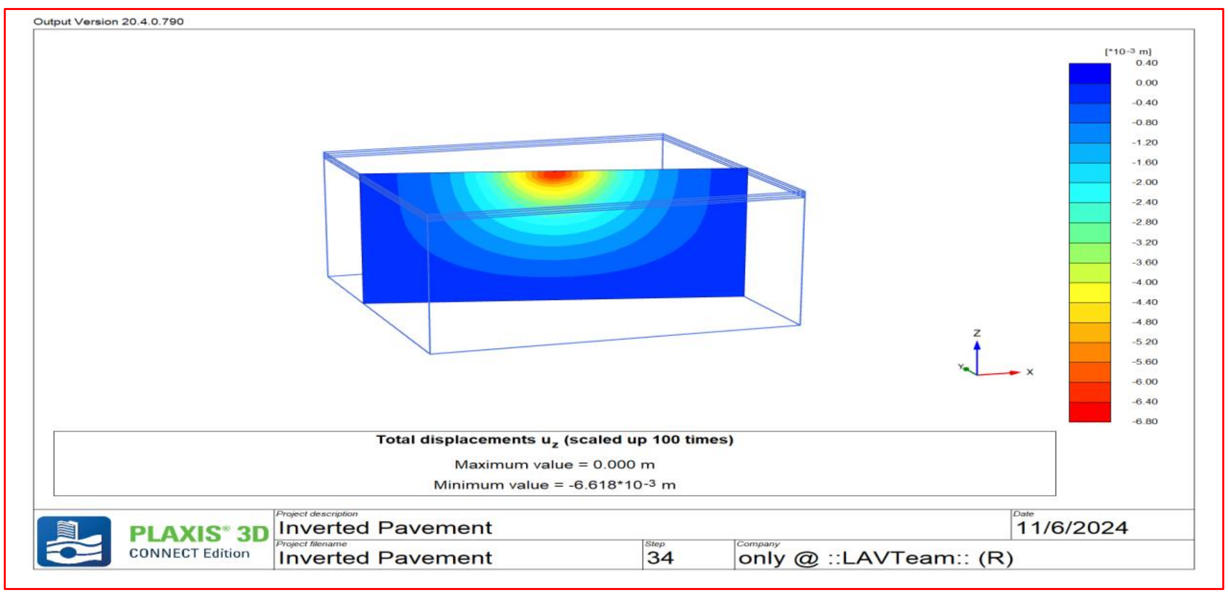


**Figure 4.15: PLAXIS 3-D output view (Sample) of total vertical displacement [m] of Inverted base pavement**

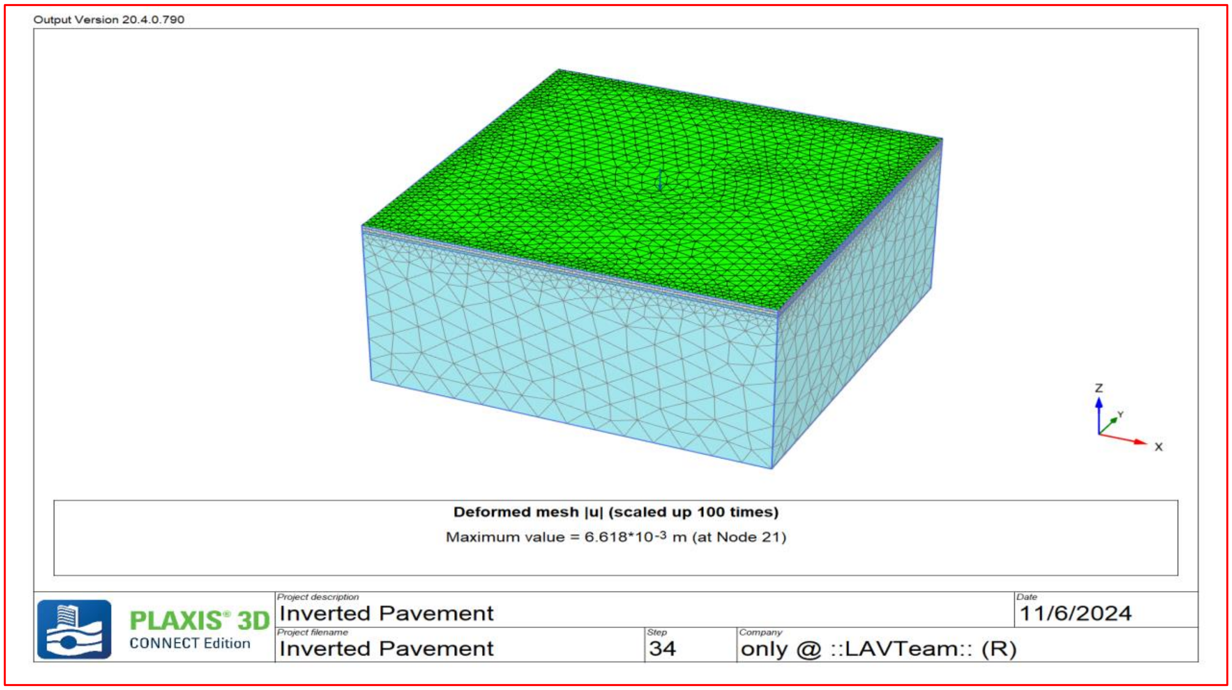


**Figure 4.16: PLAXIS 3-D output view (Sample) of the deformed mesh of Inverted base pavement**

In areas of heavy loading, deformation measurements often show that inverted pavement systems experience less rutting and vertical displacement in the subgrade than flexible pavements. This suggests that the CTB layer's stiffness effectively protects the subgrade from excessive deformation, which is particularly advantageous in regions with weak subgrades.

2. Stress Distribution

The stress distribution within the inverted pavement layers provides valuable insights into load transfer efficiency. Stress contour plots from PLAXIS 3D typically show that the CTB layer absorbs and spreads the load, minimizing stress concentrations on the subgrade. This load-spreading capability of the CTB layer results in lower stress levels within the subgrade compared to flexible pavements, where stress is more directly transmitted to the lower layers.

In the granular interlayer, which lies between the CTB and the subgrade, stresses are moderate, helping to ensure a smoother transition and reducing stress peaks that could cause damage. This configuration highlights the benefit of inverted pavements, where the high-stiffness CTB layer enhances load distribution across the layers, reducing the potential for deformation in the subgrade and minimizing permanent deformation (rutting) at the surface.

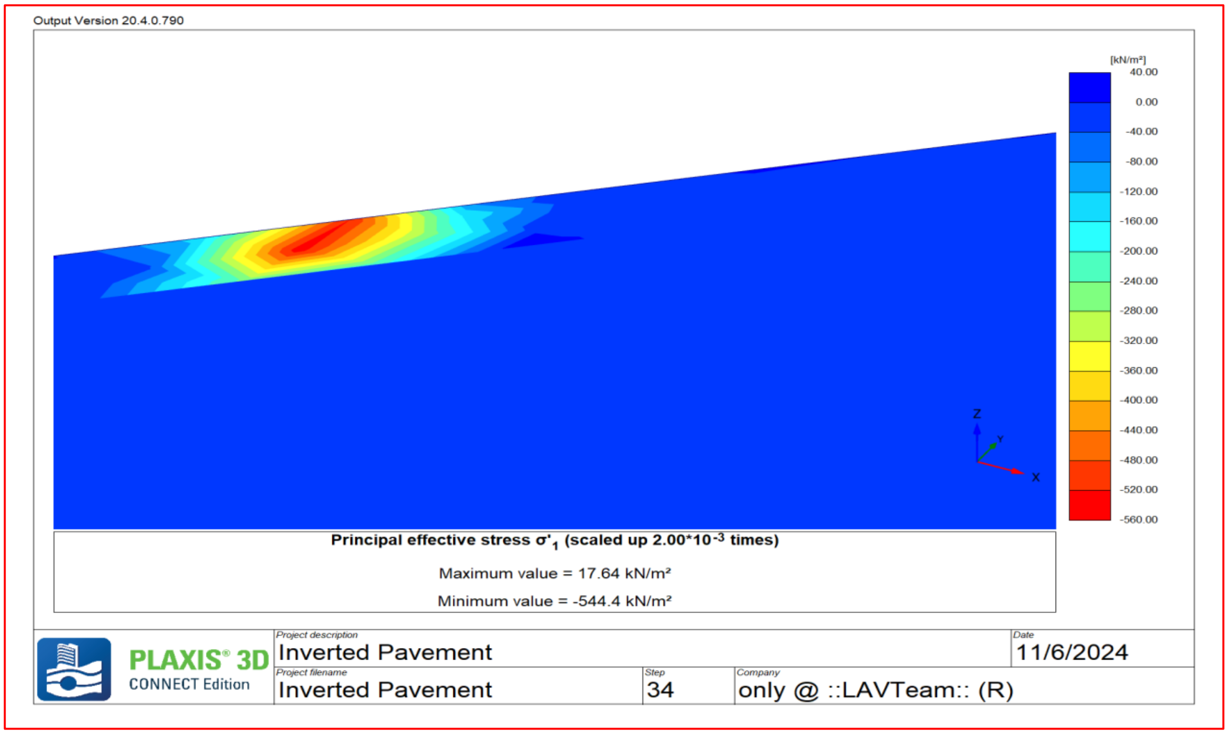


**Figure 4.17: PLAXIS 3-D output view (Sample) of principal effective stress of Inverted base pavement**

3. Strain Analysis

The strain analysis in PLAXIS 3D often reveals reduced horizontal and vertical strains within the subgrade in inverted pavement systems. The CTB layer's high modulus of elasticity mitigates strain concentrations, which translates to improved fatigue life and reduced cracking potential at the surface. The strain in the granular interlayer is also better managed, as it serves as a buffer that further mitigates stress and strain transmitted to the subgrade. This means the inverted system is less prone to fatigue and rutting under repeated loading, which is critical for heavy-traffic applications.

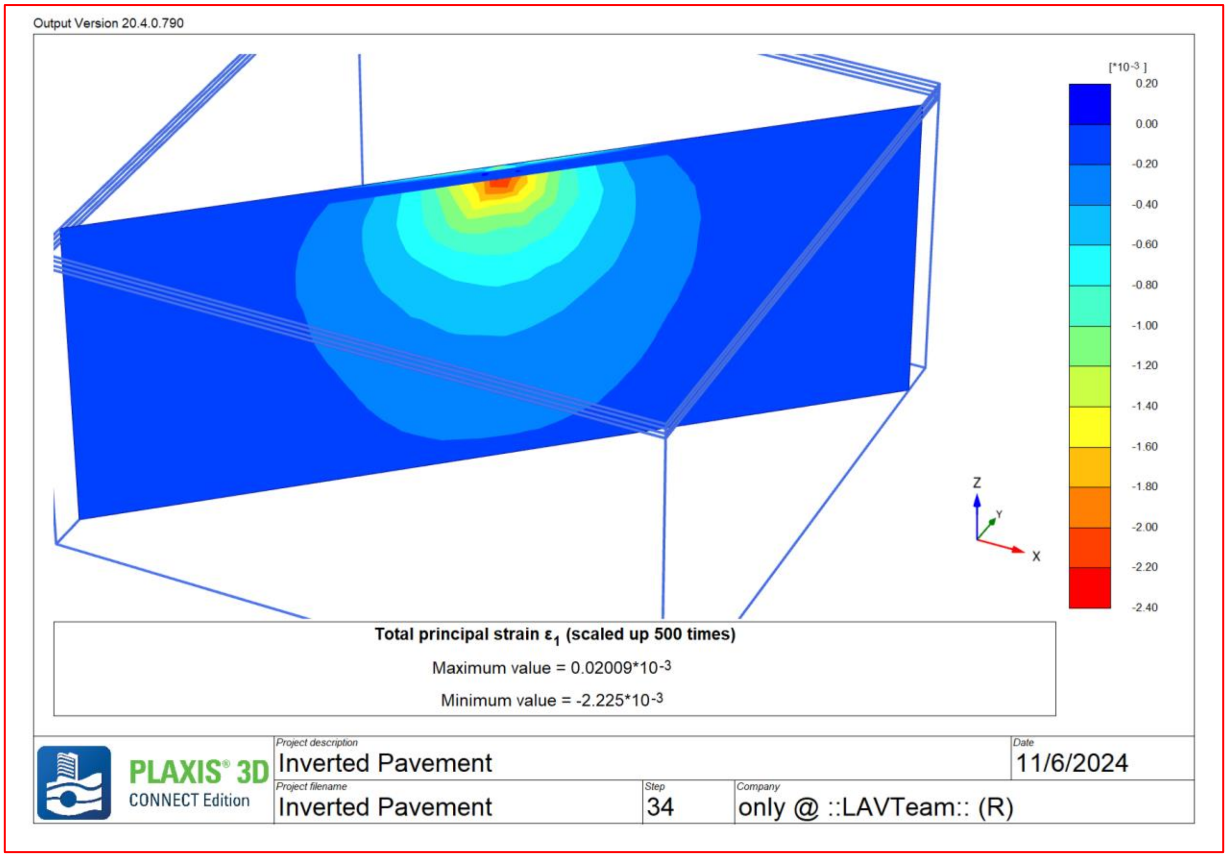


**Figure 4.18: PLAXIS 3-D output view (Sample) of the total principal strain of Inverted base pavement**

4. Fatigue and Rutting Potential

PLAXIS 3D's cyclic analysis or repeated loading simulations provide insights into fatigue resistance and rutting potential. Inverted pavement systems show enhanced resistance to fatigue due to the CTB layer's stiffness, which absorbs much of the load and mitigates stress concentrations that could lead to surface cracking. The results typically indicate that the CTB layer in the inverted pavement can handle a higher number of loading cycles before showing signs of fatigue, prolonging the pavement's service life.

The rutting potential is also significantly reduced in inverted pavement systems. The combination of a stiffer CTB layer and a supportive granular interlayer reduces plastic deformation over time, which is often observed in conventional flexible pavements. The reduced rutting potential means the inverted pavement surface remains smoother for longer periods, enhancing ride quality and reducing maintenance costs.

5. Comparison to Conventional Flexible Pavement

When compared to conventional flexible pavement, the results indicate that inverted pavement systems offer superior performance in terms of deformation control, stress distribution, and fatigue resistance. Conventional flexible pavements often experience greater deformation, stress concentration within the subgrade, and higher rutting potential, especially in areas with weaker subgrades. The PLAXIS 3D analysis shows that the CTB layer's role in the inverted pavement system effectively alleviates these issues, leading to a more resilient pavement structure that performs well under high traffic loads and in conditions with suboptimal subgrade strength.

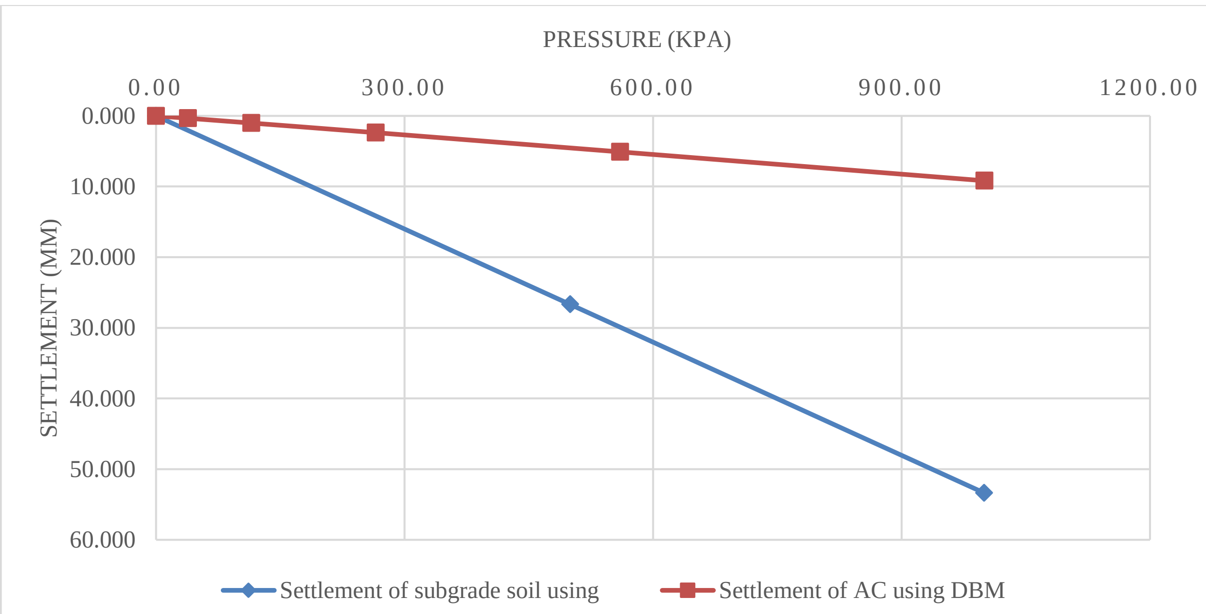


**Figure 4.19: Effect of the Settlement on Conventional flexible Pavement**

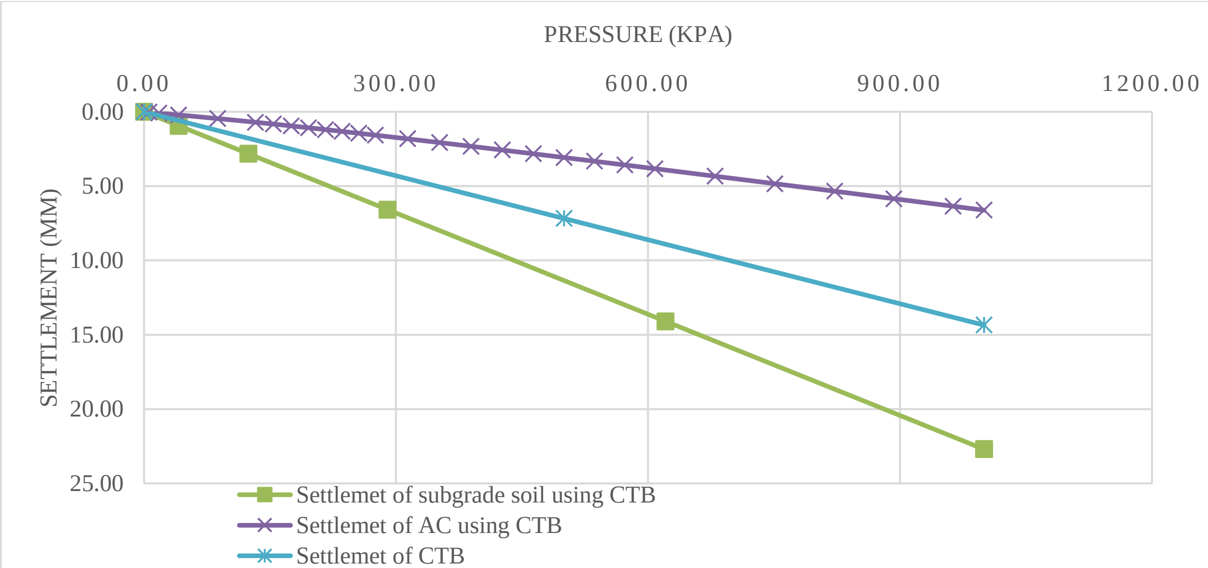


**Figure 4.20: Effect of the Settlement on Inverted base Pavement**

The findings from the PLAXIS 3D analysis support the argument that inverted pavements are a viable alternative to conventional designs, particularly in regions with weaker subgrade soils. The high stiffness of the CTB layer contributes to the overall system's ability to reduce deformation and stress within the subgrade, offering long-term benefits such as lower maintenance needs and extended pavement life. The granular interlayer also contributes to performance by enabling stress redistribution and minimizing strain in the subgrade, which reduces the potential for subgrade failure.

The reduced rutting and fatigue observed in inverted pavements further confirm that this system is suitable for heavy-load applications, making it an effective choice in high-traffic corridors where load-bearing performance is critical. The model results underscore the benefits of an inverted pavement design, particularly in terms of long-term performance and reduced lifecycle costs. However, the reliance on a cement-treated base may introduce higher initial construction costs, which should be weighed against the benefits of reduced maintenance and increased durability.

In summary, the PLAXIS 3D results suggest that inverted pavements provide significant advantages over conventional flexible pavements in terms of load-bearing capacity, stress distribution, and durability, especially in areas where the subgrade is weak or traffic loads are high.

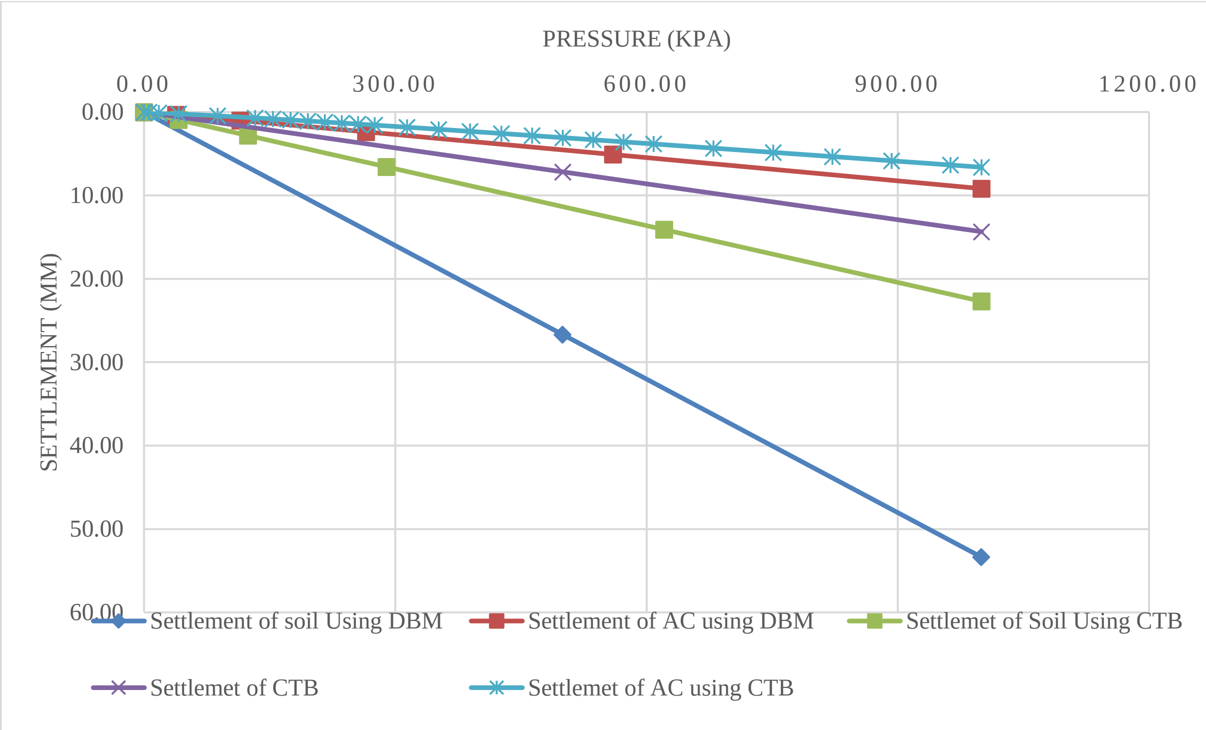


**Figure 4.21: Comparison of the settlement on the inverted base layer and conventional pavement layers**

This graph illustrates the settlement behavior of different pavement layers (conventional flexible pavement and inverted base pavement system) under various applied pressures (ranging from 0 to 1200 kPa). Here's a breakdown of the key observations and implications:

Settlement of Soil Using DBM (blue line): This layer experiences the most significant settlement among all configurations as pressure increases. It shows a steep downward trend, indicating that soil directly under DBM (Dense Bituminous Macadam) without additional stabilization is highly susceptible to deformation under load. This highlights a limitation of DBM for subgrade support in areas with high traffic loads, as the subgrade may suffer significant settlement.

Settlement of AC Using DBM (red line): The Asphalt Concrete (AC) layer placed over DBM shows a slight increase in settlement compared to other configurations but performs better than soil using DBM alone. This configuration has lower settlement, suggesting that the AC layer can bear load somewhat better when paired with DBM, though still not as effectively as the cement-treated base (CTB) configurations.

Settlement of Soil Using CTB (green line): This line shows that soil settlement significantly decreases when using a CTB layer. The soil's resistance to settlement improves, with a shallower slope, indicating that the CTB provides good structural support to the underlying soil, reducing deformation. This makes CTB a favorable option for supporting weak soils in pavement systems, as it effectively distributes the load.

Settlement of CTB (purple line): The CTB itself exhibits moderate settlement, which indicates its ability to provide a stable base with minimal deformation. This moderate settlement implies that CTB is effective in both load distribution and settlement control, making it an ideal layer for pavements subjected to high loads.

Settlement of AC Using CTB (light blue line with asterisks): This configuration shows the least settlement across all applied pressures, indicating that the AC layer over CTB provides excellent resistance to settlement. The shallow slope of this line suggests that AC paired with CTB is the most effective combination for minimizing deformation under load, which can enhance the pavement's durability and performance under traffic.

The analysis shows that using CTB as a base layer significantly reduces settlement compared to DBM, particularly when supporting the AC and soil layers. The CTB's rigidity and stiffness help distribute loads more effectively, limiting deformation in the pavement structure. This supports the idea that an inverted pavement system, where a CTB layer is used under the asphalt layers, can improve performance by reducing settlement and enhancing load-bearing capacity.

Furthermore, the graph demonstrates that conventional flexible pavement systems using DBM are less effective in controlling settlement, particularly over weak soils. The results emphasize the advantages of CTB in providing better load distribution and reducing permanent deformation (rutting), making it a suitable choice for heavily trafficked pavements or areas with poor subgrade conditions.

In summary, the graph supports the argument that inverted pavement systems with CTB offer a more resilient pavement structure with lower settlement rates, enhancing the pavement's longevity and reducing the need for frequent maintenance. This is particularly advantageous in high-traffic or weak subgrade environments.

### 4.6 Performance criteria for CTB result and discussion

The performance criteria for the CTB pavement result and discussion are detailed here using the IITPAVE software to calculate the stress, strain, and deflection of each layer. Here for a 7% CBR value, the Resilient Modulus of subgrade soil is 61.15 MPa. The subgrade is improved by borrowing a material layer whose CBR value is 20%. The resilient modulus of the existing borrow material layer is 119.72 MPa. Therefore effective CBR is to be determined using IITPAVE software. The Poisson's ratio of subgrade soil is taken as 0.35. From IITPAVE software, the maximum surface deflection is obtained as 1.44 mm. Figure 4.13 shows the IITPAVE software output for the maximum surface deflection for the subgrade soil.

```
No. of layers                 2
E values (MPa)           119.70   61.15
Mu values                  0.350.35
thicknesses (mm)         500.00
single wheel load (N)  40000.00
tyre pressure (MPa)        0.56
Single Wheel
  Z        R       SigmaZ       SigmaT      SigmaR      TaoRZ       DispZ       epZ         epT         epR
  0.00     0.00-0.5525E+00-0.4860E+00-0.4860E+00 0.0000E+00 0.1443E+01-0.1774E-02-0.1023E-02-0.1024E-02
```

**Figure 4.22 IITPAVE Software output for maximum surface deflection**

Now using the maximum surface deflection, the resilient modulus of the equivalent single layer is determined from the formula given below.

$$M_{RS} = \frac{2(1-\mu^2)pa}{\delta}$$

Where

p = contact pressure = 0.56 MPa

a = radius of circular contact area, which can be calculated using the load applied (40,000 N) and the contact pressure 'p' (0.56 MPa) = 150.8 mm

$\mu$ = Poisson's ratio

$\delta$ = Maximum surface deflection

From the above formula, the resilient modulus of the equivalent single layer is obtained as 102.92MPa but the maximum resilient modulus for subgrade is 100 MPa according to IRC. Therefore take value of 100 MPa was used in the design. The corresponding effective CBR value is 15.8%.

### 4.5.1 Subgrade rutting criteria

IITPAVE software is used in this research for the analysis of pavements. For the computation of stresses, strains, and deflections in the pavement, thicknesses and elastic properties (elastic modulus and Poisson's ratio) of different layers are the main inputs.

NR = 1.4100 x 10-08 $[1/\varepsilon v]^{4.5337}$ (for 90 % reliability)

74,629,855=1.4100*10^$^{-8}$$(1/ \varepsilon v)^{4.5337}$

Allowable vertical strain εv=0.00034

Substitute NR with design traffic to obtain allowable vertical strain εv. εv allowable = 0.000331 Now find the maximum vertical compressive strain using IITPAVE software. εv= 0.000112 which is less than the allowable strain. Hence safe. Figure 4.23 shows the IITPAVE input data for the maximum strain at the subgrade and bituminous layer.

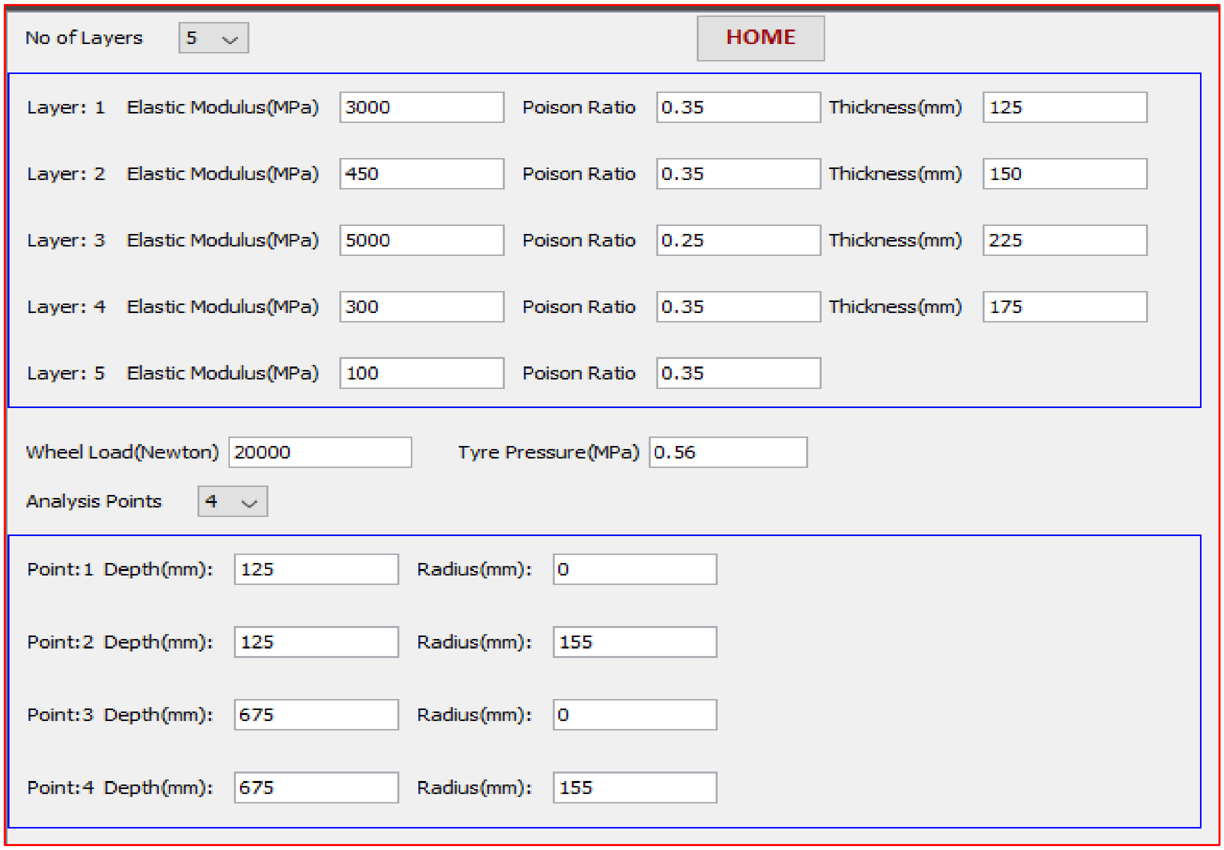


**Figure 4.23 IITPAVE input data for maximum strain at the subgrade and bituminous layer**

Figure 4.24 shows the IITPAVE output data for the maximum strain at the subgrade and bituminous layer.

```
No. of layers                 5
E values (MPa)         3000.00  450.00 5000.00  300.00  100.00
Mu values                 0.350.350.250.350.35
thicknesses (mm)        125.00  150.00  225.00  175.00
single wheel load (N) 20000.00
tyre pressure (MPa)       0.56
Dual  Wheel
  Z        R       SigmaZ      SigmaT      SigmaR      TaoRZ      DispZ      epZ        epT        epR
125.00    0.00-0.2031E+00 0.3945E+00 0.3002E+00-0.1155E-01 0.1966E+00-0.1487E-03 0.1202E-03 0.7772E-04
125.00L   0.00-0.2031E+00-0.3378E-01-0.4793E-01-0.1155E-01 0.1966E+00-0.3878E-03 0.1202E-03 0.7772E-04
125.00  155.00-0.1628E+00 0.2559E+00-0.6418E-01-0.6856E-01 0.1954E+00-0.7663E-04 0.1118E-03-0.3225E-04
125.00L 155.00-0.1628E+00-0.3613E-01-0.8414E-01-0.6857E-01 0.1954E+00-0.2682E-03 0.1118E-03-0.3225E-04
675.00    0.00-0.1067E-01 0.1218E-01 0.1076E-01-0.1394E-02 0.1429E+00-0.6232E-04 0.4048E-04 0.3411E-04
675.00L   0.00-0.1067E-01 0.2298E-03-0.2413E-03-0.1394E-02 0.1429E+00-0.1066E-03 0.4048E-04 0.3412E-04
675.00  155.00-0.1120E-01 0.1287E-01 0.1202E-01-0.1726E-02 0.1450E+00-0.6637E-04 0.4194E-04 0.3811E-04
675.00L 155.00-0.1120E-01 0.2689E-03-0.1483E-04-0.1726E-02 0.1450E+00-0.1129E-03 0.4194E-04 0.3811E-04
```

**Figure 4.24 IITPAVE Output data for the maximum strain for subgrade and bituminous layer**

### 4.5.2 Fatigue cracking criteria for bituminous layer

Following performance models are used for fatigue cracking check for bituminous layer for different percentage of reliability. Here 90% reliability is considered since the design traffic is more than 20msa.

74,629,855=0.5161*2.35*10^-4(1/Ɛt)^3.89*(1/3000)^0.854

Ɛt=0.000156, therefore the allowable tensile strain Ɛt=0.000156

Maximum strain at bottom of the bituminous layer is obtained using IITPAVE software. From the IITPAVE software the maximum strain is 0.000111. Therefore the allowable tensile strain is greater than the maximum strain. The design is safe.

### 4.5.3 Fatigue Performance Models for Cement Treated Base (CTB)

Here RF is taken as 1 for design traffic of more than 10 msa, E is taken as 5000 MPa, and limiting tensile strain is obtained by substituting the N with design traffic.

74,629,855= [(113000/5000^0.804+191/Ɛt)]^12

74,629,855=((119.98+191)/ Ɛt)$^{12}$

(74,629,855)$^{1/12}$=(310.98/ Ɛt)

Ɛt=41.47

The limiting tensile strain is 41.47 microstrains

Now using IITPAVE software, determine the tensile strain at the bottom of CTB for 80 KN standard axle (single axle dual wheels) load with 0.80 MPa contact pressure. Figure 4.20 shows the IITPAVE input data for the maximum tensile strain at the cement-treated base (CTB) layer.

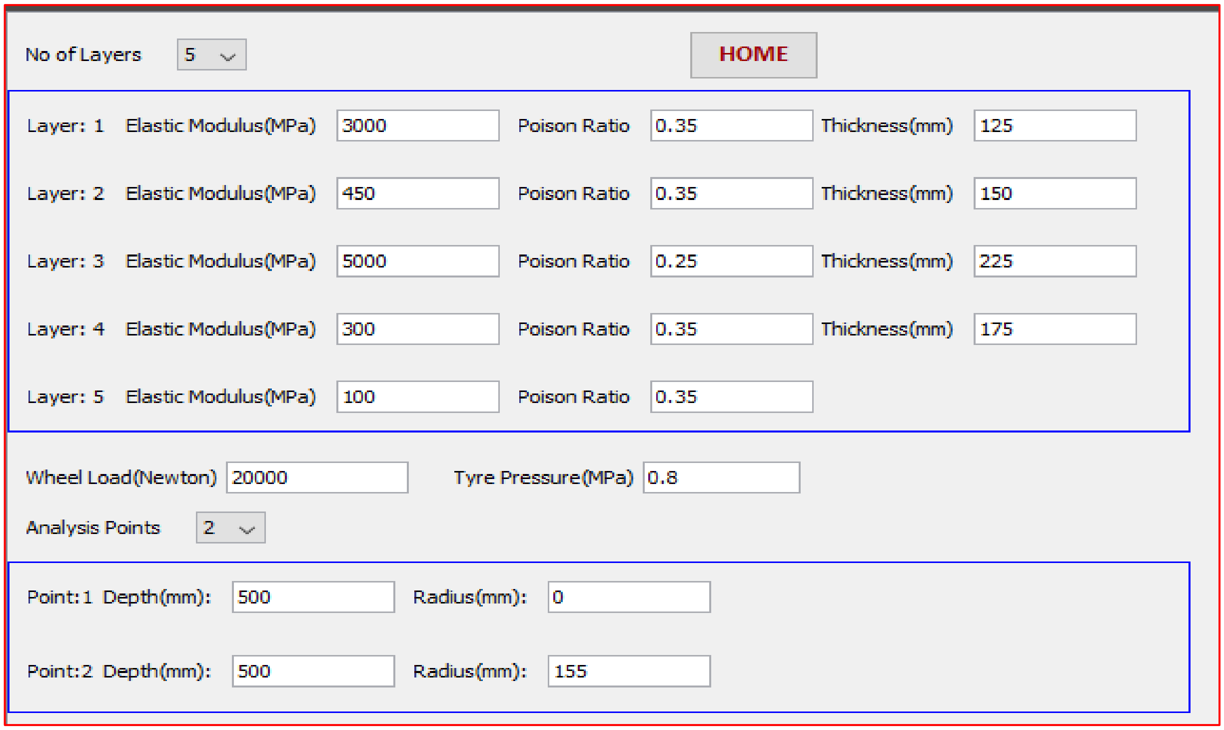


Figure 4.25 IITPAVE Software input data maximum tensile strain for CTB

Figure 4.26 shows the IITPAVE output data for the maximum tensile strain at the cement-treated base (CTB) layer.

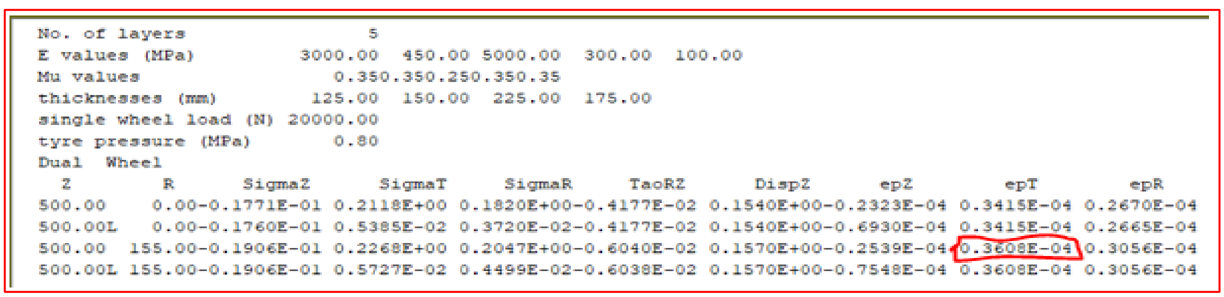

```
No. of layers                  5
E values (MPa)          3000.00   450.00 5000.00   300.00   100.00
Mu values                  0.350.350.250.350.35
thicknesses (mm)         125.00   150.00   225.00   175.00
single wheel load (N) 20000.00
tyre pressure (MPa)        0.80
Dual   Wheel
  Z         R       SigmaZ       SigmaT      SigmaR      TaoRZ       DispZ       epZ         epT         epR
500.00     0.00-0.1771E-01 0.2118E+00 0.1820E+00-0.4177E-02 0.1540E+00-0.2323E-04 0.3415E-04 0.2670E-04
500.00L    0.00-0.1760E-01 0.5385E-02 0.3720E-02-0.4177E-02 0.1540E+00-0.6930E-04 0.3415E-04 0.2665E-04
500.00   155.00-0.1906E-01 0.2268E+00 0.2047E+00-0.6040E-02 0.1570E+00-0.2539E-04 0.3608E-04 0.3056E-04
500.00L  155.00-0.1906E-01 0.5727E-02 0.4499E-02-0.6038E-02 0.1570E+00-0.7548E-04 0.3608E-04 0.3056E-04
```

**Figure 4.26 IITPAVE Software output data maximum tensile strain for CTB**

Maximum tensile strain =36.08 microstrains which is less than the limiting value. Hence safe.

## 4.6 Cost Comparison of Cement-Treated Base (CTB) and Conventional Pavement

The cost comparison between Cement-Treated Base (CTB) pavement and conventional flexible pavement methods was carried out to evaluate the economic feasibility of using CTB in road construction. The analysis considered various cost components, including material costs, construction expenses, and long-term maintenance costs.

### 4.6.1 Material Costs

The material costs for CTB were compared with those of traditional granular base and sub-base materials. CTB required the addition of cement, contributing to a slightly higher initial material cost. However, the reduction in base thickness due to CTB's higher strength and stiffness counterbalanced this additional cost. In contrast, conventional pavement required larger quantities of granular materials to meet structural requirements, increasing material costs. The optimized material use in CTB construction resulted in a 15-20% reduction in overall material costs.

### 4.6.2 Discussion for cost comparison CTB and Conventional Pavement

The findings of this cost comparison indicate that CTB pavements offer substantial economic benefits in road construction, particularly in regions like Ethiopia, where pavement performance is often compromised by subgrade conditions and overloading. The reduced base thickness in CTB pavements optimizes material use, leading to cost savings in materials and construction. Furthermore, the long-term durability and reduced maintenance needs of CTB pavements contribute to significant lifecycle cost reductions, making CTB a more sustainable and economically viable option than conventional pavement methods.

Given these advantages, the adoption of CTB in road construction projects in Ethiopia can provide cost savings and longer-lasting infrastructure, ultimately reducing the frequency of road repairs and the associated economic burdens. These findings support the recommendation for the wider implementation of CTB as a preferred pavement method in Ethiopian road construction.

# 5.0 CONCLUSION AND RECOMMENDATION

## 5.1 Conclusion

This investigation examines the characteristics of cement-treated base (CTB) materials. A comprehensive review of the existing literature is employed to explore the theoretical framework, operational mechanisms, and essential requirements of CTB. Empirical laboratory assessments are conducted to evaluate the mechanical properties and performance attributes of this material. Experimental procedures are undertaken to ascertain and validate the unconfined compressive strength outcomes for various combinations of cementitious materials incorporated into the aggregate matrix. Following the stipulations set forth by the Ethiopian Road Administration (ERA) and Ministry of Road Transport and Highways (MoRTH), the resultant data are deemed satisfactory.

This study aims to comprehensively investigate the geotechnical properties of the subgrade soil, explore the concept of cement-treated base (CTB) material, simulate the performance of the pavement using advanced numerical modeling techniques such as PLAXIS 3D and IITPAVE Software**,** and assess the economic feasibility of using CTB materials compared to conventional pavement alternatives.

- ✓ The investigation of the subgrade soil's geotechnical properties will provide critical insights into the behavior of the soil under different loading conditions, helping to design a more stable and durable pavement structure. Understanding the soil's physical characteristics is crucial for optimizing the pavement design and ensuring long-term performance, especially given the challenging nature of soils like **expansive clays** often encountered in urban environments such as Addis Ababa.
- ✓ Through the study of **cement-treated base materials**, this research will explore a sustainable and cost-effective alternative to conventional pavement methods. By optimizing the mix design and determining the best **application rates** of cement and aggregate, the study will contribute to more resilient and durable pavement structures.
- ✓ The simulation of pavement performance using PLAXIS 3D and IITPAVE Software will offer valuable insights into the behavior of the pavement under traffic loads, including stress**,** strain**,** deflection, and deformation, allowing for a more precise

prediction of pavement performance. These modeling tools will help evaluate the rutting, fatigue cracking, and overall durability of the pavement, providing a more refined and reliable pavement design.

- ✓ Finally, the cost comparison between CTB materials and traditional pavement methods will provide important economic data to assess the cost-effectiveness and long-term benefits of using CTB for road construction. Flexible pavements developed with CTB have reduced construction costs for high-volume roads by 15-20%, according to the cost estimates for flexible pavements using bound and unbound layers. This analysis will help decision-makers make informed choices, promoting the adoption of more sustainable, efficient, and cost-effective construction practices.

## 5.2 Recommendations

Based on the findings of this research, the following recommendations are proposed for future work and practical applications in road construction using Cement-Treated Base (CTB) materials:

- ✓ Adoption of CTB for Road Construction in Ethiopia: Encourage the integration of CTB in road construction projects to leverage its enhanced performance and cost-effectiveness.
- ✓ Further Research on Optimizing Cement Content: Conduct studies to identify the optimal cement content for CTB to maximize strength and durability while minimizing costs.
- ✓ Long-Term Performance Evaluation: Utilize the Falling Weight Deflectometer (FWD) and the Benkelman Beam Deflection Method for comprehensive long-term performance evaluations of CTB pavements to assess their resilience under traffic loads.

# REFERENCES


Adaska, W. S., & Luhr, D. R. (2016). *Control Of Reflective Cracking In Cement-Stabilized Pavements Control Of Reflective Cracking In Cement " Control Of Reflective Cracking In Cement Stabilized Pavements " 5th International RILEM Conferene, Limoges , France , May 2004. March*.

Adu-Osei, A. (2000). *Characterization of unbound granular layers in flexible pavements. Report No.ICAR/502-3*. 260. https://repositories.lib.utexas.edu/bitstream/handle/2152/35440/502-3.pdf?sequence=2&isAllowed=y

ASTM D-421. (1998). ASTM D 421 – 85: Standard Practice for Dry Preparation of Soil Samples for Particle-Size Analysis and Determination of Soil Constants 1. *Annual Book of ASTM Standards*, *04.08*(4), 7–8.

ASTM D-422. (2007). Standard Test Method for Particle-Size Analysis of Soils. *Astm*, *D422-63*(Reapproved), 1–8.

ASTM D-427. (2004). Standard Test Method for Shrinkage Factors of Soils by the Mercury Method. *ASTM International*, *i*(March), 1–4.

Asutroads. (2017). *Pavement Design*. 204.

Biswal, D. R., Chandra Sahoo, U., & Ranjan Dash, S. (2020). Structural response of an inverted pavement with stabilized base by numerical approach considering isotropic and anisotropic properties of unbound layers. *Road Materials and Pavement Design*, *21*(8), 2160–2179. https://doi.org/10.1080/14680629.2019.1595701

Bressi, S., Primavera, M., & Santos, J. (2022). A comparative life cycle assessment study with uncertainty analysis of cement treated base (CTB) pavement layers containing recycled asphalt pavement (RAP) materials. *Resources, Conservation and Recycling*, *180*. https://doi.org/10.1016/j.resconrec.2022.106160

Brita, D. A., Tratada, G., & Cimento, C. O. M. (2015). *Influência Do Tipo De Cimento Nas Características Mecânicas Da Brita Graduada Tratada COM CIMENTO Verônica*

*Janaína Melo Barreto Nunes Fernando Silva Albuquerque*. 1233–1244.

Chhabra, R. S., Ransinchung, G. D. R. N., & Islam, S. S. (2021). Performance analysis of cement-treated base layer by incorporating reclaimed asphalt pavement material and chemical stabilizer. *Construction and Building Materials*, *298*, 123866. https://doi.org/10.1016/j.conbuildmat.2021.123866

Cortes. (2010). *INVERTED BASE PAVEMENT STRUCTURES*. *December*.

Cortes, D. D., Asce, M., Shin, H., Santamarina, J. C., & Asce, M. (2012). *Numerical Simulation of Inverted Pavement Systems*. *3*(December), 1507–1519. https://doi.org/10.1061/(ASCE)TE.1943-5436.0000472.

Daniel, E., & Velasquez, R. (2023). *ScholarWorks @ UTEP Characterization And Modeling Of Unbound And Cementitiously Stabilized Materials For Structural Analysis Of Multilayer Pavement Systems Doctoral Program in Civil Engineering*.

De Almeida. (2021). *Performance Evaluation Of Inverted Pavements : Comparative Analysis Of South African And Brazilian Experiences Dissertation Summary Performance Evaluation Of Inverted Pavements : Comparative Analysis Of South African And Brazilian Experiences*. *January*.

Dutra, R. P. (2017). *Fev 2017 NORMA DNIT 407/2017 - ES*.

Ferri, S. (2013). *Critérios de aceitação e controle da qualidade da execução de camadas de fundação de pavimentos novos através de métodos deflectométricos*.

Forest. (2017). *Long-Term Performance Of Granular Bases Including The Effect Of Wet-Dry Cycles On Inverted Base Pavement Performance*.

Guidelines, T. (2012). *For the Design of Flexible Pavements Indian Roads Congress*.

Hasan, U., Whyte, A., Al Jassmi, H., & Hasan, A. (2022). Lifecycle Cost Analysis of Recycled Asphalt Pavements: Determining Cost of Recycled Materials for an Urban Highway Section. *CivilEng*, *3*(2), 316–331. https://doi.org/10.3390/civileng3020019

Hassani, A., Taghipoor, M., & Karimi, M. M. (2020). A state of the art of semi-flexible pavements: Introduction, design, and performance. *Construction and Building Materials*, *253*, 119196. https://doi.org/10.1016/j.conbuildmat.2020.119196

Huang. (2004). *Pavement Analysis and Design - Second Edition 2004_Huang.pdf*.

IRC:37-2018. (n.d.). *No Title*.

IRC:37-2018. (2018). GUIDELINES FOR THE DESIGN OF FLEXIBLE PAVEMENTS (Fourth Revision). *Proceedings of the Institute of Acoustics 1989 Spring …*, *August*.

IRC. (2010). Guidelines for soil and granular material stabilization using cement, lime, and fly ash. *Indian Roads Congress, SP 89_Part 1*, *53*(9), 1689–1699.

Jiang, X., Huang, B., Titi, H., & Polaczyk, P. (2022). *Evaluating the Performance of Inverted Pavements in Tennessee*.

Jiang, X., Titi, H., Ma, Y., Polaczyk, P., Zhang, M., Gabrielson, J., Bai, Y., & Huang, B. (2022). Evaluating the performance of inverted pavement structures using the accelerated pavement test (APT). *Construction and Building Materials*, *346*, 128489. https://doi.org/10.1016/J.CONBUILDMAT.2022.128489

Jiang, X., Zhang, M., Xiao, R., Polaczyk, P., Bai, Y., & Huang, B. (2021). An investigation of structural responses of inverted pavements by numerical approaches considering nonlinear stress-dependent properties of the unbound aggregate layer. *Construction and Building Materials*, *303*(July), 124505. https://doi.org/10.1016/j.conbuildmat.2021.124505

Khan, S., Ph., D., Nagabhushana, M. N., Hossain, K., & Tiwari, D. (2022). *Performance Evaluation of Fly Ash–Based Inverted Pavement System*. *148*(2), 1–11. https://doi.org/10.1061/JPEODX.0000363

Li, Q., Xiao, D. X., Wang, K. C. P., Hall, K. D., & Qiu, Y. (2011). Mechanistic-empirical pavement design guide (MEPDG): a bird's-eye view. *Journal of Modern Transportation*, *19*(2), 114–133. https://doi.org/10.1007/bf03325749

Metcalf, J. B., Romanoschi, S. A., Li, Y., Rasoulian, M., Metcalf, J. B., Rouge, B., Romanoschi, S. A., Rouge, B., & Rouge, B. (1999). *THE FIRST FULL-SCALE ACCELERATED PAVEMENT TEST IN LOUISIANA : 504*.

Papadopoulos, E., & Santamarina, J. C. (2017a). Inverted base pavements : construction and performance. *International Journal of Pavement Engineering*, *8436*(May), 0. https://doi.org/10.1080/10298436.2017.1326237

Papadopoulos, E., & Santamarina, J. C. (2017b). Inverted base pavements : construction and performance. *International Journal of Pavement Engineering*, *8436*(November), 0. https://doi.org/10.1080/10298436.2017.1326237

Patel, D., Kumar, R., Chauhan, K. A., & Patel, S. (2019). Experimental and Modeling Studies of Resilient Modulus and Permanent Strain of Stabilized Fly Ash. *Journal of Materials in Civil Engineering*, *31*(8), 4–9. https://doi.org/10.1061/(ASCE)mt.1943-5533.0002798

Plati, C. (2019). Sustainability factors in pavement materials, design, and preservation strategies: A literature review. *Construction and Building Materials*, *211*, 539–555. https://doi.org/10.1016/j.conbuildmat.2019.03.242

Plati, C., & Pomoni, M. (2019). Impact of Traffic Volume on Pavement Macrotexture and Skid Resistance Long-Term Performance. *Transportation Research Record*, *2673*(2), 314–322. https://doi.org/10.1177/0361198118821343

Rivki, M., Bachtiar, A. M., Informatika, T., Teknik, F., & Indonesia, U. K. (n.d.). *No 主観的健康感を中心とした在宅高齢者における 健康関連指標に関する共分散構造分析Title* (Issue 112).

Schwartz, C. W. (2007). Implementation of the NCHRP 1-37A Design Guide Final Report Volume 1 : Summary of Findings and Implementation Plan. *Design*, *1*(February 2007), 111.

Singh, A. K., & Sahoo, J. P. (2020). Analysis and design of two-layered flexible pavement systems: A new mechanistic approach. *Computers and Geotechnics*, *117*(September 2019), 103238. https://doi.org/10.1016/j.compgeo.2019.103238

Solla, M., Pérez-Gracia, V., & Fontul, S. (2021). Review of GPR application on transport infrastructures: Troubleshooting and best practices. *Remote Sensing*, *13*(4), 1–5. https://doi.org/10.3390/rs13040672

T-180, A. (n.d.). *T 180-95 Modified Proctor.pdf*.

Taha, R., Al-Harthy, A., Al-Shamsi, K., & Al-Zubeidi, M. (2002). Cement Stabilization of Reclaimed Asphalt Pavement Aggregate for Road Bases and Subbases. *Journal of Materials in Civil Engineering*, *14*(3), 239–245. https://doi.org/10.1061/(ASCE)0899-1561(2002)14:3(239)

Theyse, H. L., De Beer, M., & Rust, F. C. (1996). Overview of South African mechanistic pavement design method. *Transportation Research Record*, *1539*, 6–17. https://doi.org/10.3141/1539-02

Tian, Y., Xiang, P., Liu, S., Ling, J., & Tang, R. (2021). Improving airport runway rigid pavement design using influence surfaces. *Construction and Building Materials*, *284*, 122702. https://doi.org/10.1016/j.conbuildmat.2021.122702

TRH4. (1996). *TECHNICAL RECOMMEND FOR HIGI-1WAYS*. 1–101.

Visser, A. T. (2017). ScienceDirect Potential of South African road technology for application in China. *Journal of Traffic and Transportation Engineering (English Edition)*, 3–7. https://doi.org/10.1016/j.jtte.2017.03.004

Zvonarić, M., Barišić, I., Galić, M., & Minažek, K. (2021). Influence of laboratory compaction method on compaction and strength characteristics of unbound and cement-bound mixtures. *Applied Sciences (Switzerland)*, *11*(11). https://doi.org/10.3390/app11114750

# ANNEX-1

# SUBGRADE SOIL TEST RESULT

## Subgrade Soil test result

**Summary of Test Results**

| Station (KM) | Depth (cm) | Visual Discription | Sieve pass(%) | | | | | | Atterberg Limits (%) | | | AASHTO SOIL CLASSIFICATION | MDD ($g/cm^3$) | OMC (%) | NMC (%) | % CBR | | | | Swell (%) | Swell at 93% MDD | 93% MDD | 95% MDD | CBR at 93% MDD | CBR at 95% MDD |
|---|---|---|---|---|---|---|---|---|---|---|---|---|---|---|---|---|---|---|---|---|---|---|---|---|---|
| | | | 25.0 | 9.5 | 4.75 | 2.00 | 0.425 | 0.075 | LL | PL | PI | | | | | No. of Blows | Dry Density (g/cc) | 2.54 mm | 5.08 mm | | | | | | |
| 0+580 | 120.0 | Black cotton soil | 92 | 78.3 | 75.6 | 71.6 | 64.4 | 55.1 | 56 | 28 | 28 | A-7-6 (12) | 1.64 | 19.70 | 6.67 | 10 | 1.39 | 1.1 | 1.0 | 9.54 | 9.1 | 1.53 | 1.53 | 2 | 2 |
| | | | | | | | | | | | | | | | | 30 | 1.56 | 1.6 | 1.6 | 9.05 | | | | | |
| | | | | | | | | | | | | | | | | 65 | 1.68 | 1.9 | 1.7 | 8.50 | | | | | |
| 0+940 | 120.0 | Black cotton soil | 100 | 100 | 100 | 100 | 100 | 99 | 69 | 33 | 36 | A-7-5 (41) | 1.47 | 22.40 | 8.02 | 10 | 1.25 | 0.9 | 0.9 | 11.93 | 11.6 | 1.36 | 1.39 | 1 | 1 |
| | | | | | | | | | | | | | | | | 30 | 1.38 | 1.3 | 1.3 | 11.57 | | | | | |
| | | | | | | | | | | | | | | | | 65 | 1.50 | 1.7 | 1.6 | 11.19 | | | | | |
| 1+300 | 120.0 | Black cotton soil | 100 | 98 | 96 | 95 | 90 | 84 | 63 | 30 | 32 | A-7-6 (31) | 1.57 | 16.00 | 7.87 | 10 | 1.43 | 0.9 | 0.9 | 14.81 | 14.7 | 1.46 | 1.49 | 1 | 1 |
| | | | | | | | | | | | | | | | | 30 | 1.56 | 1.0 | 1.0 | 14.30 | | | | | |
| | | | | | | | | | | | | | | | | 65 | 1.62 | 1.2 | 1.2 | 13.99 | | | | | |
| 1+380 | 150.0 | Black cotton soil | 60 | 50 | 46.3 | 43.4 | 39.6 | 36.8 | 54 | 28 | 26 | A-7-6 (3) | 1.68 | 19.0 | 9.7 | 10 | 1.31 | 1.1 | 1.4 | 7.73 | 6.90 | 1.56 | 1.60 | 3 | 3 |
| | | | | | | | | | | | | | | | | 30 | 1.47 | 2.4 | 2.4 | 7.26 | | | | | |
| | | | | | | | | | | | | | | | | 65 | 1.52 | 2.5 | 2.6 | 6.74 | | | | | |

# ANNEX-2

# CRUSHED BASE COURSE TEST RESULT

| RESEARCH TITLE | Subgrade Investigation and Performance Characteristics of Cement-Treated Base Materials for Enhancement of Road Pavement Systems: In Case of Addis Ababa | | |
|---|---|---|---|
| Types of Material:- | Cement Treated Crushed Base Course, (CTB) | Lab. Reference No.:- | CFHWE/YZ/Lab-012/2024 |
| Sampling Location:- | Bole Bulbula Quarry | Date of Sampling:- | 22/3/2024 |
| Sample From: | Stock Pile | Date of Report:- | 19/4/2024 |
| Sampled By:- | YARED ZIKUALA MULUGETA | Cement Type:- | Dangote OPC 42.5Mpa |

**TEST RESULT SUMMARY FOR CRUSHED BASE COURSE MATERIAL**

| TYPE OF MATERIAL | ITEM DESCRIPTION | Test Result | ERA Specification |
|---|---|---|---|
| CRUSHED BASE COURSE | PI | N.P | ≤6 |
| | CBR at 100% MDD | 116 | ≥100 |
| | Swell at 100% MDD | 0 | ≤1.5% |
| | MDD g/cc | 2.11 | ------------ |
| | OMC % | 9 | ------------ |
| | ACV | 13 | ≤25% |
| | TFV | 90 | ≥75% |
| | FI | 21 | ≤30% |
| | SSS (fine.Agg,) | 2.98 | <12% |
| | SSS (CoarseAgg.) | 2.68 | <12% |
| | LAA | 14 | ≤45% |

# ANNEX-3

# CEMENT TREATED BASE TEST RESULT

| Contractor | Client | Supervision Consultant |
|---|---|---|
| CHINA FIRST HIGHWAY ENGINEERING CO. LTD<br>中交第一公路工程局有限公司 | የአዲስ አበባ ከተማ<br>Addis Ababa City<br>መንገዶች ባለስልጣን<br>Roads Authority | STADIA Engineering Work Consulting Plc |

## SUMMARY FOR CEMENT TREATED BASE MATERIAL CTB MIX DESIGN

| | | | |
|---|---|---|---|
| *RESEARCH TITLE* | *Investigation of Subgrade and Performance Characteristics of Cement-Treated Base Materials for Road Pavement Systems Enhancement: In the Case of Addis Ababa* | | |
| Types of Material:- | Cement Treated Crushed Base Course, (CTB) | Lab. Reference No.:- | CFHWE/YZ/Lab-011/2024 |
| Sampling Location:- | Bole Bulbula Quarry | Date of Sampling:- | 19/3/2024 |
| Sample From: | Stock Pile | Testing Date:- | 20/4/2024 |
| Sampled By:- | YARED ZIKUALA MULUGETA | Cement Type:- | Dangote OPC 42.5Mpa |
| Admixture:- | 0.03% used in the mix, (Type of Admixture Retarder, (Sodium Gluconate)) | Tested By:- | YARED ZIKUALA MULUGETA |

| SPECIMEN REFERENCE | CEMENT CONTENT (%) | COMPACTION DATA | | ATTERBERG LIMITS DATA | | | UNCONFINED COMPRESSIVE STRENGTH (UCS) (4.5-7MPa) | | | | | |
|---|---|---|---|---|---|---|---|---|---|---|---|---|
| | | MAXIMUM DRY DENSITY ($Kg/m^3$) | OPTIMUM MOISTURE CONTENT (%) | LL % | PL % | PI % | DRY DENSITY ($Kg/m^3$) | MOISTURE CONTENT (%) | 7 DAY COMPRESSIVE STRENGTH | | 28 DAY COMPRESSIVE STRENGTH | |
| | | | | | | | | | INDIVIDUAL (Mpa) | AVERAGE (Mpa) | INDIVIDUAL (Mpa) | AVERAGE (Mpa) |
| CTB-1 | | | | | | | 2080 | 8.2 | 2.21 | | 4.03 | |
| CTB-2 | 2.0 | 2.09 | 8.40 | NP | NP | NP | 2076 | 8.3 | 2.25 | 2.26 | 3.99 | 4.02 |
| CTB-3 | | | | | | | 2082 | 8.2 | 2.33 | | 4.03 | |
| CTB-4 | | | | | | | 2047 | 9.0 | 3.27 | | 5.94 | |
| CTB-5 | 3.0 | 2.11 | 7.6 | NP | NP | NP | 2052 | 8.9 | 3.23 | 3.23 | 5.98 | 6.00 |
| CTB-6 | | | | | | | 2047 | 8.8 | 3.18 | | 6.07 | |
| CTB-7 | | | | | | | 2029 | 9.7 | 4.20 | | 7.55 | |
| CTB-8 | 4.0 | 2.12 | 7.5 | NP | NP | NP | 2036 | 9.7 | 4.16 | 4.19 | 7.47 | 7.51 |
| CTB-9 | | | | | | | 2032 | 9.8 | 4.20 | | 7.51 | |
| CTB-10 | | | | | | | 2013 | 10.2 | 5.18 | | 8.06 | |
| CTB-11 | 5.0 | 2.14 | 6.8 | NP | NP | NP | 2011 | 10.2 | 5.26 | 5.22 | 8.11 | 8.11 |
| CTB-12 | | | | | | | | | 5.22 | | 8.15 | |
| CTB-13 | | | | | | | | | 6.15 | | 9.1 | |
| CTB-14 | 6.0 | 2.16 | 6.4 | NP | NP | NP | | | 6.20 | 6.21 | 9.0 | 9.05 |
| CTB-15 | | | | | | | 2015 | 10.4 | 6.28 | | 9.0 | |

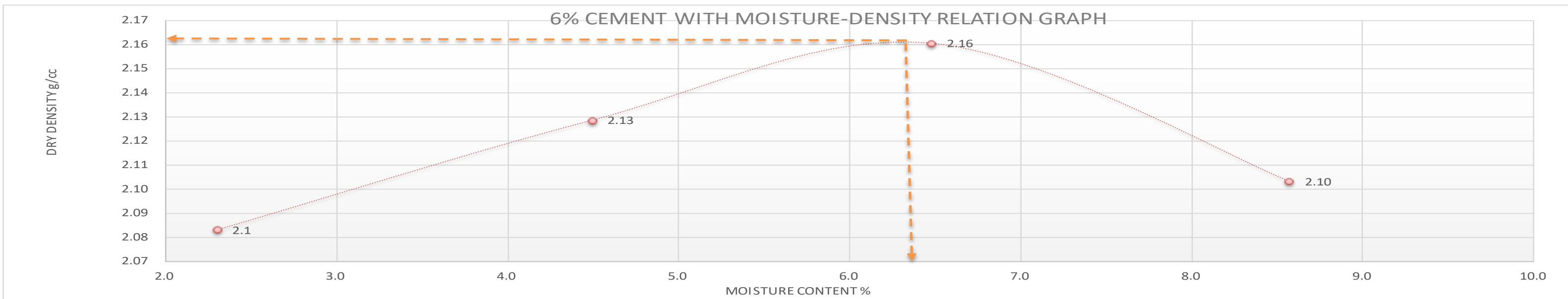


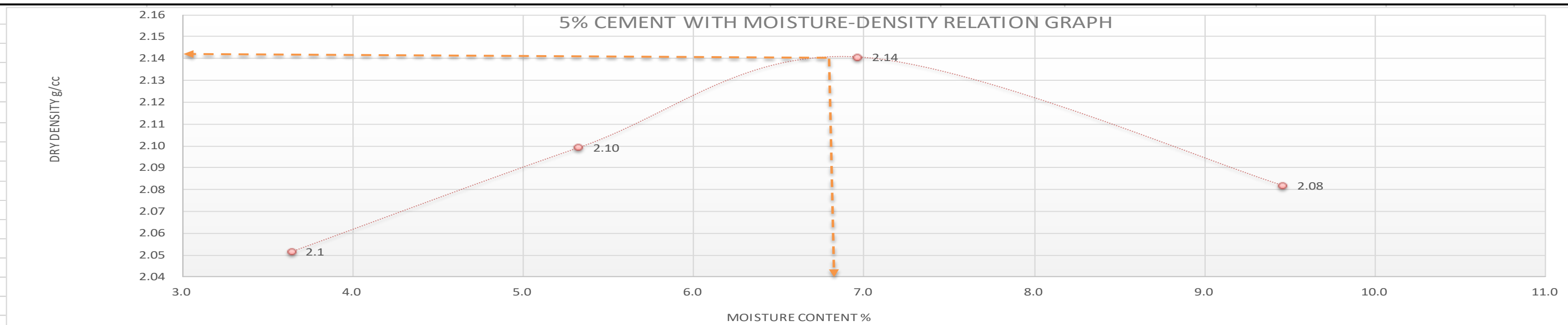


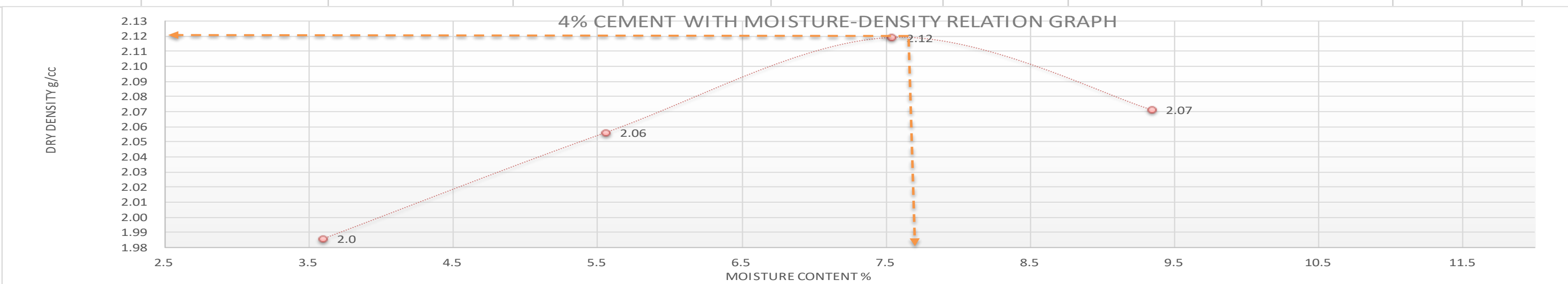


**According to MORT&H recommendation, after obtaining the OMC with respect of% of cement, we need to cast the cubes each of three no of set reqd, & after age of 7days moist curing compressive strength we will find out. Then multiplyng the Comresssive Strenth * 0.75 to find out the Unconfined Compressive Strength (UCS).**

**Now as per the graphical form & requirement of target UCS say 5.22 N.mm2 we will find out the cement content from the graph 5.0 %.**

**Now after obtaining the cement content with respect to the target UCS as per the requirement, we need to prepare the mixture with design cement content (5.0%), OMC (6.80% found earlier) & blended Agg.After that preaper the moulds as per the modified proctor test & find out the final MDD Vs OMC graph & for conformity test cast three no of cylinderical cubes to check the the target UCS at age of 7 days moist curing condition & MDD/OMC**

## SUMMARY FOR CEMENT TREATED BASE MATERIAL MIX DESIGN

| SL NO | % OF CEMENT | % OF AGG. | MDD gm/cc | OMC % | Compressive Strength N/mm2 | Unconfined Compressive Strength UCS N/mm2 |
|---|---|---|---|---|---|---|
| 1 | 2.00 | 98.00 | 2.09 | 8.40 | 3.02 | 2.26 |
| 2 | 3.00 | 97.00 | 2.11 | 7.60 | 4.30 | 3.23 |
| 3 | 4.00 | 96.00 | 2.12 | 7.50 | 5.58 | 4.19 |
| 4 | 5.00 | 95.00 | 2.14 | 6.80 | 6.96 | 5.22 |
| 5 | 6.00 | 94.00 | 2.16 | 6.40 | 8.28 | 6.21 |

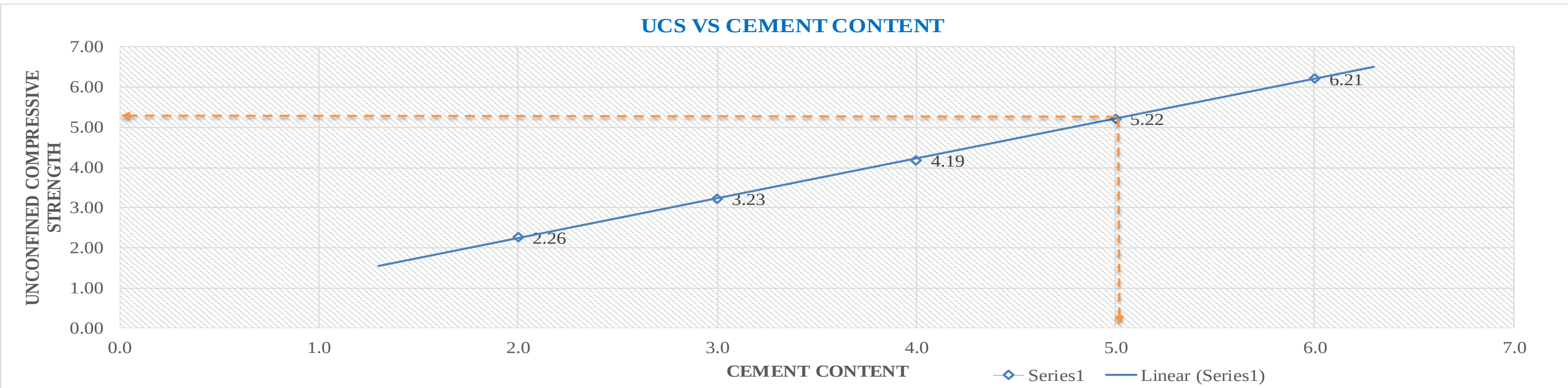


**According to MORT&H recommendation, after obtaining the OMC with respect of% of cement, we need to cast the cubes each of three no of set reqd, & after age of 7days moist curing compressive strength we will find out. Then multiplyng the Comressive Strenth * 0.75 to find out the Unconfined Compressive Strength (UCS).**

**Now as per the graphical form & requirement of target UCS say 5.22 N.mm2 we will find out the cement content from the graph 5.0 %.**

**Now after obtaining the cement content with respect to the target UCS as per the requirement, we need to prepare the mixture with design cement content (5.00%), OMC (6.80% found earlier) & blended Agg. After that prepared the moulds as per the modified proctor test & find out the final MDD Vs OMC graph & for conformity test cast three no of cyliner or cubes to check the the target UCS at age of 7 days moist curing condition & MDD/OMC also for the same.**

| RESEARCH TITLE | Subgrade Investigation and Performance Characteristics of Cement-Treated Base Materials for Enhancement of Road Pavement Systems: In Case of Addis Ababa | | |
|---|---|---|---|
| Types of Material:- | Cement Treated Crushed Base Course, (CTB) | Lab. Reference No.:- | CFHWE/YZ/Lab-012/2024 |
| Sampling Location:- | Bole Bulbula Quarry | Date of Sampling:- | 22/3/2024 |
| Sample From: | Stock Pile | Date of Report:- | 19/4/2024 |
| Sampled By:- | YARED ZIKUALA MULUGETA | Cement Type:- | Dangote OPC 42.5Mpa |

**PARTICLE SIZE DISTRIBUTION**

**TEST METHOD: AASHTO T 27**

| No of sample | | 1 | | | 2 | | Grading Modulas | PP | As per MORT&H Table 400-4 | |
|---|---|---|---|---|---|---|---|---|---|---|
| Dry sample weight (g) | | 3514.2 | | | 3242.2 | | | | | |
| After wash dry sample (g) | | 3304.2 | | | 3128.4 | | 2.63 | | | |
| Inch | Sieve Size(mm) | Mass of Retained Sample (g) | Cumulative Passing ( g ) | Cumulative Passing (%) | Mass of Retained Sample (g) | Cumulative Passing ( g ) | Cumulative Passing (%) | Average Passing (%) | LOWER | UPPER |
| 1 1/4 | 53 | 0.0 | 3514.2 | 100.0 | 0.0 | 3242.2 | 100.0 | 100.0 | 100.0 | 100.0 |
| 1.06 | 37.5 | 102.7 | 3411.5 | 97.1 | 103.1 | 3139.1 | 96.8 | 96.9 | 95.0 | 100.0 |
| 3/4 | 19 | 1000.3 | 2411.2 | 68.6 | 1000.2 | 2138.9 | 66.0 | 67.3 | 45.0 | 100.0 |
| 3/8 | 9.5 | 400.0 | 2011.2 | 57.2 | 400.0 | 1738.9 | 53.6 | 55.4 | 35.0 | 100.0 |
| NO 4 | 4.75 | 750.0 | 1261.2 | 35.9 | 750.0 | 988.9 | 30.5 | 33.2 | 25.0 | 100.0 |
| NO 8 | 0.6 | 500.0 | 761.2 | 21.7 | 500.0 | 488.9 | 15.1 | 18.4 | 8.0 | 65.0 |
| NO 30 | 0.3 | 250.0 | 511.2 | 14.5 | 50.0 | 438.9 | 13.5 | 14.0 | 5.0 | 40.0 |
| NO 200 | 0.075 | 300.0 | 211.2 | 6.0 | 325.0 | 113.9 | 3.5 | 4.8 | 0.0 | 10.0 |
| pan | | 1.2 | 0.0 | | 0.1 | | | | | |
| Wash loose | | 210.0 | | | 113.8 | | | | | |
| Total | | 3514.2 | | | 3242.2 | | | | | |

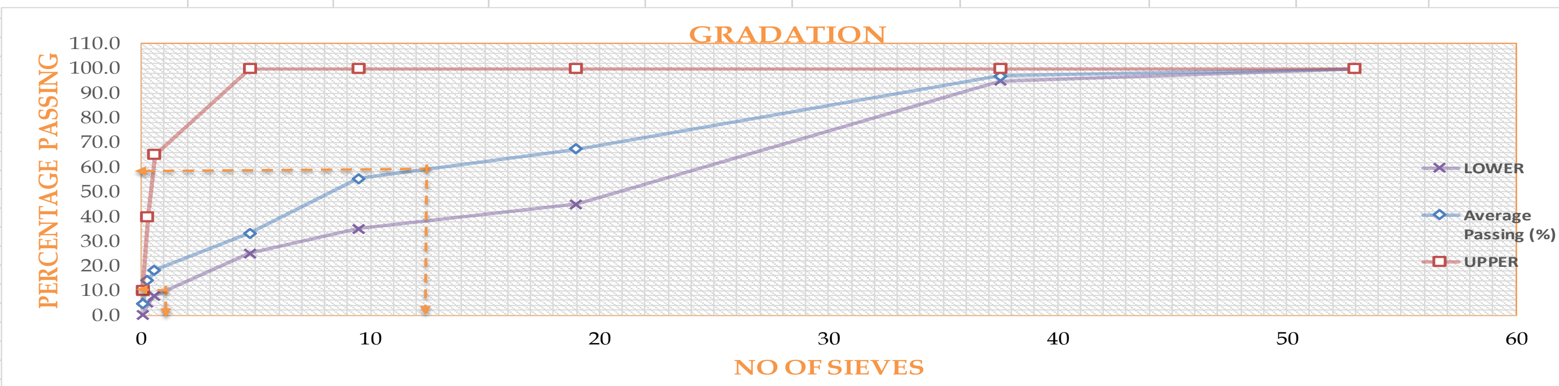

**PARTICLE SIZE DISTRIBUTION**

**TEST METHOD: AASHTO T 27**

| | | | | | | | | | | |
|---|---|---|---|---|---|---|---|---|---|---|
| No of sample | | 1 | | | 2 | | Grading Modulas | PP | As per MORT&H Table 400-4 | |
| Dry sample weight (g) | | 3514.2 | | | 3242.2 | | | | | |
| After wash dry sample (g) | | 3304.2 | | | 3128.4 | | 2.63 | | | |
| Inch | Sieve Size(mm) | Mass of Retained Sample (g) | Cumulative Passing ( g ) | Cumulative Passing (%) | Mass of Retained Sample (g) | Cumulative Passing ( g ) | Cumulative Passing (%) | Average Passing (%) | LOWER | UPPER |
| 1 1/4 | 53 | 0.0 | 3514.2 | 100.0 | 0.0 | 3242.2 | 100.0 | 100.0 | 100.0 | 100.0 |
| 1.06 | 37.5 | 102.7 | 3411.5 | 97.1 | 103.1 | 3139.1 | 96.8 | 96.9 | 95.0 | 100.0 |
| 3/4 | 19 | 1000.3 | 2411.2 | 68.6 | 1000.2 | 2138.9 | 66.0 | 67.3 | 45.0 | 100.0 |
| 3/8 | 9.5 | 400.0 | 2011.2 | 57.2 | 400.0 | 1738.9 | 53.6 | 55.4 | 35.0 | 100.0 |
| NO 4 | 4.75 | 750.0 | 1261.2 | 35.9 | 750.0 | 988.9 | 30.5 | 33.2 | 25.0 | 100.0 |
| NO 8 | 0.6 | 500.0 | 761.2 | 21.7 | 500.0 | 488.9 | 15.1 | 18.4 | 8.0 | 65.0 |
| NO 30 | 0.3 | 250.0 | 511.2 | 14.5 | 50.0 | 438.9 | 13.5 | 14.0 | 5.0 | 40.0 |
| NO 200 | 0.075 | 300.0 | 211.2 | 6.0 | 325.0 | 113.9 | 3.5 | 4.8 | 0.0 | 10.0 |
| pan | | 1.2 | 0.0 | | 0.1 | | | | | |
| Wash loose | | 210.0 | | | 113.8 | | | | | |
| Total | | 3514.2 | | | 3242.2 | | | | | |

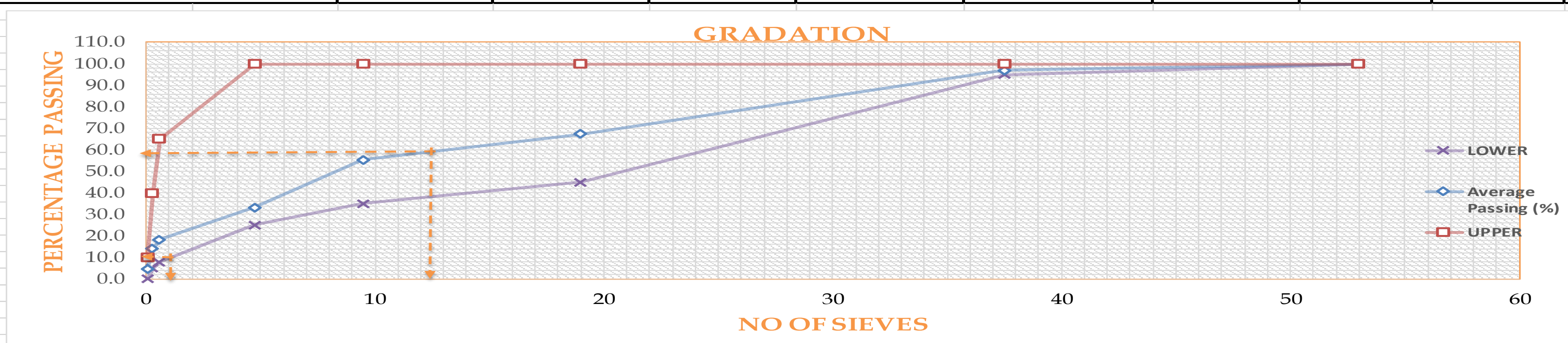


| | | | | | |
|---|---|---|---|---|---|
| UNIFORMITY COEFFICIENT CU=D60/D10 | | | | | |
| COEFFICENT OF UNIFORMITY | D60 | 13.00 | CU= D60/D10 | 32.5 | Should be more than >5 as per MORT&H specification |
| | D10 | 0.40 | | | |
| PI found for blended materials passing from 425 micron sieve- NP (Non Plastic) | | | | | Should not > 6 |
| LIQUID LIMIT | | | | | LL not more than 25 % |
| PLASTIC MODULUS=PI X % PASSING 75 MICRON SIEVE-Found NP | | | | | Should not >60 |
| REMARKS: | After obating the individual Gradation of each materials 20 mm, 10 mm & 06 mm down with designated sieves as per the specification, combined gradtion will be achived by this values | | | | |

| RESEARCH TITLE | Subgrade Investigation and Performance Characteristics of Cement-Treated Base Materials for Enhancement of Road Pavement Systems: In Case of Addis Ababa | | |
|---|---|---|---|
| **Types of Material:-** | **CRUSHED BASE COURSE** | **Lab. Reference No.:-** | **CFHWE/YZ/Lab-012/2024** |
| **Sampling Location:-** | **Bole Bulbula Quarry** | **Date of Sampling:-** | **22/3/2024** |
| **Sample From:** | **Stock Pile** | **Date of Report:-** | **19/4/2024** |
| **Sampled By:-** | **YARED ZIKUALA MULUGETA** | **Cement Type:-** | **Dangote OPC 42.5Mpa** |

## AGGREGATE CRUSHING VALUE

## TEST METHOD : BS:812 Part 110 (1990)

| TRIAL No. | 1 | 2 | 3 | |
|---|---|---|---|---|
| Mass of sample (14mm pass and 10mm Retain) | 2634 | 2626 | 2638 | AGGREGATE IMPACT VALUE MAXIMUM 40 AS PER MORT & H |
| Mass of sample retained on B.S Sieve,2.36mm | 2344 | 2311 | 2346 | |
| Mass of sample passing B.S Sieve,2.36mm | 290 | 315 | 320 | |
| Aggregate Crushing Value (ACV) | 11.01 | 12.00 | 12.13 | |
| Average ACV | **11.7** | | | |

# ANNEX-3

# Cost Comparison

Cost comparison for cement treated base CTB and Conventional Asphalt Pavement

| COST COMPARISON FOR CEMENT TREATED BASE (CTB) AND CONVENTIONAL ASPHALT PAVEMENT | | | | | | | |
|---|---|---|---|---|---|---|---|
| PAY ITEM | DESCRIPTION | UNIT | RATE IN ETB | QUANTITIES OF DBM DESIGN | QUANTITIES OF CTB DESIGN | AMOUNT FOR DBM DESIGN | AMOUNT FOR CTB DESIGN |
| 1 | Crushed stone subbase unstablized compacted to 97% of AACRA test S-11 density compacted layer thickness of maximum 200mm | M3 | 578.68 | 0.18 | 0.18 | 101.27 | 101.27 |
| 2 | Crushed stone base Crack relief layer unstablized compacted to 100% of AACRA test S-11 density compacted layer thickness of maximum 150mm | M3 | 644.22 | | 0.15 | | 96.63 |
| 3 | Cement treated base course with thickness of 225mm | M2 | 779.45 | | 1 | | 779.45 |
| 4 | Dense Bitumen Makadam Base (DBM) | | | | | | |
| 5 | 80mm compacted later thickness 37.5mm nominal aggregate size with 60/70 penetration grade bitumen | M2 | 492.35 | 1 | | 492.35 | |
| 6 | 70mm compacted later thickness 37.5mm nominal aggregate size with 60/70 penetration grade bitumen | M2 | 430.8 | 1 | | 430.8 | |
| 7 | 70mm compacted later thickness 37.5mm nominal aggregate size with 60/70 penetration grade bitumen | M2 | 430.8 | 1 | | 430.8 | |
| 8 | supply and spray of MC-30 Cut Back Asphalt Prime coat application rate 1lit/m2 | L | 37.27 | 1.1 | 1.1 | 41 | 41 |
| 9 | supply and spray of Tack coat with grade 30 bitumen emulsion application rate 0.3 lit/m3 | L | 44.98 | 1.2 | 0.3 | 53.98 | 13.49 |
| 10 | 50mm compacted later thickness with60/70 penetration grade (PG) bitumen | M2 | 314.14 | 1 | | 314.14 | |
| 11 | 70mm compacted later thickness with60/70 penetration grade (PG) bitumen | M2 | 439.8 | | 1 | | 439.8 |
| 12 | Dense graded asphalt (AC) in wearing surface | | | | | | |
| 13 | 40mm compacted later thickness with60/70 penetration grade (PG) bitumen | M2 | 259.21 | 1 | 1 | 259.21 | |
| 14 | 50mm compacted later thickness with60/70 penetration grade (PG) bitumen | M2 | 356.41 | | | | 356.41 |
| 15 | **TOTAL** | | | | | **2123.55** | **1828.05** |

Cost Comparison for CTB and DBM per square meter

| Cost Per Square Meter (Birr) | | Saving Cost Per Square Meter | Total Quantity (m2) | Total Saving Amount | Estimated Adjustment Factor | Adjustment Amount |
|---|---|---|---|---|---|---|
| Conventional Design | CTB Design | | | | | |
| 2123.54 | 1828.05 | 295.49 | 53808.06 | 15,899,743.65 | 1.78 | **28,301,543.70** |

Total expected price adjustment and saving amount for CTB and DBM Pavement

| Pavement Type | Original Amount | Expected Price Adjustment Factor | Adjusted Amount |
|---|---|---|---|
| expected price adjustment with pavement DBM | 114,263,674.50 | 1.78 | 203,389,340.61 |
| Expected price adjustment with pavement CTB | 98,363,766.13 | 1.78 | 175,087,503.71 |
| **Difference** | | | **28,301,836.90** |

Table A-1 FEA on the effect of settlement on inverted pavement (CTB)

| | | | | | | |
|---|---|---|---|---|---|---|
| 10.00 | 8.00 | 0.00 | 0.00 | 0.00 | 0.00 | AC |
| 11.00 | 8.00 | 0.01 | 0.00 | 5.93 | 0.03 | |
| 12.00 | 9.00 | 0.02 | 0.00 | 17.78 | 0.09 | |
| 13.00 | 10.00 | 0.04 | 0.00 | 41.43 | 0.21 | |
| 14.00 | 11.00 | 0.09 | 0.00 | 87.86 | 0.46 | |
| 15.00 | 12.00 | 0.13 | 0.00 | 132.50 | 0.70 | |
| 16.00 | 13.00 | 0.15 | 0.00 | 153.96 | 0.82 | |
| 17.00 | 14.00 | 0.18 | 0.00 | 175.12 | 0.95 | |
| 18.00 | 15.00 | 0.20 | 0.00 | 195.68 | 1.07 | |
| 19.00 | 16.00 | 0.22 | 0.00 | 215.99 | 1.20 | |
| 20.00 | 17.00 | 0.24 | 0.00 | 235.99 | 1.32 | |
| 21.00 | 18.00 | 0.26 | 0.00 | 255.78 | 1.45 | |
| 22.00 | 19.00 | 0.28 | 0.00 | 275.35 | 1.57 | |
| 23.00 | 20.00 | 0.31 | 0.00 | 313.94 | 1.82 | |
| 24.00 | 21.00 | 0.35 | 0.00 | 351.94 | 2.07 | |
| 25.00 | 22.00 | 0.39 | 0.00 | 389.46 | 2.32 | |
| 26.00 | 23.00 | 0.43 | 0.00 | 426.62 | 2.57 | |
| 27.00 | 24.00 | 0.46 | 0.00 | 463.45 | 2.82 | |
| 28.00 | 25.00 | 0.50 | 0.00 | 500.02 | 3.07 | |
| 29.00 | 26.00 | 0.54 | 0.00 | 536.36 | 3.33 | |
| 30.00 | 27.00 | 0.57 | 0.00 | 572.51 | 3.58 | |
| 31.00 | 28.00 | 0.61 | 0.00 | 608.49 | 3.83 | |
| 32.00 | 29.00 | 0.68 | 0.00 | 680.06 | 4.33 | |
| 33.00 | 30.00 | 0.75 | 0.00 | 751.30 | 4.84 | |
| 34.00 | 31.00 | 0.82 | -0.01 | 822.20 | 5.34 | |
| 35.00 | 32.00 | 0.89 | -0.01 | 892.79 | 5.85 | |
| 36.00 | 33.00 | 0.96 | -0.01 | 963.15 | 6.35 | |
| 37.00 | 34.00 | 1.00 | -0.01 | 1000.00 | 6.62 | |

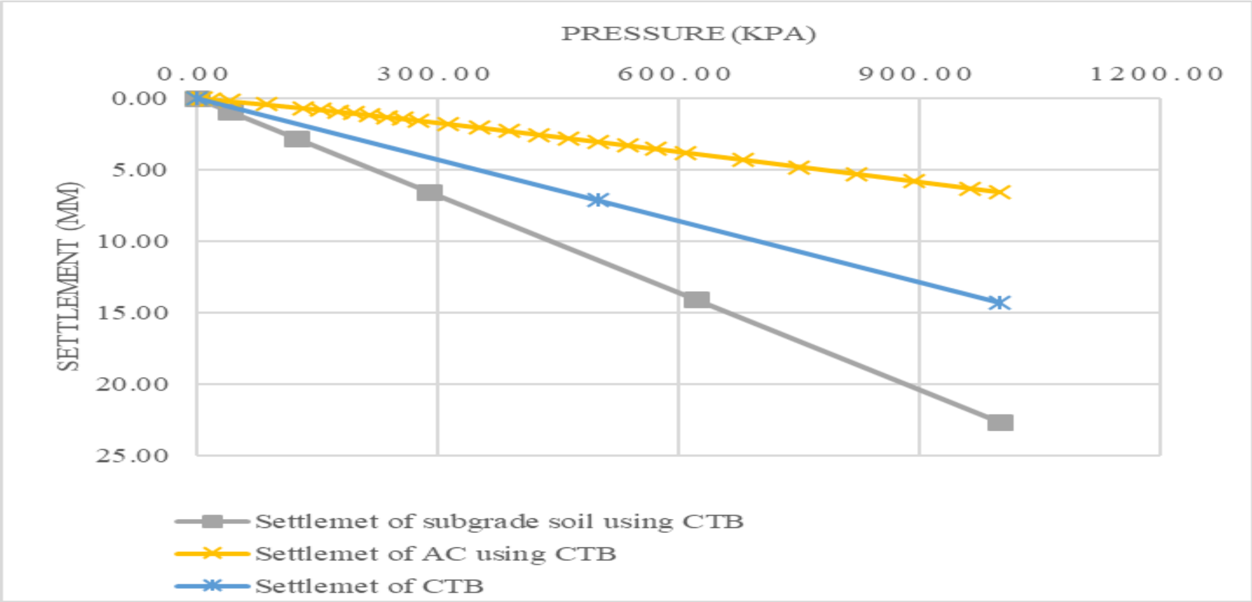

Table A-2 FEA on the effect of settlement on conventional pavement

| Point | Step | ΣMstage [] | u_z [m] | Stress (kPa) | Settlement (mm) | Loaction of Settlement |
|---|---|---|---|---|---|---|
| 1.00 | 1.00 | 0.00 | 0.00 | 0.00 | 0.000 | Soil |
| 2.00 | 1.00 | 0.50 | -0.02 | 499.87 | 26.681 | |
| 3.00 | 2.00 | 1.00 | -0.04 | 999.74 | 53.362 | |
| 4.00 | 3.00 | 0.00 | 0.00 | 0.00 | 0.000 | Asphalt |
| 5.00 | 3.00 | 0.04 | 0.00 | 38.38 | 0.339 | |
| 6.00 | 4.00 | 0.11 | 0.00 | 114.99 | 1.018 | |
| 7.00 | 5.00 | 0.27 | 0.00 | 265.16 | 2.376 | |
| 8.00 | 6.00 | 0.56 | 0.00 | 560.22 | 5.097 | |
| 9.00 | 7.00 | 1.00 | -0.01 | 1000.00 | 9.182 | |

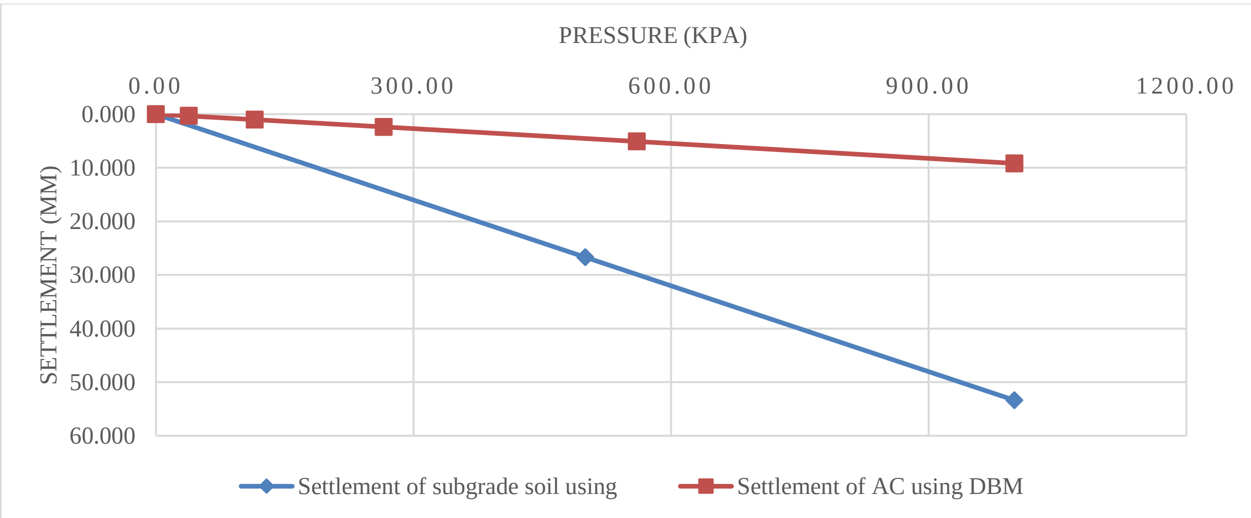

## Table A-3 FEA on the effect of settlement on conventional pavement and Inverted Pavement

| Soil with DBM | | AC with DMB | | Soil with CTB | | Soil with CTB | | AC with CTB | |
|---|---|---|---|---|---|---|---|---|---|
| Stress (kPa) | Settlement (mm) | Stress (kPa) | Settlement (mm) | Pressura (kN/m2) | Settlement (mm) | Pressura (kN/m2) | Settlement (mm) | Pressura (kN/m2) | Settlement (mm) |
| 0.00 | 0.00 | 0.00 | 0.00 | 0.00 | 0.00 | 0.00 | 0.00 | 0.00 | 0.00 |
| 499.87 | 26.68 | 38.38 | 0.34 | 41.40 | 0.94 | 500.00 | 7.17 | 5.93 | 0.03 |
| 999.74 | 53.36 | 114.99 | 1.02 | 124.20 | 2.82 | 1000.00 | 14.35 | 17.78 | 0.09 |
| | | 265.16 | 2.38 | 289.80 | 6.58 | | | 41.43 | 0.21 |
| | | 560.22 | 5.10 | 621.00 | 14.10 | | | 87.86 | 0.46 |
| | | 1000.00 | 9.18 | 1000.00 | 22.70 | | | 132.50 | 0.70 |
| | | | | | | | | 153.96 | 0.82 |
| | | | | | | | | 175.12 | 0.95 |
| | | | | | | | | 195.68 | 1.07 |
| | | | | | | | | 215.99 | 1.20 |
| | | | | | | | | 235.99 | 1.32 |
| | | | | | | | | 255.78 | 1.45 |
| | | | | | | | | 275.35 | 1.57 |
| | | | | | | | | 313.94 | 1.82 |
| | | | | | | | | 351.94 | 2.07 |
| | | | | | | | | 389.46 | 2.32 |
| | | | | | | | | 426.62 | 2.57 |
| | | | | | | | | 463.45 | 2.82 |
| | | | | | | | | 500.02 | 3.07 |
| | | | | | | | | 536.36 | 3.33 |
| | | | | | | | | 572.51 | 3.58 |
| | | | | | | | | 608.49 | 3.83 |
| | | | | | | | | 680.06 | 4.33 |
| | | | | | | | | 751.30 | 4.84 |
| | | | | | | | | 822.20 | 5.34 |
| | | | | | | | | 892.79 | 5.85 |
| | | | | | | | | 963.15 | 6.35 |
| | | | | | | | | 1000.00 | 6.62 |